Light-Guide Solar Concentrator with Dual Axis Tracking System

UCF

COLLEGE OF ENGINEERING AND COMPUTER SCIENCE

Senior Design 1, Spring 2018

Group C

Kyle Merritt	kyle.merritt@knights.ucf.edu	Photonics
Matthew Armogan	matthew.armogan@knights.ucf.edu	Computer Engineering
Justin Kolnick	justinkolnick@knights.ucf.edu	Computer Engineering

Table of Contents

List of Figures

List of Tables

1 Executive Summary

Concentrated photovoltaic (CPV) devices have the potential to be a major player in the renewable energy market. These devices allow a smaller number of solar cells to be used, because the light is concentrated into a small area. Using fewer solar cells means that more expensive, higher efficiency solar cells can be used. However, a major disadvantage of these devices is that they are bulky and hard to manufacture. In this work, we present a more compact solution that still offers a concentration factor of 6. This solution is also scalable and, once manufacturing methods become mature, the cost to manufacture this device will be lower than traditional solutions.

In addition to the concentrator, we present an android app to control the system. The android app is innovative in that it allows the user to understand the status of their system easily and in detail. The app attempts to bridge the gap between technical data and non-technical users by displaying power generation over time, current status, and empowering the user to control their system manually. The mobile app will also allow the user to monitor the status of their system anywhere they can connect to the internet. This app also calculates the amount of money the user has saved by using the system and how long it will be until the user has made enough money to pay for the system.

The concentrator will only function properly when it is directly facing the sun. Therefore, a dual axis tracking system is required. This tracking system and various other electronics will be controlled by an embedded processor. The embedded processor will send status data to a server where it will be stored. The android app will access the data on the server whenever necessary. Using this architecture, data about the status of the system can be available at a moment's notice. The embedded processor will also ensure that the maximum power point is achieved through the use of a MPPT circuit and algorithm. By measuring the voltage and current at the solar cell and the battery we can ensure that the voltage at the battery is sufficient, yet low enough to maximize the current flowing through and therefore reducing the charge time of the battery. To maximize the battery longevity, a current cap is placed to not overload the battery.

This entire system functions as one complete unit, maximizing the energy captured from the sun and utilizing it in some of the most efficient ways possible to ensure that the user is getting the most out of their renewable energy source.

2 Project Description

The following section outlines a general description of the project including background information regarding solar technology, the motivation for building the device, as well as a basic overview of our design plan and requirement specifications.

2.1 Project Background

Over the past 45 years, the electricity demands of the population of the world have continued to increase. This trend is likely to continue. As seen in Figure 1, the large majority of electricity is generated using fossil thermal methods. This presents a problem because of supply limit concerns and the contribution of excess CO2 emissions to climate change [2]. However, we can see a little bit of hope within Figure 1 as well. Over the past 5 years, the portion of electricity generation from non-hydro renewables has been growing, while fossil thermal electricity generation has begun to plateau. In 2015, The United Nations set 17 sustainable development goals [3]. Goal 7 is to ensure access to affordable, reliable, sustainable and modern energy for all people. Part of this goal is to increase the share of renewable energy in final energy consumption. Essentially, we need to make the gray area of Figure 1 larger and the blue area smaller.

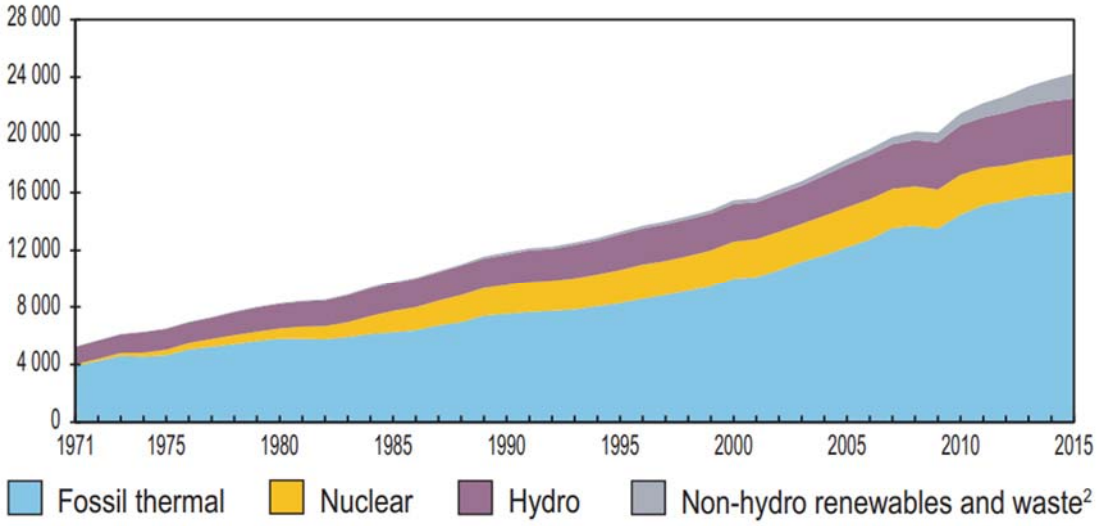

Figure 1: World Electricity Generation from 1971 to 2015 By Fuel (TWh) [1] Based on IEA data from "Key world energy statistics" © OECD/IEA [2017], www.iea.org/statistics, Licence: www.iea.org/t&c; as modified by [Group C]. Permission Requested from: IEA

To accomplish that, countries must be willing to implement new technologies on a large scale. One of the goals of this project is to introduce a new technology that will reduce the cost per watt of solar energy.

A second goal of the project is to make solar energy tracking systems easier to use and understand. By making these systems easy to use, the rate of adoption can be increased. Over the past 5 years, home automation has become increasingly common. Devices like the nest thermostat, smart lighting and smart door locks, allow users to control their devices easily via Android or IOS applications. We want to apply that idea to a solar energy system. In the context of solar energy systems, a companion application can allow a user to easily control the system, educate the user about the system, and reduce buyer's remorse by clearly showing the amount of money the user has saved by using the system.

2.2 Motivation

The motivation for any photovoltaic solar concentrator is to reduce the surface area of solar cells required to capture a given amount of solar energy. When the surface area is reduced, more expensive solar cells, such as multijunction solar cells, can be used while staying within a given budget. These more expensive solar cells have higher efficiency percentages of up to 46% which represents a significant improvement over the 20% efficiencies of silicon solar cells.

The advantage of a LGC over traditional solar concentrators is that the former is more compact and easier to install. Traditional solar concentrators use large parabolic mirrors to focus the light to a point that is above the mirror where the solar cells are positioned. On the other hand, LGCs require no large curved surfaces to concentrate light and the solar cells are not positioned above the mirror. Instead, the LGC redirects light to either side (see Figure 1.) This removes the need to create an additional mounting system for the solar cells. When considering the scale of a solar farm, this simplicity offers a substantial reduction in cost.

2.3 Objectives

The primary goal of our design is to concentrate energy with the concentrator into a solar cell, store this energy in a rechargeable battery, and make information about the status of the system available for the user. A secondary goal is to create a design that is more compact than existing solar concentrators. Our design is unlike most other designs in that it is a planar shape rather than a parabolic shape. Once the sunlight is concentrated only to the cell, we need to effectively charge a battery using a maximum power point tracking algorithm to ensure we are maximizing the energy that the solar cell produces. We then need to implement an algorithm to track the sun in order to maximize the sunlight hitting our device. This is the main function of the system, but expanding what our system is doing into an

easy-to-digest format is vital in broadening our market and user base. These goals can be broken down into the following subsections.

Concentrator Objectives:

- Solar energy will be concentrated by bending light using layered gradient index material
- Light will enter from the large side of a glass plate and exit out two of the smaller sides.
- The reflection layer will consist of prisms with mirrors deposited onto each hypotenuse.

Hardware Objectives:

- Servos will be used to rotate the concentrator. The servos will be controlled using a microcontroller.
- A high efficiency solar cell will be used in order to maximize the power output of our system.
- A maximum power point tracking algorithm will be implemented to ensure maximum power output of the system.
- The system will be user friendly. It will bridge the gap between solar engineering jargon and the non-technical end user.

Embedded Software Objectives:

- The embedded software will read data from optical sensors.
- The embedded software will read data from temperature sensors.
- The embedded software will monitor the voltage of the battery.
- The embedded software will Interface with the mobile application to accept various commands input by the user.
- The embedded software will read and translate energy output from the MPPT PCB to the mobile application.

Mobile Software Objectives:

- The mobile software will provide an interface to remotely control the position of the solar concentrator.
- The mobile software will display important energy statistics from the solar cells.
- The mobile software will be able to communicate to the microcontroller via a wireless network.
- The mobile software will display temperature statistics from the solar cells.
- The mobile software will display power generation vs time to visualize what times of day the device is most effective.
- The mobile software will compare the power generation of the system to that of a traditional solar panel.
- The mobile software will display battery life statistics.
- The mobile software will display the current tilt angles of the concentrators.
- The mobile software will display the systems long term value through a payback timer and multiple graphs and metrics.

- The mobile software will display the efficiency of each individual solar cell so that shading issues can be troubleshot.
- The mobile software will allow the user to change the current tracking mode of the system.

Our user needs to know how effective the device is. This includes how much energy its storing and how efficient the system is compared to other solar energy options. To accomplish this, we are implementing a mobile application that communicates via WiFi with a microcontroller embedded in the device. Users will be able to easily see metrics such as battery storage, energy absorption, and movement decisions of the solar tracking software. Creating a user interface that makes technical information comprehensible to a non-technical user is challenging. Visual representations of our information using functional colors and graphs will assist in bridging this gap. Whenever possible, non-technical language will be used to ensure the user is not overwhelmed.

2.4 Design Overview

This design consists of five primary components, a solar concentrator, solar tracking system, electrical power control system, an embedded microcontroller and a mobile application. When light is incident on the solar concentrator at a 90 degree angle, that light is focused and redirected to the edges where the solar cells are mounted. The solar cells are connected in parallel to a buck converter which is connected in parallel to the batteries. The microcontroller will control the voltage that the buck converter operates at to keep the solar cells operating at their maximum power point.

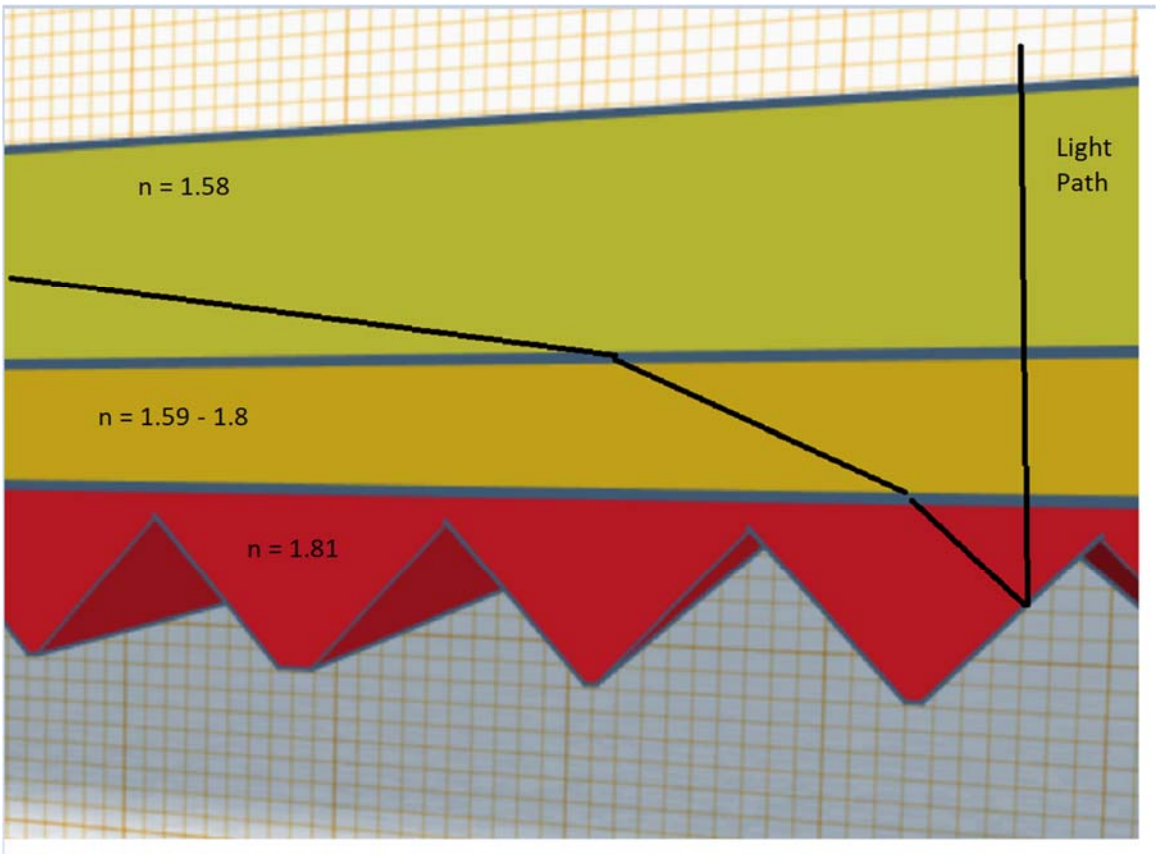

Figure 2: Light Guide Concentrator with Light Path

Because the optical components required are difficult and expensive to manufacture, the scale of this prototype will be on the order of 20 cm by 2cm. The small size allows us to use relatively simple servos to keep the concentrator perpendicular to the path of the solar radiation. These servos will be controlled by the microcontroller. There will be a sensor mounted at each corner of the solar concentrator at a 45 degree angle from the surface. When the signals from two of these sensors are not equal, the microcontroller will change the position of one of the servos in small increments until they are equal.

Figure 3 is the hardware diagram for our design project. The microcontroller will send information about the status of the system to the mobile application via a wifi chip. This information will include, servo positions, solar cell voltage and current, solar cell temperature, battery charge percentage, and estimated battery degradation. The mobile application will forward this information to the user and also store certain portions of the data so that the status of the device can be tracked over time. Temperature vs time and power generation vs time charts will be available to the user.

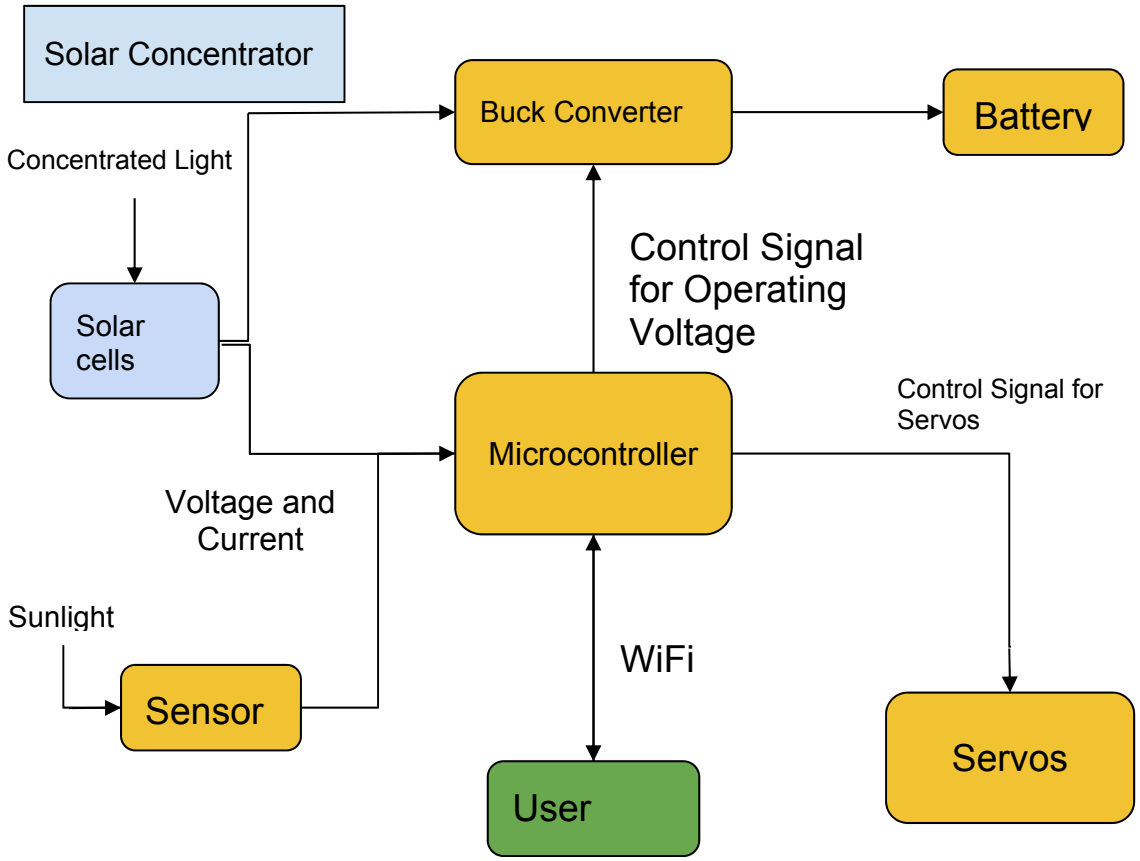

Figure 3: Hardware Diagram

Figure 4 is the software diagram for our design project. The microcontroller and servos will be powered by the batteries that the solar cells have charged. A DC to DC converter will be required for the microcontroller and the servos. Since the system will not run if the batteries are not charged, a backup battery charger will be provided with the prototype.

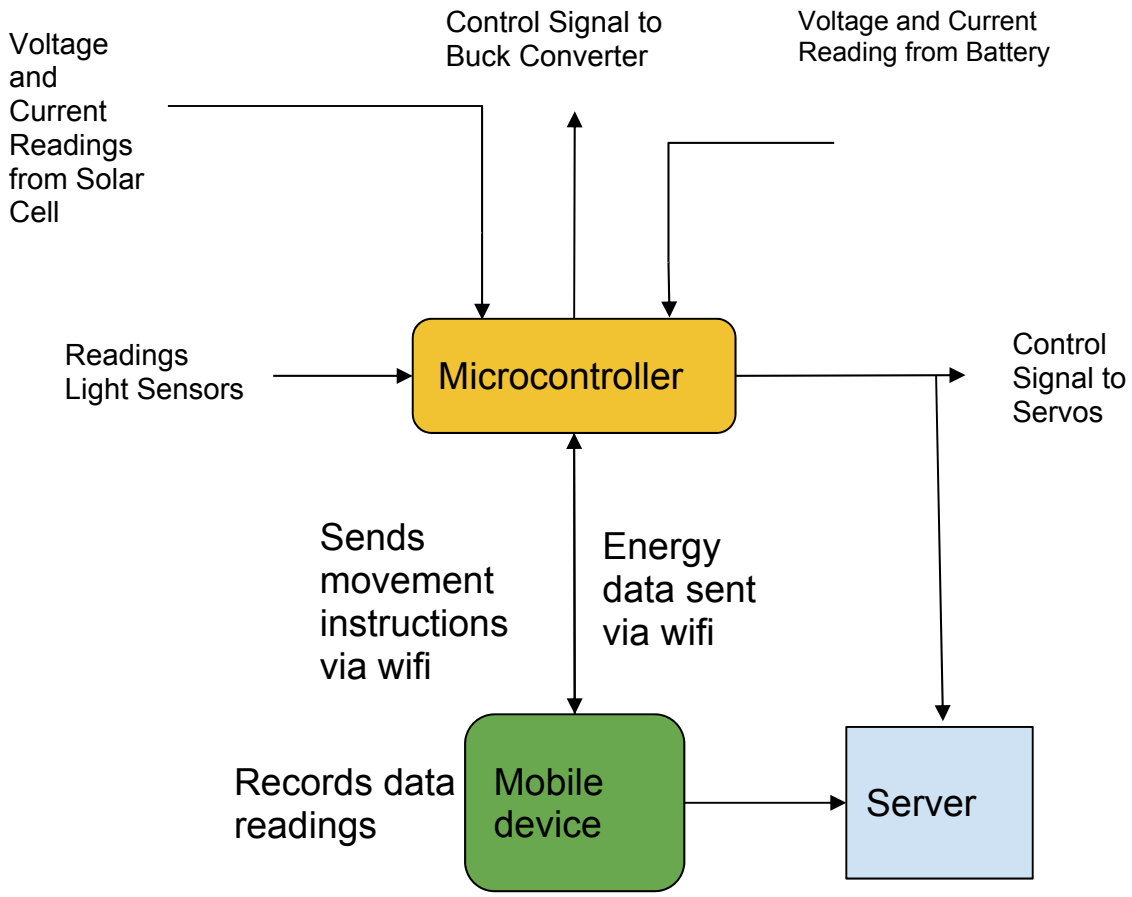

Figure 4: Software Diagram

Figure 5 is the electrical diagram for our design project. Each of these blocks represent an electrical circuit where current flows through. The arrows represent the flow of current through each electrical device.

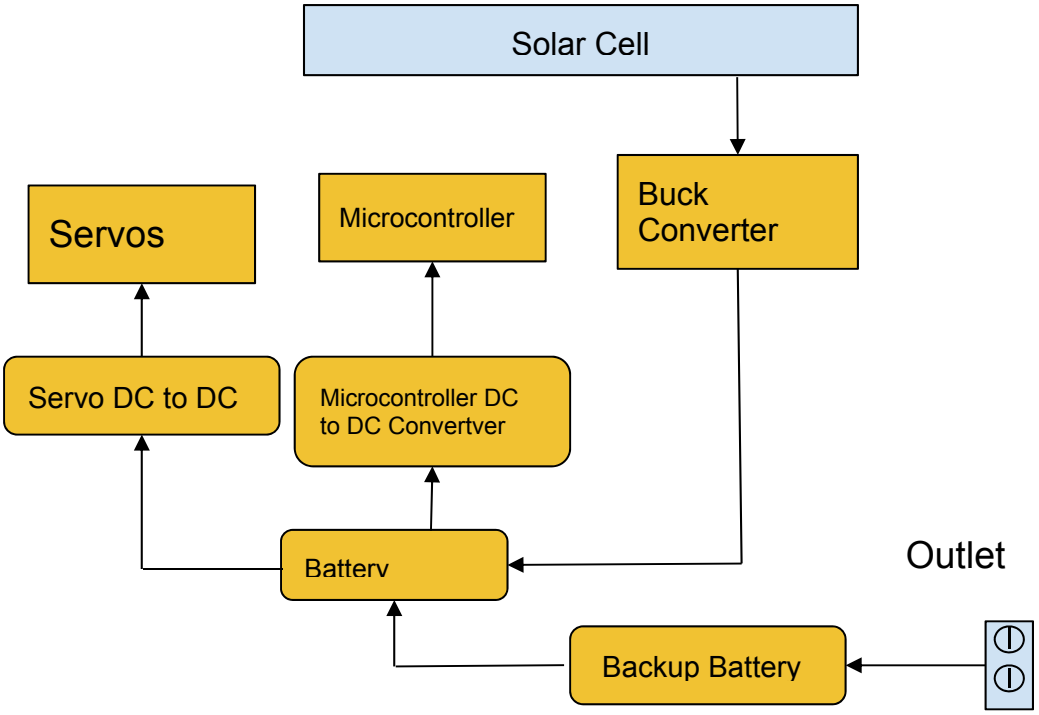

Figure 5: Electrical Diagram

2.5 Requirement Specifications

These are the specifications that we have chosen for our design. Each specification is modeled as a quantitative value. The specifications are broken into 4 subsections, concentrator, tracking, electrical and microcontroller.

Table 1: Requirement Specifications

1.00	The solar concentrator will have a concentration value above C = 6.
1.01	The solar concentrator will be less than 5 cm thick.
1.02	The concentrator will consist of 4 layers, a reflection layer, two gradient index layers and a hard plastic upper layer.
1.03	The concentrator will have a mass of less than 1 kg
2.01	The system will track from east to west automatically from -60 degrees to 60 degrees.
2.02	The system will track from north to south automatically from 0 degrees to 55 degrees.
2.03	The servos will be able to rotate with a torque force above 2 kg/cm
2.04	The MPPT algorithm will be able to track the maximum power point within

	5 seconds.
3.00	The minimum power output greater than 0.5 Watts.
3.01	The 280mAh battery will fully charge in 2 hours. (C=1)
4.00	The circuitry for all components of the microcontroller will be kept to 1 PCB.
5.00	The mobile application will notify the user of battery health degradation after the battery capacity drops below 80% design capacity.
5.01	The mobile application will notify the user to replace the connected battery after the battery capacity drops below 60% design capacity.

Key
1.XX: Concentrator Requirements
2.XX: Tracking System Requirements
3.XX: Electrical System Requirements
4.XX: Microcontroller Requirements
5.XX: Software Requirements

2.6 Marketing and Engineering Requirements

The following section describes requirement trade offs between engineering specifications and marketing specifications. These trade offs help us determine the importance of building towards engineering requirement specifications while keeping in mind the use and functionality of the device to the target demographic we intend to market this product to.

2.6.1 House of Quality

Table 2 is the house of quality table for the project. This table clarifies the relationship between engineering requirements and marketing requirements. This allows us to justify target figures for specific engineering requirements.

Table 2: House of Quality

	Engineering Requirements							
		Efficiency (+)	Weight (-)	Quality (+)	Dimensions (+)	Cost (-)	Power Output (+)	Sensor Accuracy (+)
Ma	Ease of Use (+)	↑	↑	↓	↑	↑	↑	↑
	High Performance (+)	↑	↑		↑	↑		
	Energy Cost (-)	↑	↑	↓		↑	↑	↑
	Quality (+)	↑	↑	↓	↑	↑		
	Durability (+)		↑		↑		↑	↑
	Smartphone app (+)	↑	↑		↑		↑	↑
	User Interface (+)							
	Target	46%	30lbs			~$820 -$910	50W/hr	

Table 3 depicts the relationship between each engineering requirement and each other engineering requirement. This is useful when considering the trade offs between them. This allows us to understand the importance of engineering specifications in relation to others when determining target values for our requirements specifications

Table 3: Relationship Between Engineering Requirements

	Engineering Requirements						
Eng.		Efficiency	Weight	Quality	Dimensions	Power Output	Sensor Accuracy
	Efficiency					↑	↑
	Weight			↑	↑		
	Quality		↑				
	Dimensions		↑			↑	
	Power Output	↑			↑		↑
	Sensor Accuracy	↑				↑	

Key
(+) Increases requirements
(-) Decreases requirements
↑ Positive correlation
↓ Negative correlation

3 Research

In order to realize this project design, a background in solar energy and other competing technologies was required. Also, studying the operating principles of various hardware and software components was necessary to properly integrate them. An understanding of these topics also allowed us to make informed choices when choosing components. The following section reviews existing products as well as research on the solar energy and related technologies.

3.1 Existing Products

The products below are all existing solar energy technologies that compete with our design. While many other products exist relating to solar energy, including concentrated photovoltaics, this project has been designed to specific objectives to meet the needs of the consumer as a unique addition to the CPV market.

3.1.1 Photovoltaic Solar Panels

Likely the most popular form of solar installation today is the photovoltaic solar panel. This design has been the lead product in solar technology since the sector boom in the early 2000s. Traditional photovoltaic solar panels use large PN junction solar cells to move electrons and create current when hit by sunlight. When the sunlight hits the N-type semiconductor, electrons are knocked loose from their atoms and these electrons. Figure 6 below shows the cross section of a solar cell.

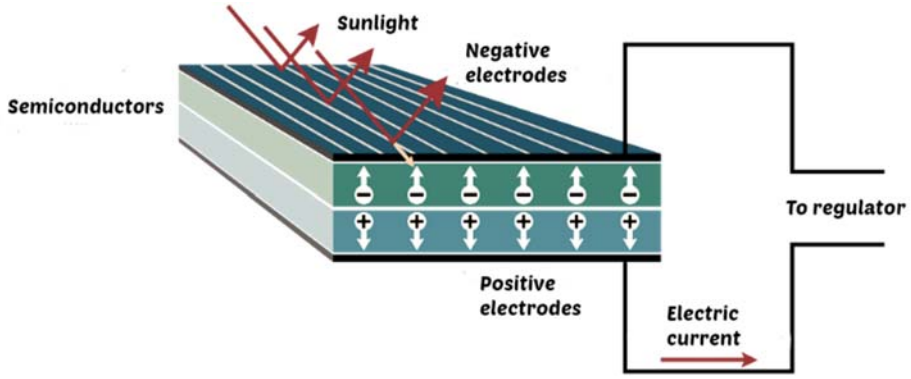

Figure 6: Cross section of a solar cell
Permission Requested from: Value Walk

This solar panel design in practice can cover a large area, however their failure point lies within their efficiency. Solar cell efficiency is based on many variables including its reflectance, thermodynamic efficiency, charge carrier separation, and conduction efficiency. Reflectance efficiency deals with the materials ability to reflect radiant energy. Thermodynamic efficiency is a theoretical hard limit on conversion of sunlight to electricity. The hard limit is found to be 86% based on the

temperature of the Sun's surface where the photons are produced. This efficiency percentage is known as the Chambadal-Novikov limit. Charge carrier separation is in relation to the energy cost in pulling an electron away from its atom. Conduction efficiency describes the heat energy lost through the collisions created within the NP junction.

Traditional solar panel designs fall victim to low efficiency due to the size of the panel, which is in most cases an array of six by ten solar cells with an efficiency of approximately 20% per cell. In comparison to our design, we are concentrating the solar energy into each end of the solar panel, meaning that we can buy two solar cells instead of sixty. This decrease in quantity allows us to increase the quality of our solar cell. Due to the high price of multijunction solar cells, this project uses normal mono crystalline solar cells but still proves that the solar concentrator will work with multijunction solar cells.

3.1.2 Tracking Solar Panel Without Concentrator

The main purpose of solar panels are to generate as much power as possible while requiring the minimum cost to do so. To be able to do this, the photovoltaic array panels have to be pointed directly at the sun to be able to absorb the maximum amount of irradiance. The optimal point to do so is when the sunlight beam is covering the entire surface area of the panel and is at an incidence angle of 0°. This can be achieved by having a tracking system attached to the base of the solar panel to follow the movement of the sun consistently throughout the day and adjust the angle of incidence accordingly. Some tracking systems that have been built already are single (one)-axis tracking systems which track the sun in an east-west motion and dual(two)-axis tracking systems that follow the sun in an east-west and north-south motion.

The statistics in figure 7 came from a study conducted by the National Renewable Energy Laboratory that compared energy generation between a fixed-tilt solar panel pointed in the south direction at an angle of 25° relative to the surface of the Earth, a single-axis solar panel and a dual-axis solar panel. The study shows that over the entire United States single-axis solar panels generated 12-24% more electricity than the fixed tilt, and dual-axis solar panels generated 30-44% more electricity than the fixed tilt solar panel[31].

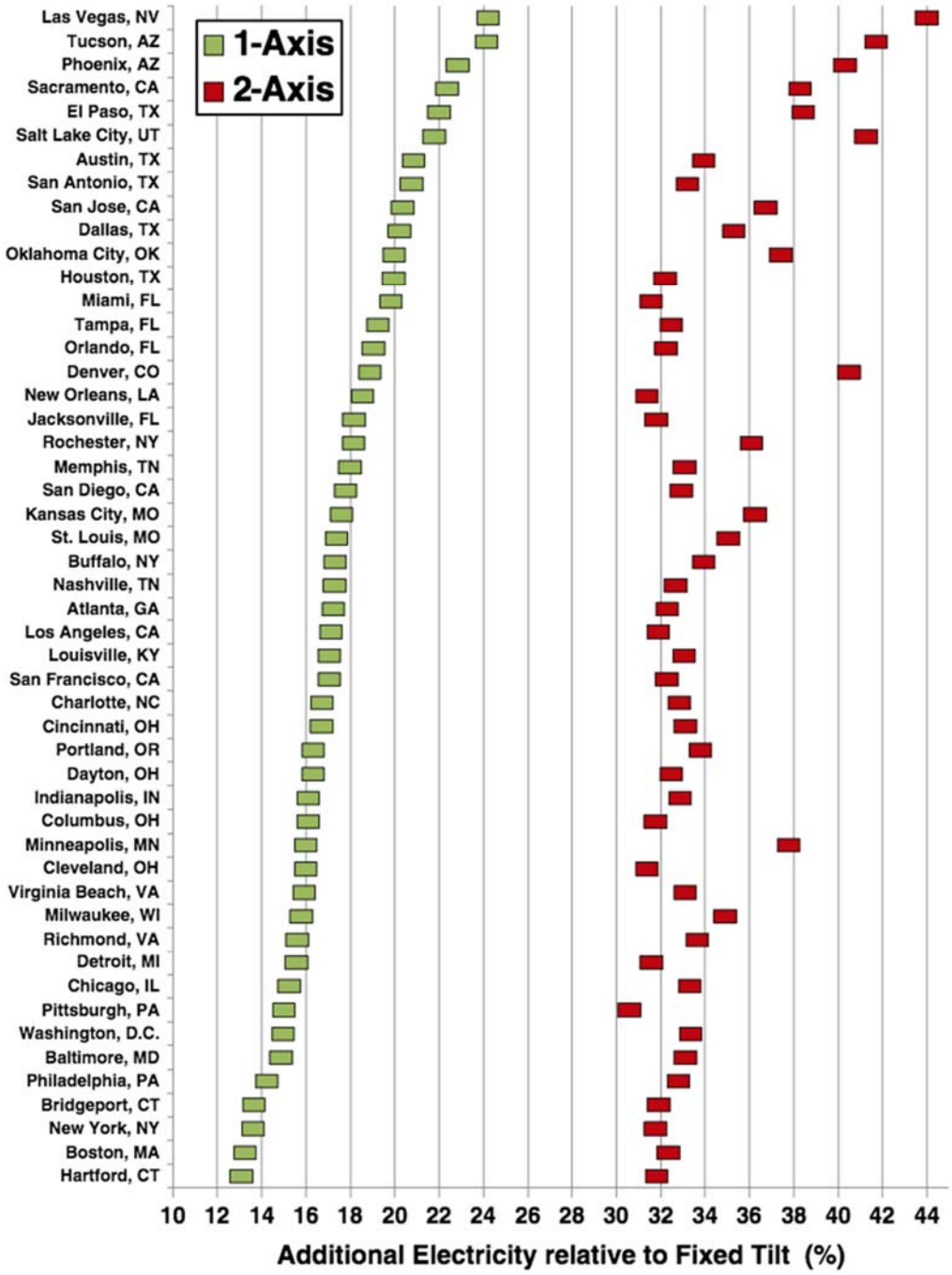

Figure 7: Additional generation from one-axis and two-axis tracking photovoltaic systems relative to a south-facing fixed tilt system for the United States [31] Permission Requested from: Progress in Photovoltaics

Logically, this would make single-axis and dual-axis solar tracking panels seem like the better way to generate electricity, but there are other factors that decide whether tracking solar panels are more beneficial to use than a fixed-tilt solar panel. The price of installation and maintenance of tracking solar panels are

typically more costly than just implementing a fixed-tilt solar panel depending on location and how much energy cost the owner is saving per unit. Depending on the location of the owner, if he/she is living in an area that receives minimal sunlight over the course of the year then the cost of having a solar tracking unit compared to a fixed axis system may not be worth investing. Mounting structures and tracking software may also cause the cost tracking solar panels to be so high that using a fixed-tilt solar panel would cause a greater return on investment in the long run. [28]

3.1.3 Parabolic Solar Concentrator

The parabolic solar concentrator is another type of solar concentrator that harvests solar energy for electrical use. Instead of the standard looking solar panel that is composed of an array of solar cells grouped together, this type of solar concentrator uses a parabolic dish which is made up of reflection panels to reflect sunlight toward a single focus point. At the focal point where all of the sun rays intersect is a power conversion unit that is composed of a thermal receiver and generator. The thermal receiver can be composed of tubes or heat pipes that are filled with a fluid or gas. When it absorbs the beams of solar energy that is reflected from the parabolic dish it increases the temperature of the fluid. The heat from the fluid is then transferred to the generator. The generator system takes the thermal energy produced and converts it to electrical energy [6]. The solar concentrator implements a dual axis tracking system, which can track the sun in a more direct circular path than a single axis tracker, which follows the movement of the sun across a horizontal plane. An illustration of the solar concentrator is seen below in Figure 8.

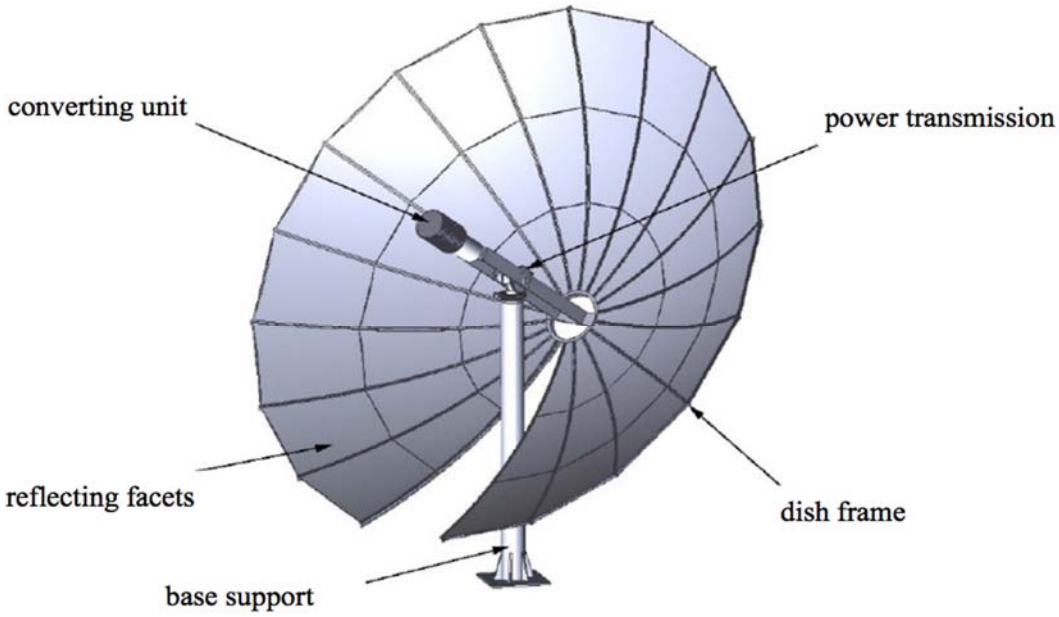

Figure 8: Parabolic Solar Concentrator [29]
Permission Requested from: Alexandria Engineering Journal

One of the main benefits of using a parabolic dish-shaped solar concentrator is that it currently has “the highest efficiency in the conversion of solar energy to electricity with an efficiency of 29.4% achieved” [5]. Compared to it, regular flat solar panels are only able to convert less than 14% of solar energy into electricity [7]. Our solar concentrator design is predicted to convert solar energy to electrical energy at an efficiency rating of up to 46%.

3.1.4 Solar Thermal Power Generation

Another existing method used to harness power from solar energy is to utilize the heat generated when sunlight is incident on a material. The simplest form of this is a solar water heater. The sunlight is incident on a material that is easily heated such as copper, and that metal is in contact with water. The water is heated via thermal conduction and then can be used. This method reduces the amount of electricity required to heat water for a home or building.

Highly concentrated solar energy can be used to heat water or other liquids beyond their boiling point. The expansion of these liquids can be used to power a steam engine that powers an electric generator. The disadvantage of this method is that there are four different types of losses, optical losses, thermal losses, mechanical losses and electrical losses. The efficiency of these systems is directly proportional to their size. A more compact system is going to be less efficient. The photovoltaic solar concentrator described in this paper has the advantage that it is efficient even at small scales.

3.1.5 SolarEdge monitoring application

The SolarEdge monitoring application allows the user to remotely monitor the energy generation from their solar devices. Types of measurements available are current system power, energy generation, graph display of daily power, weekly and yearly energy production, and weather forecast.

3.1.6 MyEnlighten application

Built by Enphase Energy, MyEnlighten is a solar monitoring app built for the system owner that tracks the Enphase System installed on his or her property. It verifies the system's health and performance, displays energy production by month, day or hour, and analyzes performance against historical weather data.

3.2 Relevant Technologies

The following section consists of research regarding technologies that we are likely to find present in our own project design. Through research of these topics, we will be able to understand the necessary components that we will need to fulfill the requirements of our design.

3.2.1 Photovoltaic Solar Cells

Photovoltaic solar cells are electrical devices that generate electricity when exposed to light. Solar cells are commonly implemented with a PN junction. Whenever a semiconductor is exposed to light, some portion of the photons are absorbed by the material, causing a electron-hole pair to be created as shown in Figure 9. In a semiconductor that is not a PN junction, these electrons and holes diffuse in random directions and are likely to recombine before they are useful. However, because a PN junction has a built in electric field, if the electron-hole pair is generated within a PN junction, the electron and hole are pushed to opposite sides of the cell. This movement of charges is a current that can be used as electrical power.

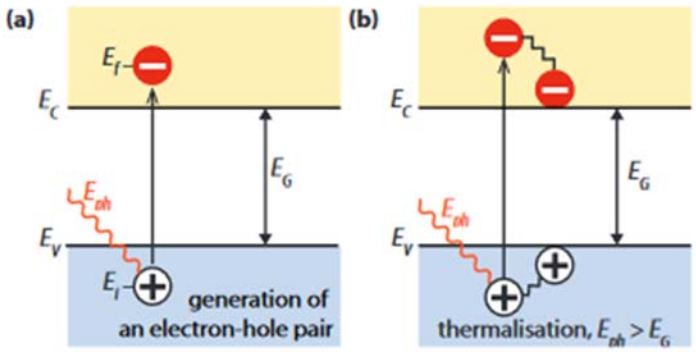

Figure 9: Electron Hole Pair Generation

To use this power, the solar cell must be placed in a circuit and to analyze the circuit containing the solar cell, we must assign it an equivalent circuit. Two possible equivalent circuits are shown in Figure 10. It should be noted that the diode in the equivalent circuit is forward biased which differs from a circuit for an optical sensor. The next step is to add some type of energy storage as shown in Figure 9. Common energy storage devices used are capacitors and batteries. These simple circuits all have a problem that the solar cells operate at a constant voltage, which means they are usually not operating at optimal efficiency. This problem is addressed in the section about maximum power point tracking (3.2.6).

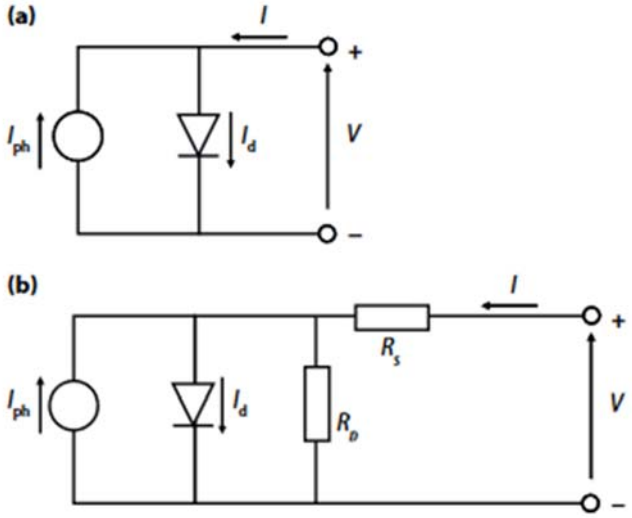

Figure 10: Solar Cell Equivalent Circuits: (a) Ideal Solar Cell (b) Solar Cell with Series and Shunt Resistances [10]
Permission Requested from: KED PLANT INSIDER

The most basic solar cell circuit is to put it in parallel with a load such as a fan or a light as shown in Figure 11. However, this circuit very unreliable, because it only ever runs when the cell is exposed to light. Figure 12 utilizes capacitors of different forms to allow the power output to be maintainable.

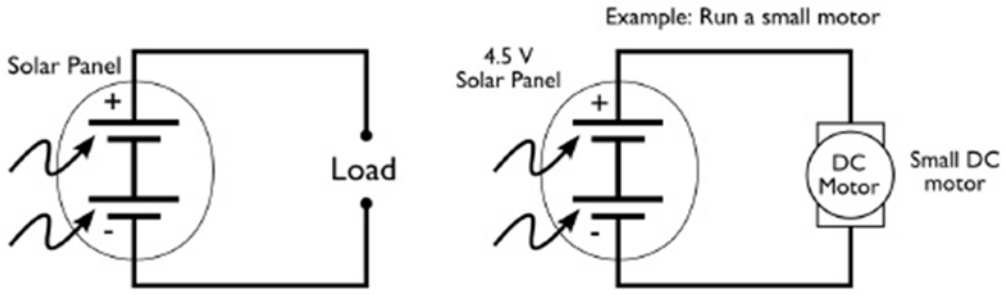

Figure 11: Simple Solar Cell Circuits [10]
Permission Requested from: KED PLANT INSIDER

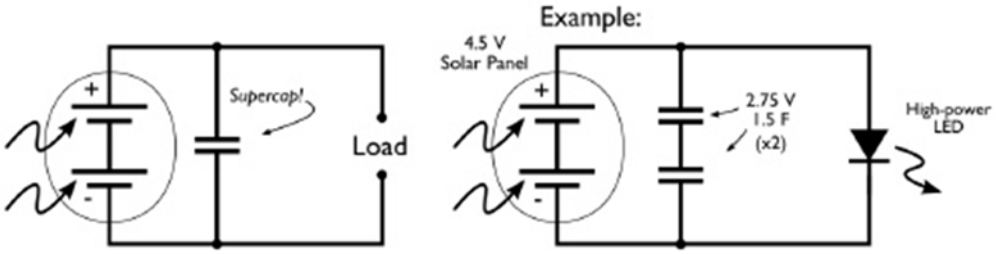

Figure 12: Solar Cell Circuit with Capacitors as Storage [10]
Permission Requested from: KED PLANT INSIDER

3.2.2 Optical Sensors: Photodiodes

The operating principle and structure of a photodiode configured as an optical sensor is similar to that of a solar cell. Both components are can be implemented using PN junctions and both work by absorbing photons and generating, but optical sensors are usually reverse biased. A typical simple photodiode circuit is shown in Figure 13. In this circuit, Vout is directly proportional to Ev1. Although Ev1 can be found from Vout and the other circuit parameters, in the context of our application it will be sufficient to compare the Vout of each optical sensor circuit.

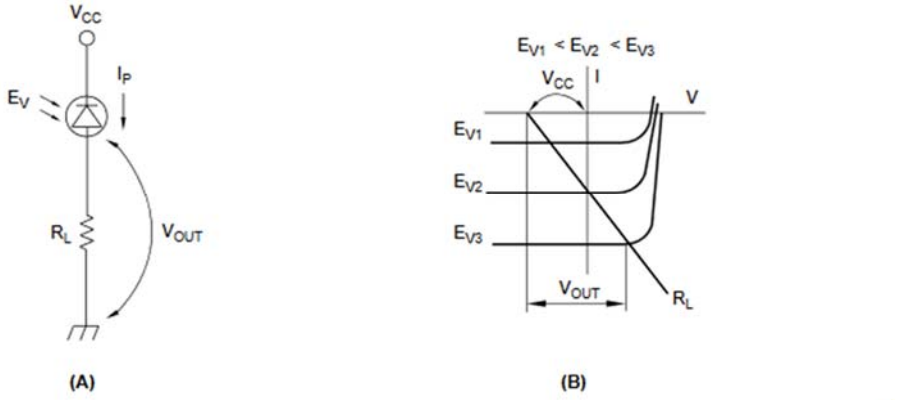

Figure 13: (a) Photodiode Circuit (b) Photodiode I-V Curve
Permission Requested from: UCF CREOL

3.2.3 Solar Concentrators

In this section several parameters used to characterize solar concentrators will be discussed. As discussed in the introduction, the purpose of a solar concentrator is to concentrate solar radiation into a smaller area and thus reduce the area of optical absorbers required. To quantify that goal, we can compare the aperture area, A_a, to the absorber area, A_{abs}, which gives us the concentration factor, C. [12]

$$C = A_a / A_{abs}$$

A higher C value usually means a more effective solar concentrator, however, a higher C usually reduces the acceptance angle. The acceptance angle, $theta_A$, defines how far the angle of the ray can deviate from the normal and still be incident on the absorber. A third important parameter is optical efficiency, eta_O. Optical efficiency is defined as the ratio of the energy incident on the absorber to the energy incident on the aperture. [12]

$$\eta_O = E_{abs} / E_a$$

Optical losses are caused by absorption at the surfaces of mirrors, absorption within optical materials, and unwanted reflections at interfaces between materials. These losses may be reduced by using mirrors with low absorbance and anti-reflection coatings.

3.2.4 Glass Component Assembly Methods

This project requires an optical component that is made up of multiple subcomponents. Therefore, an investigation of how to combine these subcomponents while minimizing optical losses was required. In other works, using an epoxy with a refractive index that matches the refractive index of one or both of the subcomponents has been found to be effective [14]. A small, even coat of index matched epoxy will be applied to one of the components. A device such as a vice will be used to compress the two components together as much as possible in order to force any excess epoxy out of the interface. Any excess epoxy will be removed.

3.2.5 Gradient Index Glass Fabrication Methods

Two methods of gradient index glass fabrication were investigated for this project, ion exchange [9] and molten glass batching [8]. Ion exchange occurs when glass is exposed to a liquid admixture, which is usually a molten salt. Over time, ions in the admixture are exchanged for different ions within the glass. It takes more time for ions to diffuse deeper into the glass. Therefore once the process is complete, the concentration of new ions is higher at the surface of the glass and is less further

away from the surface. The gradient of new ions creates a gradient refractive index. The advantages of this method are that it is relatively simple to perform and it only requires lower temperatures than molten glass batching. The disadvantages of this method is that it takes a lot of time for ions to diffuse into the glass which could prevent rapid manufacturing, the total change in refractive index is limited to around 0.2, and the ions that create the largest change in refractive index are dangerous heavy metals like Thallium.

In the case of molten glass batching, a number of different glasses with the desired variation in refractive index are melted in separate containers. These molten glasses are then combined in a single crucible and then allowed to settle. The higher density glasses, which are usually higher refractive index, will sink to the bottom of the mixture while less dense glasses will float to the top. Eventually, at the interfaces between these glasses, they will mix slightly to form a gradient index. An advantage of this method are that the total change in refractive index can be arbitrarily large, because it is determined by which glasses are chosen. Another advantage is the components used are glass frits which are generally safe to use. The biggest disadvantage of this method is that it requires very high temperatures and therefore very expensive crucibles and furnaces. This method shares the disadvantage of a slow manufacturing time with ion exchange.

3.2.6 Mirror Deposition Technique

This section will describe the method that will be used to deposit the mirror onto the bottom surface of the concentrator. The process contains three steps, cleaning the glass, sensitizing the glass, and depositing the mirror. To clean the glass, it is first washed with hot water and concentrated detergent. It is then cleaned with a soft cloth. After rinsing well, it is cleaned with Cerium Oxide which is also known as “Optician’s Rouge.” After scrubbing, the glass is rinsed with warm tap water, then sprayed with distilled water. The surface of the glass then must be sensitized. The surface is covered by a solution that is called a “Tinning” solution. This solution, which is Stannous Chloride, acts as a reagent in the reaction that deposits the silver onto the surface. The surface is covered with the solution and it is left to sit for 30 seconds. Then, the excess solution is removed by tilting the glass. Lastly, the silver solution is added to the surface. The silver solution is allowed to stay on the surface for 5 minutes. During that time, it will change colors multiple times. Once the time is up, the surface is cleaned and a mirror has been deposited.

3.2.7 Maximum Power Point Tracking

In order to operate the photovoltaic cells at peak efficiency, we need to ensure that the cells are producing their maximum power point. This is determined through the use of a maximum power point tracking algorithm and an additional DC-DC converter. This circuit controls the voltage at which the photovoltaic cells operate, ensuring that the photovoltaic cells are operating at peak efficiency through the

tradeoff of current and voltage. Maximum power produced by photovoltaic cells can vary with solar radiation, ambient temperature, and solar cell temperature. A block diagram of the MPPT is seen below.

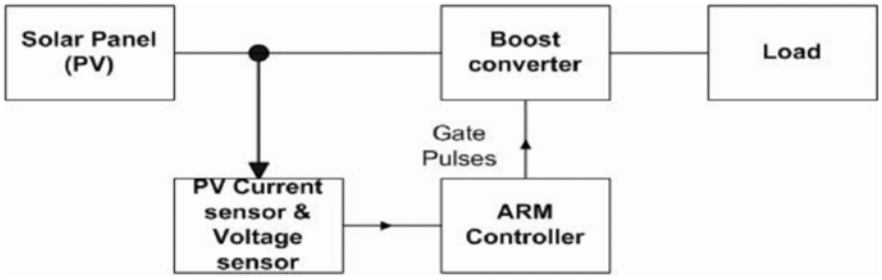

Figure 14: MPPT Block Diagram
Permission Requested from: Gutierrez

Choosing the algorithm in which we are monitoring and controlling the buck boost switches is vital to the performance of the MPPT system. Hill-climbing is one of the more popular algorithms with incremental conductance being a close second; note both are not photovoltaic array dependent meaning that they apply to general graph applications rather than simply to solar photovoltaic arrays. Table 4 depicts the comparisons of multiple MPPT algorithms from which we chose from.

Table 4: MPPT Algorithm Comparisons

MPPT Technique	PV Array Dependent?	True MPPT?	Analog or Digital?	Periodic Tuning?	Convergence Speed	Implementation Complexity	Sensed Parameters
Hill-climbing/P&O	No	Yes	Both	No	Varies	Low	Voltage, Current
IncCond	No	Yes	Digital	No	Varies	Medium	Voltage, Current
Fractional V_{OC}	Yes	No	Both	Yes	Medium	Low	Voltage
Fractional I_{SC}	Yes	No	Both	Yes	Medium	Medium	Current
Fuzzy Logic Control	Yes	Yes	Digital	Yes	Fast	High	Varies
Neural Network	Yes	Yes	Digital	Yes	Fast	High	Varies
RCC	No	Yes	Analog	No	Fast	Low	Voltage, Current
Current Sweep	Yes	Yes	Digital	Yes	Slow	High	Voltage, Current
DC Link Capacitor Droop Control	No	No	Both	No	Medium	Low	Voltage
Load I or V Maximization	No	No	Analog	No	Fast	Low	Voltage, Current
dP/dV or dP/dI Feedback Control	No	Yes	Digital	No	Fast	Medium	Voltage, Current
Array Reconfiguration	Yes	No	Digital	Yes	Slow	High	Voltage, Current
Linear Current Control	Yes	No	Digital	Yes	Fast	Medium	Irradiance
I_{MPP} & V_{MPP} Computation	Yes	Yes	Digital	Yes	N/A	Medium	Irradiance, Temperature
State-based MPPT	Yes	Yes	Both	Yes	Fast	High	Voltage, Current
OCC MPPT	Yes	No	Both	Yes	Fast	Medium	Current
BFV	Yes	No	Both	Yes	N/A	Low	None
LRCM	Yes	No	Digital	No	N/A	High	Voltage, Current
Slide Control	No	Yes	Digital	No	Fast	Medium	Voltage, Current

Permission Requested from: Gutierrez

The maximum power point tracking algorithm we will use is known as the hill-climbing algorithm. This maximum power point is the point where the maximum voltage achieves a maximum power level. Increasing the voltage past this point results in a decrease in power.

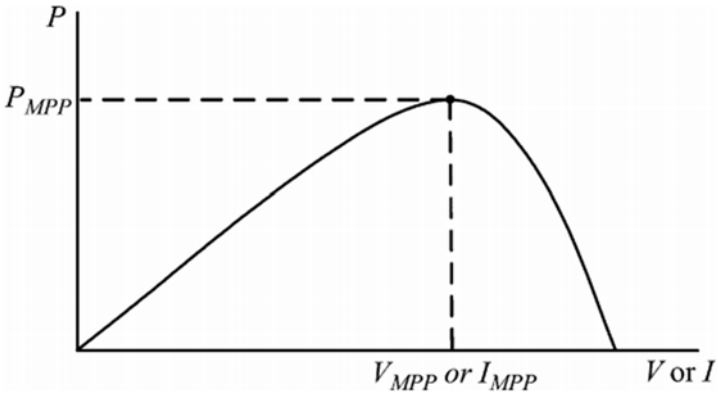

Figure 15: MPPT Graph

If the controller increases the voltage and then the power increases, then we know we are at too low of a voltage and need to shift the voltage upwards to reach the maximum power point. Similarly if the voltage increases and the power decreases, then the voltage is too high and needs to be reduced to achieve the maximum power point. This behavior is detailed in Table 5 and Figure 15.

Table 5: Hill Climbing Algorithm

Change in Voltage	Change in Power	Next Change in Voltage
Positive	Positive	Positive
Positive	Negative	Negative
Negative	Positive	Negative
Negative	Negative	Positive

3.2.8 DC-DC Converter

For the connection of a solar cell to a battery, there must be some voltage and current monitoring occurring in order to maintain a high enough input voltage for the battery to accept charge, but also low enough to not waste or lose energy. This monitor must also be able to resolve high voltages into a minimum load acceptance voltage in order to charge the battery. In turn this reduced voltage will increase the current flowing to the battery and charge the battery faster. To tackle this problem, we will use a form of a DC-DC Converter.

The buck-boost circuit is a very popular DC-DC converter that relies on an inductor and diodes to regulate the voltage between the voltage source and the load. When both of the switches are closed, the voltage source Vin stores its charge in the inductor and immediately goes to ground. When both of the switches are open, the

inductor is able to discharge and flow over the load. The capacitor is included to smooth out the signal.

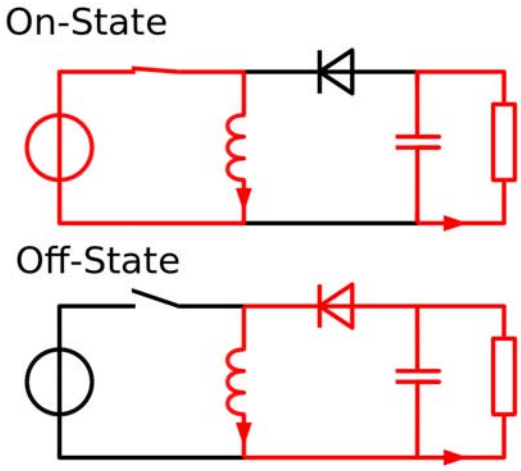

Figure 16: Example DC-DC Buck Boost Converter (CC License)

Depending on the rate at which the switch opens and closes, the current will vary as the inductor contains a greater charge or a lesser charge. This begs the question of how to determine when to switch the circuit open and closed. Utilizing the MPPT hill climbing algorithm from above, we can replace this circuit's switches with a pulse width modulated signal and a N-type mosfet to switch the solar cell output connection to the inductor within the DC-DC Buck Boost converter circuit. This design is depicted in Figure 17.

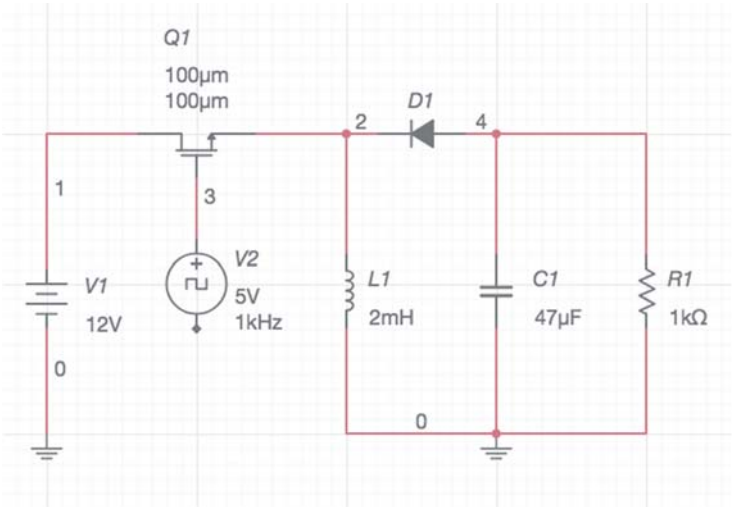

Figure 17: Preliminary DC-DC Circuit Design

In Figure 17, we see that the NMOS Gate is connected to a PWM signal, and therefore the voltage source V1 will be connected and disconnected at a frequency of 1kHz. This allows the inductor to briefly charge and subsequently discharge over

the 1kΩ resistor load. This will allow is to control the amount of current supplied to the load depending on the voltage from V1.

3.2.9 Battery

There are many batteries available with many different specifications. Choosing the correct battery requires an understanding of the relationship between these specifications and the application. Capacity, power, depth of discharge, and speed of discharge are important factors when deciding on a battery. A battery with a low capacity and a high power rating would be able to run a large number of devices, but only for a short time. In contrast, a battery with a high capacity and a low power rating would be able to store a large amount of energy and power a smaller number of devices for a longer time. Both forms have their place in solar energy, however it depends on the output power of the solar cells to the battery and the desired output of the battery.

Lithium-ion batteries are rechargeable batteries that store energy by moving electrons from the positive electrode to the negative electrode, and vise versa during discharge. These batteries are some of the most popular options on the market in battery technology today, specifically for home electronics due to their small footprint, high energy density and low energy release discharge rate. The tradeoff point is their high cost.

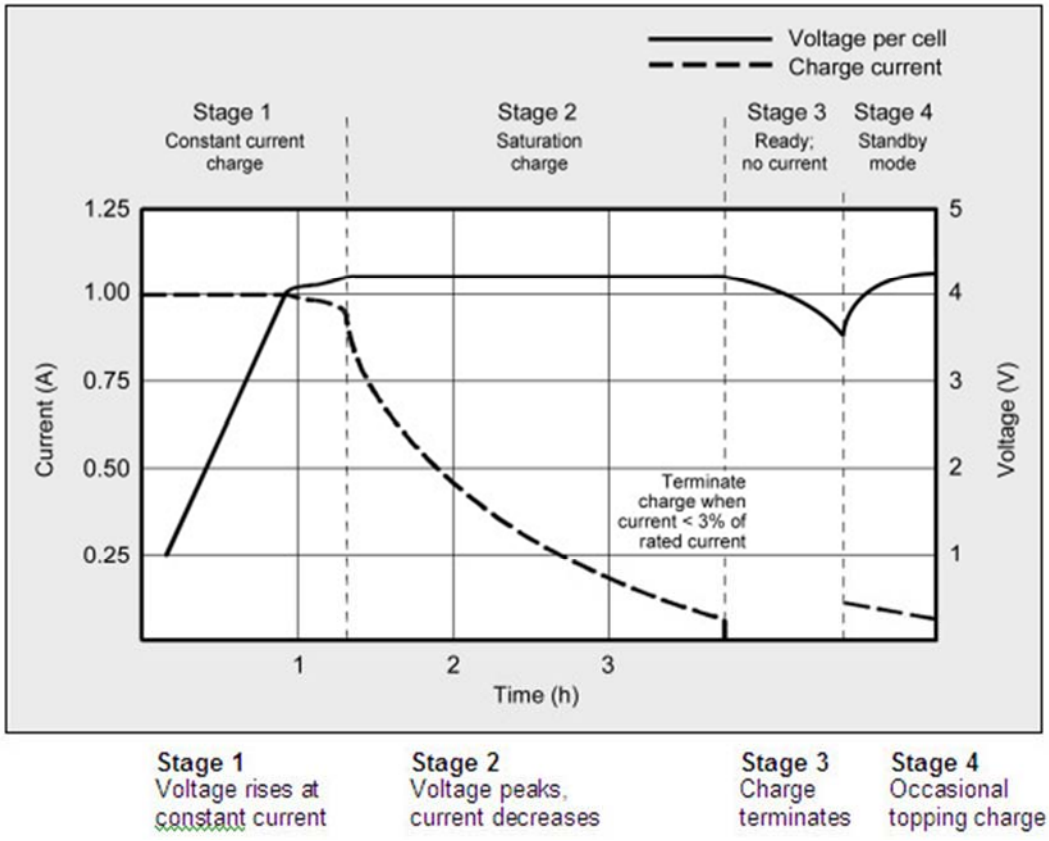

Figure 18: Lithium-ion Battery Charging Over Time

Permission Requested from: Battery University

Lithium Cobalt Oxide (LiCoO2) batteries are some of the most commonly used batteries in mobile phones, laptops and digital cameras in today's market. They were introduced in 1991, and have since stabilized in price within the battery market. The battery contains a cobalt oxide cathode and a graphite carbon anode that moves lithium ions from the anode to the layered cathode. The main drawback of batteries with this material makeup consist of its short life span, low thermal stability, and limited load capacity. In addition, Cobalt is also a significantly expensive material. The cycle life for batteries with this makeup is around 500-1000 cycles on average. [22] Figure 19 depicts the common trade off variables with Lithium Cobalt Oxide batteries.

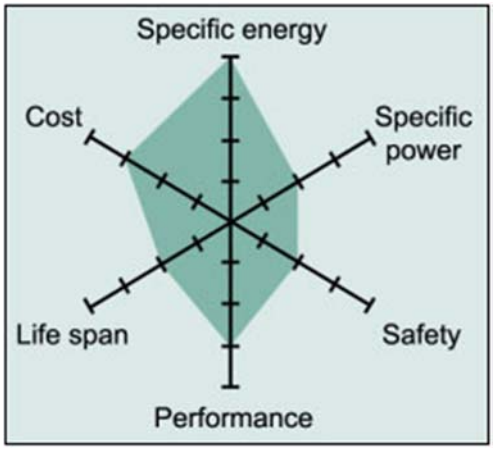

Figure 19: Lithium Cobalt Oxide Trade Offs
Permission Requested from: Battery University

Lithium Manganese Oxide (LiMn2O4) batteries were introduced in 1983 and later realized in 1996 by Moli energy. The Manganese Oxide structure differs, as it is a three dimensional lattice structure that allows Lithium-ions to pass through its holes. This updated structure improves ion flow between the layers, which in turn improves current handling by decreasing internal resistance. The main downside to these batteries is decreased storage capacity. Li-manganese batteries are mostly used for power tools, medical instruments, as well as hybrid and electric vehicles. [22]

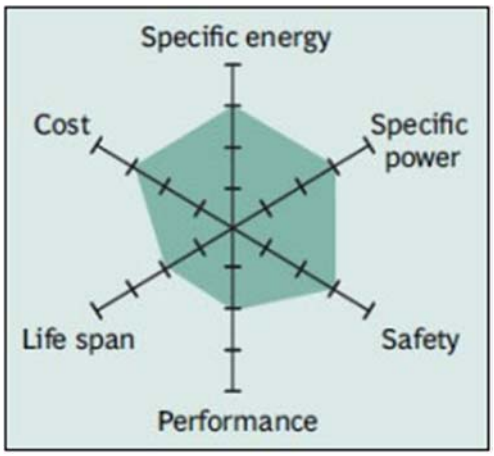

Figure 20: Lithium Manganese Oxide Trade Offs
Permission Requested from: Battery University

Arguably the most successful Lithium-ion battery is the Lithium Nickel Manganese Cobalt Oxide (LiNiMnCoO2 or NMC) battery. Nickel is known for its high energy and poor stability, while Manganese maintains the lattice structure which provides low internal resistance but gives low energy outputs. With the combination of these elements, we can use their strengths together to create a low internal resistance, high energy, stable battery system. Due to its low temperature, this battery is sought after for application where temperature control is a concern, such as electric cars, which can reach high temperature when exposed to sunlight for extended periods. NMC is also known as the battery of choice for electric bicycles and other electric powertrains. [22]

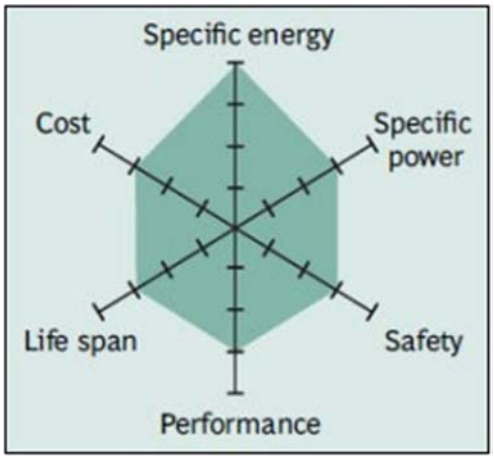

Figure 21: Lithium Nickel Manganese Cobalt Oxide Trade Offs
Permission Requested from: Battery University

Lead-acid batteries are one of the oldest types of rechargeable batteries that also function by the movement of electrons. During discharge, the lead dioxide (positive plate) and lead (negative plate) react with the electrolyte of sulfuric acid to create lead sulfate, water and energy. During charging, the lead sulfate and water are

electro-chemically converted to lead, lead oxide and sulfuric acid by an external charging source.

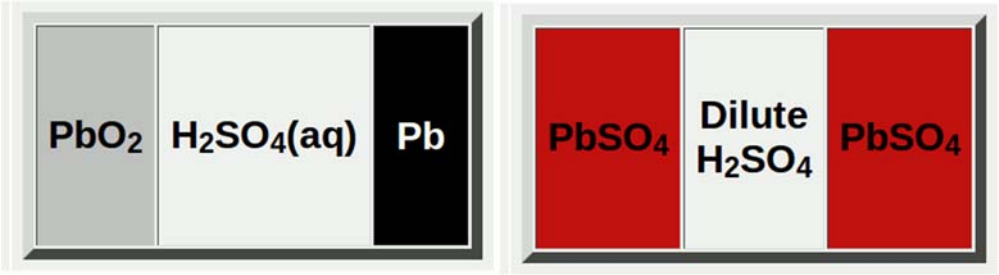

Figure 22: Lead-acid Battery Charged, Discharged (Left to Right)
Permission Requested from: Battery University

Lead-acid batteries provide one of the lowest cost to energy ratios, which is why they are used so frequently in machinery that require a large amount of energy to be stored. The tradeoffs include a heavy weight and large size conducive of the lead plates, slow charge speeds, as well as a narrower voltage range at which the battery is able to be charged.

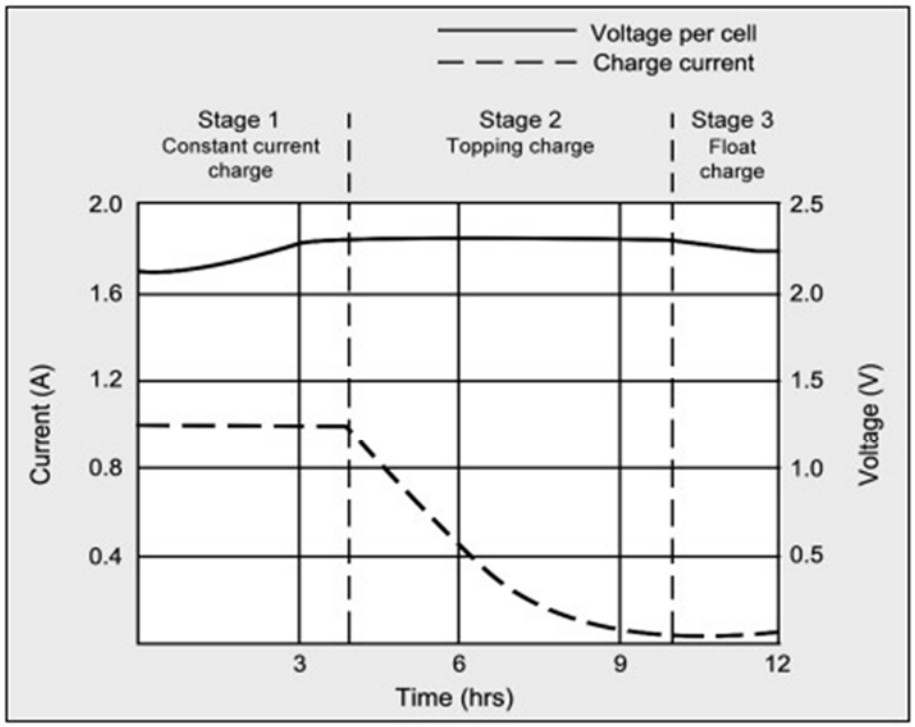

Figure 23: Lead-acid Battery Charging Over Time
Permission Requested from: Battery University

3.2.10 Servo system

A servo system is a functional mechanical device that has the ability to control the movement of other components within the overall system at a very accurate precision rate. Types of movement that is is able to do on the object are pushing it in different areas or rotating it to a precise angle. There are many industrial applications of a servo motor, the most common being used in:

- Robotics
- RC toys such as cars, helicopters, and planes
- Automatic door openers
- Solar tracking systems

Figure 24 shows the hardware design of a servo. It is composed of a controller, an AC or DC powered rotary motor, an amplifier, and a feedback mechanism. A pulse signal is sent to the controller, and it stores the acceleration and speed values that the motor should be moving at. Those values are sent to the amplifier which sends a specific current to the motor. The motor moves at the given speed and acceleration and is able to rotate at different angular positions. The feedback mechanism relays information about the angle position back to the controller. The controller then compares that output signal to the initial input parameters and makes the necessary adjustments to keep the device at the required position [30].

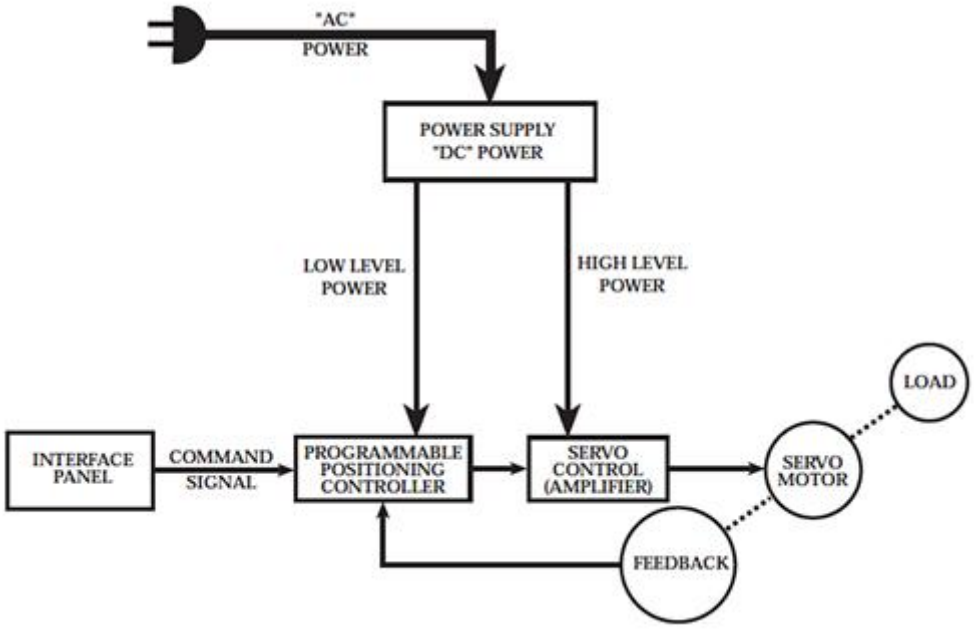

Figure 24: Servos [30]
Permission Requested from: Linear Motion Tips

In use of a single or dual-axis solar tracker, servos are implemented on the trackers to rotate the solar panels. Sensors attached to the solar panel track the movement

of the sun and send a digital pulse signal to the servo controller to tell it what angle it needs to be set at so that the rotary motor can be adjusted so that the solar panels can maintain direct exposure from the sun. This ensures that the maximum amount of solar energy is being absorbed and converted to electricity. According to GTM Research, solar trackers using single or dual axis linear actuators increased energy production of solar panels by 15-30% [11].

3.2.11 Pulse Width Modulation

A pulse width modulated signal is often used to control servo motors. A PWM signal is usually a square wave. The parameter that corresponds to the value being expressed is the duty cycle. The duty cycle of a square wave is the ratio of the time the signal is on to the period of the signal.

$$Duty\ Cycle\ = t_{on}/T_{signal}$$

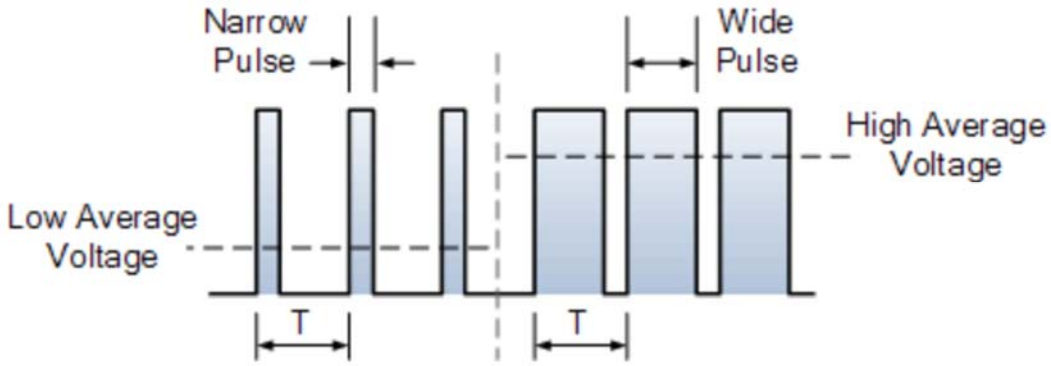

Figure 25: Pulse Width Modulated Waveform[18]
Permission Requested from: Arduino

In the case of PWM controlled servos, each duty cycle corresponds to a different position of the servo. When the duty cycle of the PWM signal changes, the position of the motor changes.

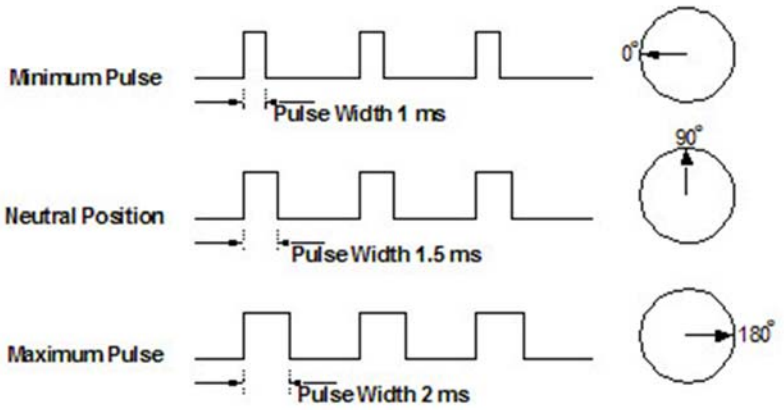

Figure 26: Servo Position vs Pulse Width
Permission Requested from: Arduino

3.3 Market Research

When designing our product, we must keep in mind our target consumer. This product could be utilized in a few different target demographics including the non-technical homeowner or the industrial solar farm. Often solar farms have the innate disadvantage of sheer size when it comes to repairing equipment that implementing our solar concentrator in a solar farm would prove costly in money and time if any of the components were to fail.

This led our gaze to the non-technical homeowner, which in recent years is a demographic that is experiencing significant growth. Namely, the solar investment tax credit (ITC) has provided the entire industry with substantial growth since 2006 in its initial passage. The ITC is a tax credit of 30% granted to solar systems on residential and commercial properties.

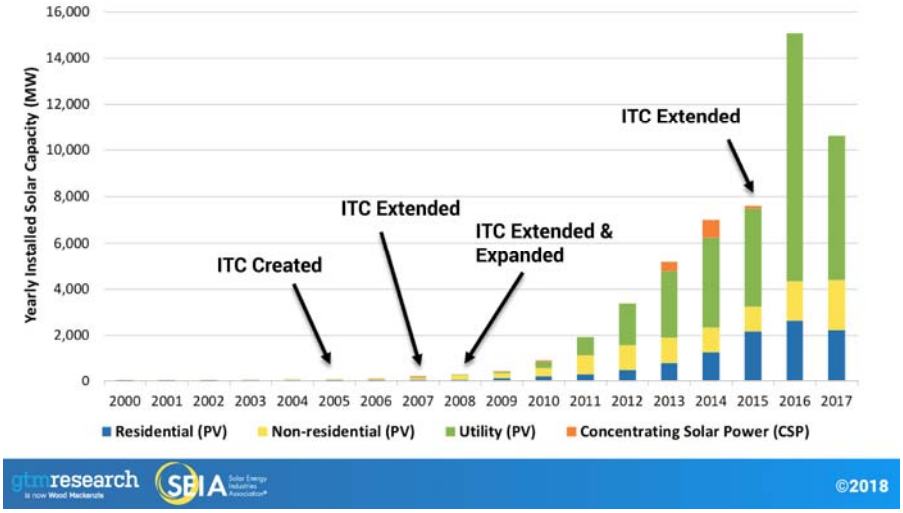

Figure 27: Yearly U.S. Solar Installations
Permission Requested from: GTM Research

The residential market for solar continues to diversify over time. Notably, California accounts for over 20,000 MW, while North Carolina sits in second with a little over 4000 MW cumulatively through 2017. The residential market however continues to diversify every year. We are seeing other states ramping up their solar installations as the price point for solar, including the soft costs of labor and maintenance drop.

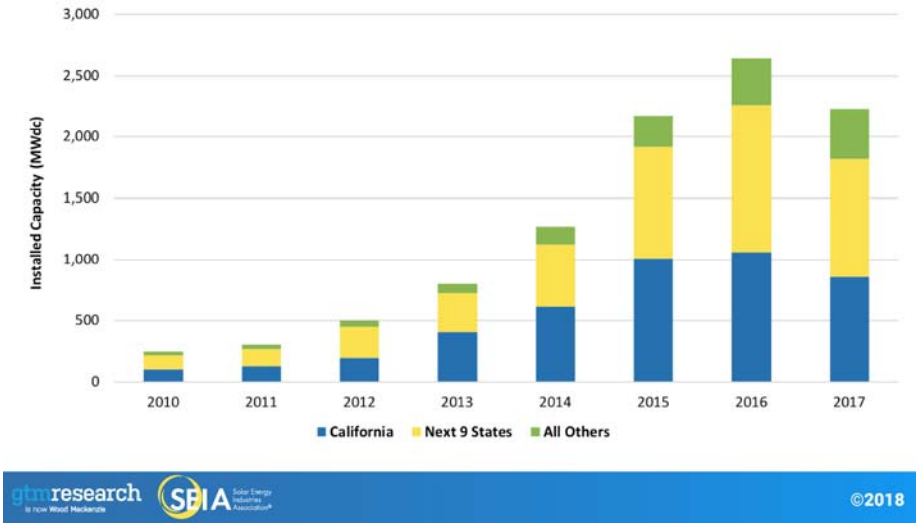

Figure 28: Annual Residents PV Installations
Permission Requested from: GTM Research

Currently, there is a small amount of concentrated photovoltaic systems in use, but this growth trend continues to grow. Two main sections break up the CPV market, namely low concentrated photovoltaic systems and high concentrated photovoltaic systems, which are used more frequently on solar farms due to their high efficiency, sometimes upwards of 43% by using some of the most efficient solar cells on the market: multijunction solar cells.

Presently, China has the largest CPV power plant in operation making Asia Pacific one of the leading markets for the global CPV market. Many CPV companies inside the US and Europe have had difficulty profiting due to the high cost in optics, but as prices drop, as the solar photovoltaic industry has continued to do, we will see a growth in successful CPV companies due to the inherit high efficiency unlike current photovoltaic systems. [25]

Some of the current companies in the US and European concentrated photovoltaic market are Ravano Green Powers (Italy), Sunpower Corporation (US), Suncoreus (US), and Soitec (France). The significant players for HCPV located in Asia include companies such as OPEL (China), Suntrix (China), and Everphoton (Taiwan).

3.4 Strategic Components and Part Selections

There are numerous parts and components that can be utilized to build our project design. This section includes a deep comparison of component options and lists the details of the parts that are being chosen.

3.4.1 Optical Components

This project requires the following optical components:

- One gradient index glass plate (n = 1.80 - 1.65)
- One gradient index glass plate (n = 1.65 - 1.59)
- One plexiglass plate (n = 1.585)
- Ten prisms with cross sections in the shape of a 30 - 60 - 90 cross section (n = 1.804)

The most difficult components to obtain are the gradient index glass plates. We were not able to make the ideal gradient index plate which would be n = 1.80 - 1.59, because we do not have access to the high temperature furnaces and crucibles required. However, early on in the project, we were able to obtain a gradient index plate (n = 1.80-1.65) from Lightpath Inc, a local Orlando company. The plate was manufactured using the molten glass batching method described in section 3.2.5. The acquisition of this plate influenced the design and selection of the rest of the optical components.

The top layer of the solar concentrator was selected next. Because the top layer is the thickest one, it contributes the most to the weight of the system. Therefore we knew we wanted use a plastic layer to reduce overall weight. Polycarbonate was selected because it has a high refractive index for a plastic. Any other plastic material would not work, because their index would be too low. Total internal reflection would occur at the interface between the gradient index glass and the plastic.

If the polycarbonate layer was mounted directly onto the gradient index plate obtained from Lightpath Inc, there would be unwanted Fresnel reflection causing a loss of 12% of the optical power. Therefore, we decided that a second gradient index layer was required that would be n = 1.65 - 1.59. We decided to fabricate the second gradient index plate using ion exchange, because it is much easier to make a gradient index plate with delta n of 0.6 than it is to make a gradient index plate with a delta n of 2.1.

To redirect the light toward the sides of the assembly, we decided to use prisms that are coated with a silver mirror. We decided to repurpose anamorphic prism pairs made of H-ZLaF2A glass. These prisms were chosen because they have a refractive index of 1.804. Silver was chosen because it has low reflection losses.

3.4.2 Solar Cells

When choosing solar cells for a solar concentrator the first parameter to consider is the level of concentration. For systems with high concentration, on the order of 100 suns and low cell surface area, it makes sense to use expensive highly efficient cells. In the case of our concentrator, our goal is to create concentration

of 6 suns. Because of this, we can modify solar cells that are intended for 1 sun for use with our system. According to A. Blakers, “the key requirements for such cells are:

1. High material quality with long minority carrier lifetimes
2. Good design of diffusions in order to minimize resistance and recombination losses
3. Excellent surface passivation
4. Good passivation of cell edges
5. Excellent reflection control and light trapping
6. Good design of metallizations in order to minimize optical and resistance losses” [21]

In the same paper, it is suggested that back contact solar cells created by Sunpower Corporation can be modified for use with linear concentrators. Since linear concentrators have similar concentration levels to the present device, our plan is to purchase and modify these solar cells. To use solar cells that are designed for non-concentrator applications with a concentrator, the contacts have to be reinforced so that they can handle higher currents. The strength of back contact solar cells is that reinforcing the positive and negative metal conductors on the back surfaces does not lead to additional shading losses.

When used in non-concentrator applications, these solar cells have efficiencies in the range of 21%. Under increased illumination, the efficiency typically drops, because of increased temperature. We expect that under an illumination of 6 suns, the efficiency will drop to somewhere between 14% and 18%.

Another option is to search for solar cells that are small enough to fit on the side of the solar concentrator and are high efficiency. In order to closely match the voltage of the battery and reduce the losses in the boost/buck converter, higher voltage solar cells were considered. Because of these concerns, solar cells from IXYS were considered. The considered part number is KXOB22-01X8F. These cells have a max power point voltage of 3.4 V and max power point current of 3.8 mA.

With the circuit arrangement shown in figure 29, the maximum power point voltage will be 3.4 V and the maximum power point current will be 22.8 mA. The problem with these solar cells is that they cannot handle the higher current that occurs when concentrated sunlight is incident on them.

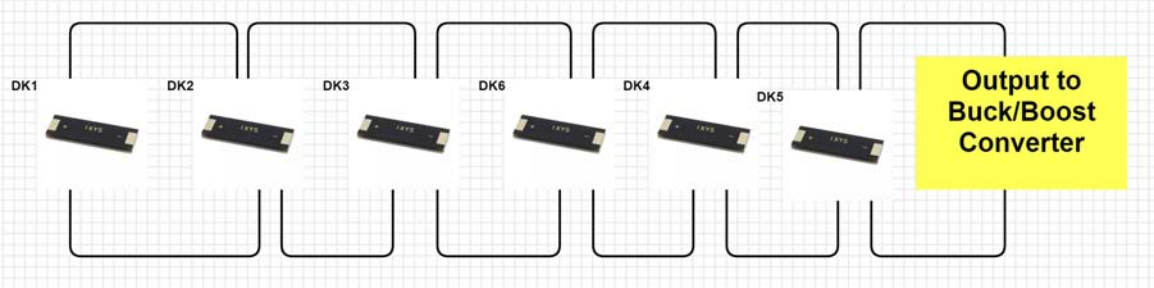

Figure 29: Solar Cell Circuit Diagram

The first option of using custom cut Maxeon solar cells manufactured by the Sunpower Corporation. These are back contact solar cells. Because they are custom cut, the voltage and current of the custom size cell is unknown until they are received. The current and voltage of each cell will be determined once they are received. The procedure for characterizing the solar cells is described in the testing section.

3.4.3 Microcontroller

For this project, we are building a custom PCB that contains a DC-DC buck-boost circuit as well as a microprocessor to handle MPPT calculations, servo commands, signals from sensors, and an open two-way communication to the mobile application for relevant information and commands. There are many microprocessors on the market to handle the number of calculations that we are requiring the device to complete. Cortex-M microcontroller cores are useful for a wide range of embedded applications, while Cortex-A and Cortex-R are more useful in high-performance applications, such as real time systems.

The Cortex-M series is built on the ARMv7-M architecture (used for Cortex-M3 and Cortex-M4), and the smaller Cortex-M0+ is built on the ARMv6-M architecture. The Cortex-M3 and Cortex-M4 are very similar cores. Each offers a performance of 1.25 DMIPS/MHz with a 3-stage pipeline, multiple 32-bit busses, clock speeds up to 200 MHz and very efficient debug options. The
significant difference is the Cortex-M4 core's capability for Digital Signal Processing (DSP). [19] Having the ability to handle DSP calculations would allow for more flexibility when determining other components of the solar concentrator system, as we would already have a built-in functionality to measure, filter, or compress continuous analog signals.

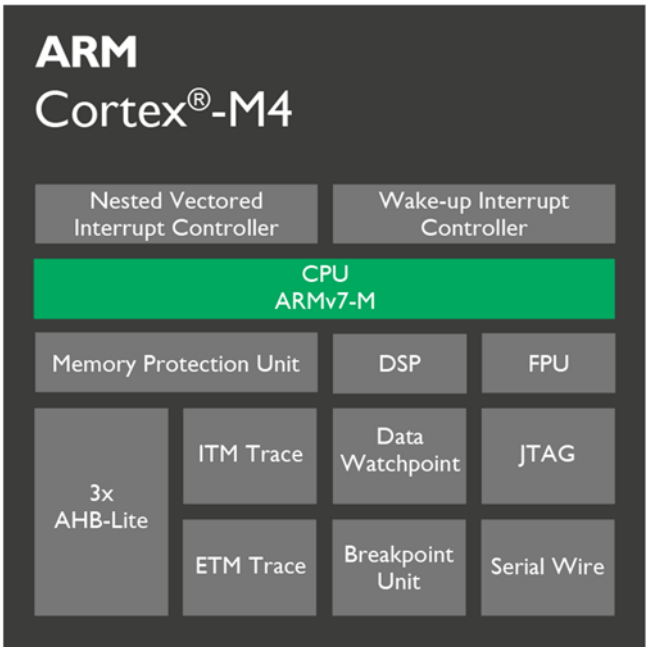

Figure 30: ARM Cortex-M4
Permission Requested from: ARM

The Cortex-M3 and Cortex-M4 has been gaining popularity as the need for simple autonomous living devices has increased. These cores are specifically designed to target this MCU market. More and more original equipment manufacturers (OEMs) are switching to a single, high-performance, low power MCU with DSP extensions, such as Cortex-M4 or Cortex-M7, to replace the common two processor design utilizing two low-power, low-performance cores such as the Cortex-M0+ or Cortex-M3. [19]

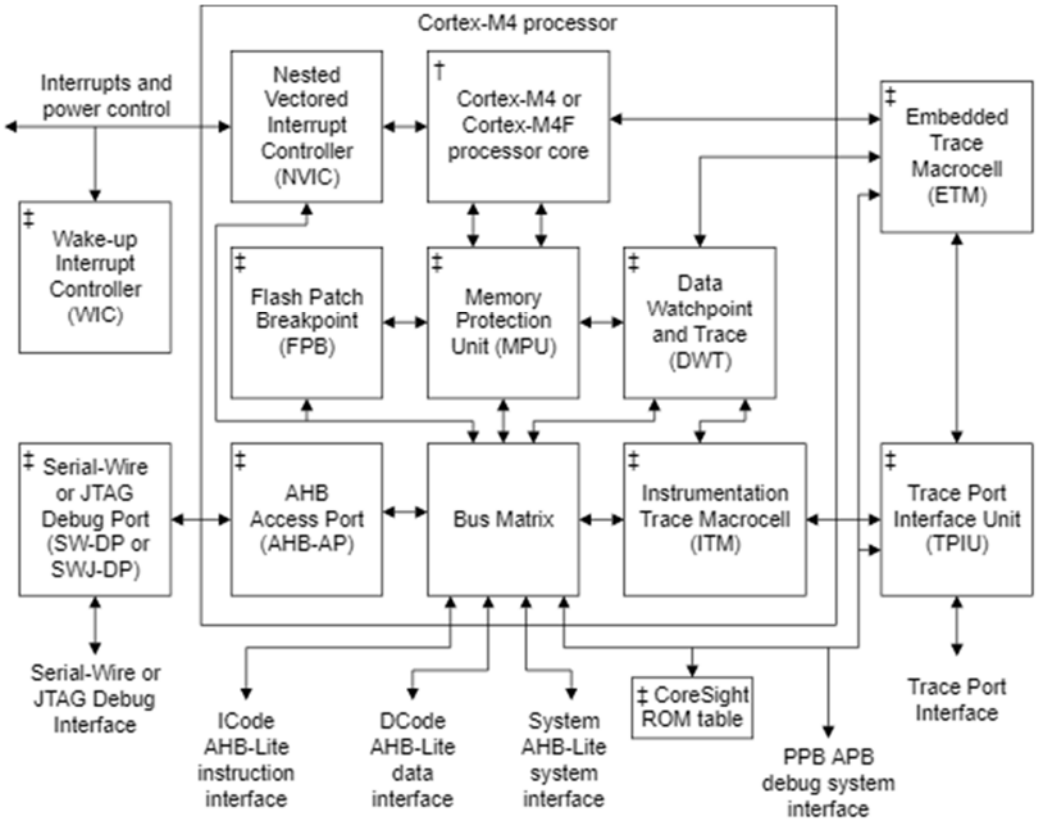

Figure 31: ARM Cortex M4 Block Diagram
Permission Requested from: ARM

Our design will require significant data communication via WiFi between the micro processing unit and the mobile application. This is required in order to send monitoring data updates and user controlled signals. When considering which chip to implement our software on, a number of single chip solutions arose. These choices are depicted in Table 6.

Table 6: Comparing Single Chip WiFi Enabled MCUs

Product	Manufacturer	Processor	ROM & RAM	Protocol	Cost
CC3200	Texas Instruments	ARM Cortex-M4 (80MHz)	None, 256KB	802.11 b/g/n	$10.66
CC3220	Texas Instruments	ARM Cortex-M4 (80MHz)	None, 256KB	802.11 b/g/n	$10.45
CC3220 MOD	Texas Instruments	ARM Cortex-M4 (80MHz)	1000KB, 256KB	802.11 b/g/n	$11.70
ESP8266	Espressif	Tensilica Xtensa L106 (80 or 160 MHz)	64KB, 64+96KB	802.11 b/g/n	$6.95 (Module)
MT7687	MediaTek	ARM Cortex-M4 (192 MHz)	64KB, 256+96KB	802.11 b/g/n	$8.64
RTL8195	RealTek	ARM Cortex-M3 (166 MHz)	1MB, 2.5MB	802.11 b/g/n	$23.99 (board)
RTL8711	RealTek	ARM Cortex-M3 (166 MHz)	512KB, 256KB	802.11 b/g/n	$4.35
CYW43340	Cypress	ARM Cortex-M3	512KB, 640KB	802.11 a/b/g/n	$6.00

Our main focus is in ARM technology, but while researching WiFi modules to handle the above described communication, the ESP8266 which features a Tensilica Xtensa L106 microprocessing unit was found to be a widely used MCU when it came to self-starter home automation projects.

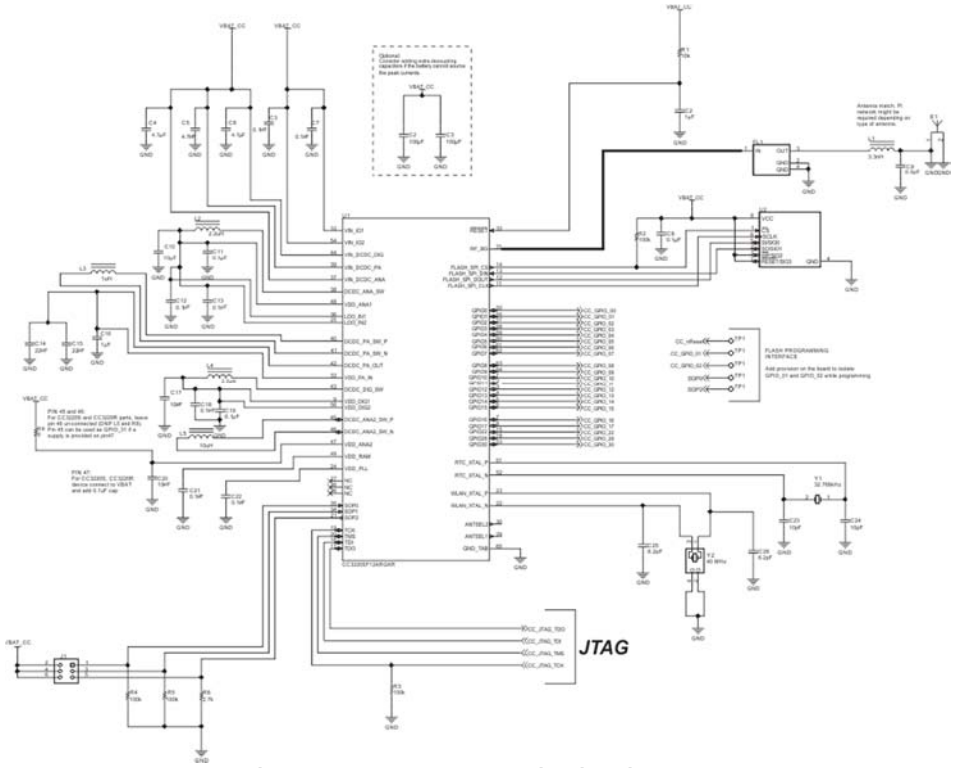

Figure 32: CC3220 Block Diagram
Permission Requested from: Texas Instruments

To design the circuit board, we are using EAGLE software and placing our components as needed on the board. The entire printed circuit board will contain all of the components needed to operate the solar concentrator device and transmit the corresponding data to the mobile application. In order to communicate with our mobile application, the microprocessor requires WiFi capability; therefore we have chosen to use the **CC3220** which integrates WiFi capability within the microprocessor. Rather than having a separate WiFi module on the board and creating an extra step in the communication protocol using I2C in order for the external WiFi module to read, we decided to use a more advanced chip to handle said protocol.

The module comes with TI's SmartConfig technology, which is a Wi-Fi setup process that allows the programmer to connect the MCU to Wi-Fi access point over an Android or iOS device.

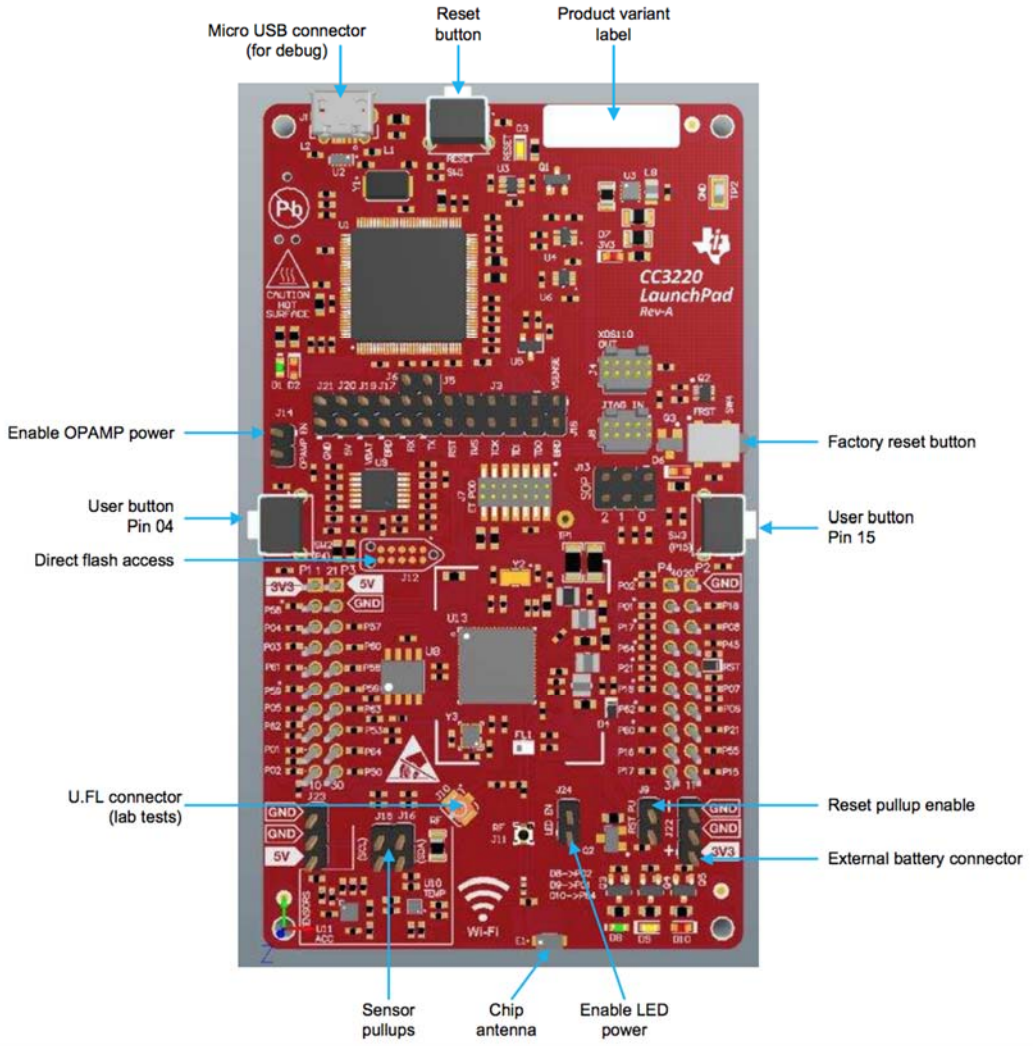

Figure 33: CC3220 Launchpad Overview
Permission Requested from: Texas Instruments

CC3220 Development board Features:

- Two separate execution environments
    - User application dedicated ARM Cortex-M4 MCU
    - Network processor MCU to run all Wi-Fi and internet logical layers
- Chip-level, Wi-Fi alliance Wi-Fi CERTIFIED
- Applications microcontroller subsystem
    - ARM Cortex-M4 Core at 80 MHz
    - Embedded Memory
        - 256 KB RAM
        - External serial Flash
    - McASP supports two I^2S channels
    - SD
    - SPI
    - I2C

- UART
- 8-bit parallel camera
- Four general-purpose timers with 16-bit PWM mode
- Watchdog timer
- 4-channel, 12-bit ADCs
- Up to 27 GPIO pins
- Debug interfaces: JTAG, cJTAG, SWD

Wi-Fi Capabilities

- IPv6 and IPv4
- Enhanced Wi-fi provisioning
- Enhanced power consumption
- Wi-Fi AP connection with up to four stations
- HTTPS support
- RESTful API support

Because we want to be able to transfer data and information over a network, there are security risks that come up that the user needs to know about in case there is an attack on the user's devices or software. Common exposure points for the devices are:

- Internet network connectivity
- Local network connectivity
- Physical access

The CC3220 MCUs come with a variety of built-in security features that reduce the risk of security attacks on the devices. The security features are listed below:

Table 7: Security Features

Security Feature	**Description**
Personal and Enterprise Wi-Fi security	802.11 standard-compliant security support (WPA/WPA2-PSK/WPA2-EAP)
Secure sockets	Transport layer security comply with SSLv3, TLS1.0/1.1/1.2. Support up to six secure sockets concurrently.
HTTPS server	Internal HTTPS server running on top of a TLS socket, with support for client authentication
Device Identity	Unmodifiable unique 128-bit number that TI stores in the device during production. It may serve as a unique device identity (UDID).

Secure key storage	On-chip asymmetric key-pair storage with built-in crypto acceleration and crypto services
Trusted root-certificate catalog	Built-in secure mechanism to ensure a CA is trusted as root of certificate chain for the purpose of TLS and for file signing.
Ti root-of-trust public key	The hardware-based mechanism that allows authenticating TI as the genuine origin of a given content (such as software service pack, trusted root-certificate catalog) using asymmetric keys.
File system security	File system security for confidentiality and integrity of data
Secure boot	Validate the integrity and authenticity of the runtime binary during boot (CC3220S and CC3220SF only)
Secure content delivery	Provides an end-to-end ability for delivering confidential information to the system independent of the security of the transport layer
Initial secure programming	Image integrity check and image confidentiality during programming, including system configurations and user files.
Debug security	Blocking the access to debug capabilities such as JTAG interface and file-by-file access from external tools
Software tamper detection	Detecting and alerting potential unauthorized manipulation of secure file content
Cloning protection	The file system is readable only by the device, which first booted this image.

3.4.4 Servos

To achieve a dual-axis solar tracker, we need to select two servos that can be controlled to rotate the solar panels from east to west from -60 degrees to 60 degrees and north to south automatically from 0 degrees to 55 degrees.. The servos we selected are the Adafruit standard, High torque, Metal gear servos.

Figure 34: Servos [37]
Permission Requested from: Adafruit

These servos are capable of rotating the solar panels. We chose these servos because they are capable of withstanding harsh weather conditions such as rain. Even though the servos would not be moving the solar panel when it rains, it's important that it would not get damaged in the rainy conditions. Table 8 shows the specification details for the servos we have chosen

Table 8: Technical Specifications for High Torque Metal Gear Servo

Power	4.8 - 6V DC max
Average Speed	4.8V: 60 degrees in 0.2 sec 6.0V: 60 degrees in 0.16 sec
Weight	62.41g
Torque	4.8V: 8.5 kg-cm / 120 oz-in 6.0V: 10 kg-cm / 140 oz-in
Size (Length x Width x Height)	40.7mm x 19.7mm x 42.9mm
Spline Count	25

3.4.5 Battery

Choosing between a lithium-ion and a lead-acid battery consists of many pros and cons. The lithium-ion battery provides a more compact energy storage solution, however they are generally more expensive than most battery solutions. The lead-acid option will be heavy and bulky, but they are much cheaper when energy storage capacity is compared. One major downside is the charge voltage level that the battery must be receiving in order to charge the battery. The solar cells used in the concentrator design will have a 12V maximum output. This applies a limitation to our battery selection as the lithium-ion battery should be charged at 4.2 ± 0.05 V/cell and the lead-acid battery should be charged at 2.30 to 2.45V/cell. Due to cost and charge voltage limitations, we chose to use a lead-acid battery.

According to the UT Institute of Agriculture, 1000 W/m^2. Since our device is 2cm x 2cm x 20cm, our maximum sunlight in one area is 4W. At its lowest efficiency, our solar cells will run at 14% efficiency, meaning that our approximate power output is around 0.54W. This is significantly low, however the device is small and more of a proof of concept than a full design, due to these constraints. The focal point of this design is in the functionality and viability of the solar concentrator, but due to the large cost of the optical elements, the functionality can be proven on a smaller scale in conjunction with a smaller battery. After these considerations, we were able to choose the correct battery applicable to our system.

Figure 35: EasyLander Battery 3.7V, 280mAh [38]
Permission Requested from: AliEpress

Using the battery comparison research, as well as size and budget constraints from our project design, we have determined to use a lithium-polymer battery of 3.7V and 280mAh. These batteries are designed for smaller toy products that require little power during use. For a preliminary battery choice, the EasyLander

3.7V, 280mAh battery (Model Number 501833) will be sufficient for the power output we are producing with the solar concentrator. This battery has a cycle life of 500-700 cycles and includes a built in PCB for charge, discharge and temperature protection.

3.4.6 Sensors

The following subsection covers the selection of the sensors used to detect the intensity of sunlight on the top face of the concentrator, as well as the sensors used to detect the temperature of the solar cells.

3.4.6.1 Optical Sensors

Comparison of photodiodes, phototransistors and photoconductors [23]. There are three optical sensors that we evaluated for use in this project were photodiodes, phototransistors, and photoconductors. Photoconductors are commonly made of Cadmium Sulfide and their resistance reduces as the light intensity increases. Photodiodes and phototransistors work via electron-hole pair generation within pn junctions. When comparing the performance of these sensors we considered linearity, stability, ruggedness and physical size. Because our application requires comparing different measurements to each other, linearity and stability were judged to be the most important properties. Ruggedness and physical size are important because the device is small as it is and a minimal amount of the aperture and absorber should be taken up by sensors.

Similar to transistors, phototransistors provide a gain to the initial light induced signal. This allows them to be used without external amplifiers at times. This application does not require amplification of the light signal, because the intensity is already high. The linearity of these devices is also limited which makes it difficult to compare values to each other. Cadmium Sulfide photoconductors also suffer from limited linearity so they were ruled out as well. Photodiodes, on the other hand, offer excellent linearity. They are also are quite compact and can be implemented with a simple circuit. A comparison of optical sensors is shown in Figure 36.

Table 1 - Comparison of Light Sensor Characteristics								
Electrical Characteristics	Photo-multiplier Tubes	Photo-diodes	Photo-transistors	CdS Photocells	Other Photo-conductors	Itegrated Circuits	Hybrids	Sensor Electronic Assembly
Available Wavelengths (µm)	0.2-0.9	0.2-2.0	0.4-1.1	0.4-0.7	2-15	0.2-1.1	0.2-15.0	0.2-15.0
Performance-to-cost ratio	Fair	Good	Excellent	Excellent	Fair	Fair	Fair	Good
Sensitivity	Excellent	Very Good	Very Good	Very Good	Very Good	Very Good	Very Good	Very Good
Linearity	Good	Excellent	Good	Good	Good	Good	Good	Good
Ambient Noise Performance	Fair	Very Good	Very Good	Very Good	Very Good	Excellent	Excellent	Excellent
Dynamic Range	Very Good	Excellent	Very Good	Good	Good	Very Good	Very Good	Very Good
Stability	Very Good	Very Good	Good	Poor	Fair	Very Good	Very Good	Very Good
Other Characteristics								
Reproducibility	Fair	Excellent	Fair	Poor	Fair	Very Good	Very Good	Very Good
Cost	High	Low	Very Low	Very Low	High	Medium	High	Medium
Ruggedness	Poor	Excellent	Excellent	Excellent	Good	Excellent	Very Good	Excellent
Physical Size	Large	Small	Small	Small	Small	Small	Medium	Medium
Ease of Customization	Poor	Easy	Fair	Fair	Poor	Poor	Poor	Fair
Cost of Customization	Very High	Low	Medium	Low	High	Very High	High	Medium
Lead time for Customization (weeks)	40	12	14	12	20	40	30	16

Figure 36: Comparison of Optical Sensors [23]
Permission Requested from: EG&G Optoelectronics

3.4.6.2 Temperature Sensors

Two types of temperature sensors were considered for this project, resistance temperature detectors (RTDs) and thermocouples. Resistance temperature detectors contains a material that changes resistance with temperature. [24] Different materials in RTDs offer different ranges of temperature sensing. A table of the temperature ranges are shown in Figure 37.

Material	Usable Temperature Range
Platinum	-450°F To 1200°F
Nickel	-150°F To 600°F
Copper	-100°F To 300°F
Nickel/Iron	32°F To 400°F

Figure 37: Temperature Ranges of RTDs
Permission Requested from: Pyromation Inc

In comparison, thermocouples contain two different junctions between two different electrical conductors. Each set of these two conductors is called a junction. One of these junctions is exposed to the area that is is to be measured and the other junction is kept away from it. The difference between these two temperatures creates a small voltage which can be used to infer the temperature of the measurement junction. Because our temperature sensor will be used outdoors, where the temperature of the whole system will be raised, thermocouples were deemed inappropriate, because they only generate a relative measurement. RTDs can measure absolute temperature and were therefore chosen. Given that we do not expect our solar cells to reach a temperature that is much higher than 70 degrees Celsius, it was determined that a Nickel/Iron RTD will be sufficient.

3.4.7 Software

To be able to make information on the solar concentrator accessible to the user as well as allow the user to establish control movement on the device, we've decided to build a mobile application that the user could download on their mobile device. There are multiple development platforms that come with tools and features that allow us to design the mobile application.

3.4.7.1 Android Studio

Android Studio is an IDE (Integrated Development Environment) designed specifically for developing Android applications. It comes with built-in features that are customized for Android developers such as:

- A Gradle-based build system that allows the programmer to build the application within and outside of the IDE.

- Included pre-existing project and code templates to make it simpler for the programmer.
- A layout editor that allows the software developer to insert and move components used in the user interface.
- A code editor that gives suggestions to the programmer
- Instant Run feature that pushes code to the app while it's running. Updates and changes are made immediately without having to restart the application.
- Android Emulator: A virtual Android device that can run and debug the application.
- Memory monitor to view the memory usage of the app over time.

3.4.7.2 React-Native

React-Native is a mobile development framework for building applications. It allows the software programmer to build a native mobile application, meaning that the application is built solely for a device and is not a web application (webpage). It is based on the React JS library, which is used to create web applications. Before, programmers would build mobile applications by using various technologies such as HTML (Hypertext Markup Language), JavaScript, and CSS (Cascading Style Sheets) to modify the view from a web application and display it on the device. React-Native applications are written using the JavaScript language. Some features of React-Native are:

- Use of JavaScript language which allows the programmer to essentially use the same code on iOS and Android devices, saving development time and cost.
- Live-reload feature that allows the programmer to see the changes made to the application immediately
- Uses the GPU (Graphics Processing Unit) instead of the CPU (Central Processing Unit) which hybrid technologies have been using before, thus increasing processing speed.

3.4.7.3 Code Composer Studio

Code Composer Studio is an integrated development environment used to develop and debug embedded applications for microcontrollers and embedded processors.

It includes:
- C/C++ compiler
- Source code editor
- Project build environment
- Debugger
- Profiler

Code Composer Studio also implements useful tools within the debugger to ensure proper memory management is enforced. For example, the step by step run feature used inline with the memory register display allows developers to see exactly where the data is being stored and at which step it is being processed. This results in easier and faster debugging.

4 Related Standards and Realistic Design Constraints

While developing our design, we must keep in mind standards and constraints that may limit or restrict the design to particular requirements. The following section outlines these related standards and design constraints.

4.1 Related Standards

The following section details related design standards for related hardware and software elements that we are including within the design. Each section hosts their respective standard(s) for the related topic.

4.1.1 Testing Photovoltaic System Standards

IEEE 1526 - Recommended Practice for Testing the Performance of Stand Alone Photovoltaic Systems [43]

The recommended practice for testing the performance of stand alone photovoltaic systems provides testing procedures to determine the performance of stand-alone photovoltaic (PV) systems, and also for verifying the design of the PV system. The standards for this practice are that complete solar systems with a defined load are only allowed to be tested and performance testing must be done in an outdoor setting under the current weather conditions over a period of about one month. These tests are intended to assist designers, manufacturers, system integrators, system users, and laboratories that will conduct the tests.

4.1.2 Solar Cell Standards

In 1976, Florida passed the Solar Energy Standards Act [15]. Under this act, the Florida Solar Energy Center is responsible for certifying all PV systems sold or manufactured in Florida. Manufacturers must apply to have their samples tested by the Florida Solar Energy Center. The center may revoke or suspend an approval of a PV system if any of the following occur:

- “Deliberate misrepresentation of documentation submitted in the application for design review and approval”
- “Claiming that one PV system approval applies to another system which has not been approved”
- “Failure to comply with a condition of approval or product labeling”
- “Failure to correct a discrepancy that is detected by the Florida Solar Energy Center after initial approval. The supplier is given 30 days in which to make the correction”

4.1.3 WiFi Communication

IEEE 802.11 is a family of WiFi communication standards set describing a series of half duplex over-the-air modulation implementation techniques that use the same protocol for wireless local area networks in the 900, 2.5, 3.6, 5, and 60 GHz frequency band.

Besides this, there isn't a "standard" for the communication protocol used, however the most commonly used are Transmission Control Protocol (TCP) and User Datagram Protocol (UDP). Some would argue that this is a standard network layer protocol as they are practically the only two used.

ANSI/IEEE 802.11-2007 - IEEE Standard for Information Technology - Telecommunications and Information Exchange Between Systems - Local and Metropolitan Area Networks - Specific Requirements - Part 11: Wireless LAN Medium Access Control (MAC) and Physical Layer (PHY) Specifications

4.1.4 Low Power Integrated Circuit Standards

IEEE 1801-2013 - IEEE Standard for Design and Verification of Low-Power Integrated Circuits

This standard is used to specify the power intent for an electronic design, for use in verification of the structure and behavior of the design in the context of a given power management architecture, and for driving implementation of that power management architecture. The method supports incremental refinement of power intent specifications required for IP-based design flows.

4.1.5 Battery Standards

IEEE 937 - IEEE Recommended Practice for Installation and Maintenance of Lead-Acid Batteries for Photovoltaic Systems [41]

This standard describes the design considerations and procedures for "storage, location, mounting, ventilation, assembly, and maintenance of lead-acid secondary batteries for photovoltaic power systems are provided". There are many safety precautions and instrumentation considerations included in the standards. Even though general recommended practices are covered, battery manufacturers may provide their own specific instructions for battery installation and maintenance.

IEEE 1013 - IEEE Recommended Practice for Sizing Lead-Acid Batteries for Stand-Alone Photovoltaic Systems [42]

This standard mentions a method for determining the energy-capacity requirements (sizing) of both vented and valve-regulated lead-acid batteries used in terrestrial stand-alone photovoltaic (PV) systems is described.

IEEE 1561 - Guide for Optimizing the Performance and Life of Lead-Acid Batteries in Remote Hybrid Power Systems [44]

Using the information provided in this guide, the performance and life of the lead-acid battery can be optimized for the particular operational strategy selected for the remote hybrid power system. The information provided is intended for use by remote hybrid system designers, system evaluators, owners and operators.

IEEE 1562 - Guide for Array and Battery Sizing in Stand-Alone Photovoltaic Systems [45]

A method for properly sizing the PV array and battery for stand-alone PV systems where PV is the only charging source is recommended (in conjunction with IEEE Std 1013(TM)). Load calculations and determination of solar radiation in the sizing of the system need special attention. Additionally, the critical nature of the load in deciding an acceptable annual availability needs to be considered.

IEEE 1661 - Guide for Test and Evaluation of Lead-Acid Batteries Used in Photovoltaic (PV) Hybrid Power Systems [46]

This guide is specifically prepared for a PV/engine generator hybrid power system, but may also be applicable to all hybrid power systems where there is at least one renewable power source, such as PV, and a dispatchable power source, such as an engine generator. Taper-charge parameters for PV hybrid systems are suggested to help in preparing the battery for a capacity test. A test procedure is provided to ensure appropriate data acquisition, battery characterization, and capacity measurements. Finally, a process to review test results and make appropriate decisions regarding the battery is provided. No cycle-life predictions are made.

IEEE P2030.3 - Draft Standard for Test Procedures for Electric Energy Storage Equipment and Systems for Electric Power Systems Applications [47]

This standard applies to applications of electric energy storage equipment and systems (electric energy storage equipment and systems, ESS) for electric power systems (electric power systems, EPS). It provides the testing items and procedures, including type test, production test, installation evaluation, commissioning test at site and periodic test, in order to verify whether ESS applied in EPS meets the safety and reliability requirements of EPS. This standard is established for users including grid operators, ESS manufactures and ESS operators.

This standard establishes test procedures for electric energy storage equipment and systems for electric power systems (EPS) applications.It is recognized that an electric energy storage equipment or systems can be a single device providing all required functions or an assembly of components, each having limited functions. Components having limited functions shall be tested for those functions in accordance with this standard.

4.1.6 Software Testing Standards

ISO/IEC/IEEE 29119 - ISO/IEC/IEEE International Standard - Software and systems engineering —Software testing [48]

The purpose of the ISO/IEC/IEEE 29119 series of software testing standards is to define an internationally-agreed set of standards for software testing that can be used by any organization when performing any form of software testing. ISO/IEC/IEEE 29119-1 facilitates the use of the other ISO/IEC/IEEE 29119 standards by introducing the concepts and vocabulary on which these standards are built, as well as providing examples of its application in practice. ISO/IEC/IEEE 29119-1 is informative, providing a starting point, context, and guidance for the other parts.

4.2 Realistic Design Constraints

This section covers constraints that have arisen while researching and developing our project.

4.2.1 Economic and Time Constraints

Time constraints are made to ensure that the research, prototype development, implementation and testing are finished in time of the project presentation deadline, which is December 2018. Research and part selection are projected to be completed at the end of the Senior Design 1 course in May 2018. Manufacturing of the PCB, single axis tracker, and software design should be completed in Senior Design 2 by Fall 2018, which will allow time to test the hardware and fix errors before the project presentation deadline. These time constraints are made so that there is a sufficient time period to add, remove or change any component that we think will provide better results or meet the deadline period.

The biggest economic constraint is the cost of the optical components. A pair of prisms costs $55 and each prim is only 1 cm by 1 cm. The smallest solar cells available are 0.7 cm by 2.2 cm. It will require 40 prisms to make a concentrator with dimensions of 2 cm by 20 cm. Forty prisms will cost $1100. Due to the high cost of the prisms and other optical components, the size of the solar concentrator prototype severely limited

4.2.2 Manufacturability and Sustainability Constraints

An ideal way to manufacture the solar concentrator is using molten batching with a custom platinum crucible in the zig-zag shape required. Multiple types of glass would be melted and then placed in the crucible. The higher density glasses will sink to the bottom of the mixture (into the zig-zag mold.) The textured side of the cooled glass would then have a mirror deposited onto it. The assembly would then be glued to a polycarbonate plate. The single gradient index component could be much thinner than the multiple gradient index and prism assembly that has been planned for the prototype.

Sustainability of electrical design being in an outdoor environment
Weatherproofing any electrical components

4.2.3 Environmental, Health and Safety Constraints

One of the health concerns related to the solar concentrator is the lead that is contained within the high index glass. Leaded glass is common in CRT monitors and TVs [16]. Recycling leaded glass is far more difficult than recycling normal soda lime glass, because removing the lead is very difficult doing so creates toxic air conditions. For the purposes of this project, Lightpath Inc has offered to recycle our leaded glass for us. If this project was ever scaled up, the manufacturers of the solar concentrators would have to offer a glass buyback program to alleviate the recycling problem.

4.2.4 Ethical, Political, and Social Constraints

In general, solar energy is perceived positively in social and ethical constraints. Besides the minor concerns about leaded glass that many optical systems share, this system is much like any other solar energy system ethically and socially. Politically, however, solar energy is at some risk. The public failures of previous solar energy projects such as solar roads and solyndra have tarnished the good reputation that solar energy had. Because of this history, it is important for anyone presenting a project about solar energy to present it clearly and honestly. All claims should be back up with experimental data and should not be exaggerated in any way.

5 Project Hardware Design Details

This section contains any and all design details related to hardware components of our design. This includes drafts of design architectures and detailed descriptions of hardware components and how they interact with each other.

5.1 Initial Design Architectures and Related Diagrams

Throughout the planning phases of our project, the initial design of the solar concentrator sun tracking hardware used two linear actuators mounted from the base to two adjacent edges of the device. These linear actuators would extend and retract, and subsequently the angle of each axis would increase and decrease as shown in Figure 38. Originally, the design was much larger than the current plan, and therefore we required a large amount of force to rotate the concentrator around both angles, especially in the East and West directions, as this axis sees the most action throughout the lifetime of the device.

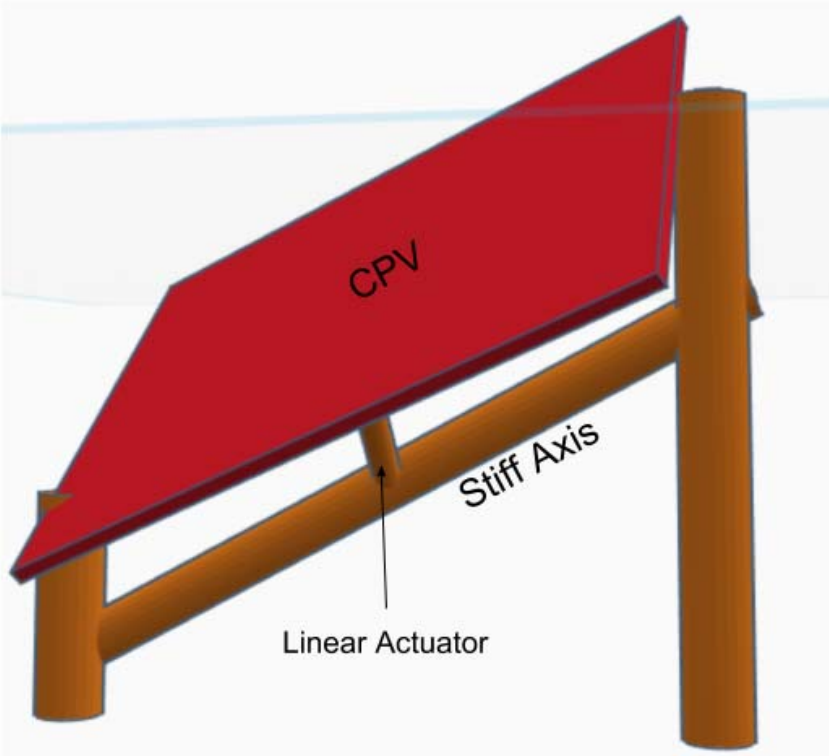

Figure 38: Preliminary Tracking Hardware

This design proved obsolete after calculating the actual dimensions of the device, which resulted in a much smaller profile due to the high cost of the optical components. This new design required less force to rotate on the axes in question; therefore, we shifted our focus to research low power servos and designs that would be able to rotate axles attached to the concentrator. When thinking small

devices, toy servos immediately stood out, but another constraint arose. The weight of the device is significant due to the thick layers of glass atop the optical elements. Due to these constraints, the servos must be able to move small dense objects, which led us to the final design plan for mounting and rotating the concentrator.

In regards to the microcontroller, the initial plan was to use a 4 switch buck-boost circuit as a DC-DC converter to control and maintain the maximum power point of the solar cell. The switching required for this design proved to be more complicated using a custom microcontroller. This evolved into the current design which controls the signal using a pulse-width modulated signal from the CC3220 microprocessor sent to the gate of an N-type mosfet. This acts as a switch for the maximum power point tracking to control the amount of power flowing and stored within the inductor of a modified buck-boost circuit.

It is important to note, that this new circuit design also bucks the voltage down from 12V to 3.7V and uses this drop to increase the flow of current into the battery. In addition, the obvious form of communication to the mobile device was WiFi, so this element made the cut in the initial design. Due to a recommendation on the CC3220 microprocessor, this device also made the cut early into the design.

5.2 Solar Concentrator

As described in section 3.4.1, the solar concentrator consists of 4 different components, a plexiglass plate, two gradient index plates and an array of prisms that are adhered to the bottom gradient index plate. Two optical principles are used to concentrate the light, refraction and specular reflection. Ideally, the light enters the polycarbonate layer at a 90 degree angle, passes through all layers and is reflected by the silver coated prism such that it forms a 60 degree angle with the normal. Then, the light will pass into progressively lower refractive index materials which will increase the angle it forms with the normal. Given the prism index of 1.804, the angle that the light makes with the normal in the polycarbonate (n = 1.57) can be found using snell's law:

$$Theta_f = sin^{-1}(1.804 * sin(60)/1.585) = 80.29$$

As described in section 3.2.3, the concentration factor is the ratio of the area of the aperture to the area of the absorber. In the case of this concentrator, the area of the aperture is the area of the plexiglass layer and the area of the absorber is the area of two of the sides of the plexiglass layer. The thickness of the plexiglass layer is determined by Theta_f and the length of the concentrator, because layer must be thick enough for light reflected on either end to pass to the other end without passing back into the gradient index material. For example, if the concentrator is 22 cm long and Theta_f is 80.29, the plexiglass layer thickness can be calculated as follows:

$$t = 22/tan(80.29) * (1 / 2) = 1.88\ cm$$

If the width of the concentrator is 2 cm, the aperture area is 44 cm^2 and the absorber area is 7.52 cm^2. The concentration factor can be found as follows:

$$C = A_a/A_{abs} = 5.84$$

The optical losses in the design will mostly come from absorbance in the silver mirrors and losses due to Fresnel reflection because of small differences in the refractive indexes. It is important to note that the closer the refraction angle gets to the critical angle, the greater the loses to Fresnel reflection becomes. Therefore, it is more important for the differences between the indexes of adjacent layers to be lower closer to the top of the stack.

5.3 MPPT Circuit Design

As described in the above research sections, the maximum power point tracking system is implemented using a buck-boost circuit design, taking advantage of a NMOS switching device to control the flow of energy through the inductor. In addition, the maximum power point tracking algorithm located on the CC3220 microprocessor utilizes a hill climbing algorithm to determine at what impedance the circuit should hold to match the internal impedance of the solar cell system.

As shown in Figure 39, the maximum power point circuit design has the form of a pulse width modulated and NMOS controlled gate switch that regulates the current entering the inductor. As the pulse is given, the n-type mosfet allows signal to pass from the drain to the source. This fills the inductor with current, and as the pulse turns off, the inductor releases the stored current into the right side of the circuit. The occurs since the pulse signal is no longer provided, removing the connection to the left side of the circuit. The 470uF capacitance is one of many capacitors that can regulate the voltage entering the battery, to ensure that the voltage is one of sustenance for the battery to enter the charging phase.

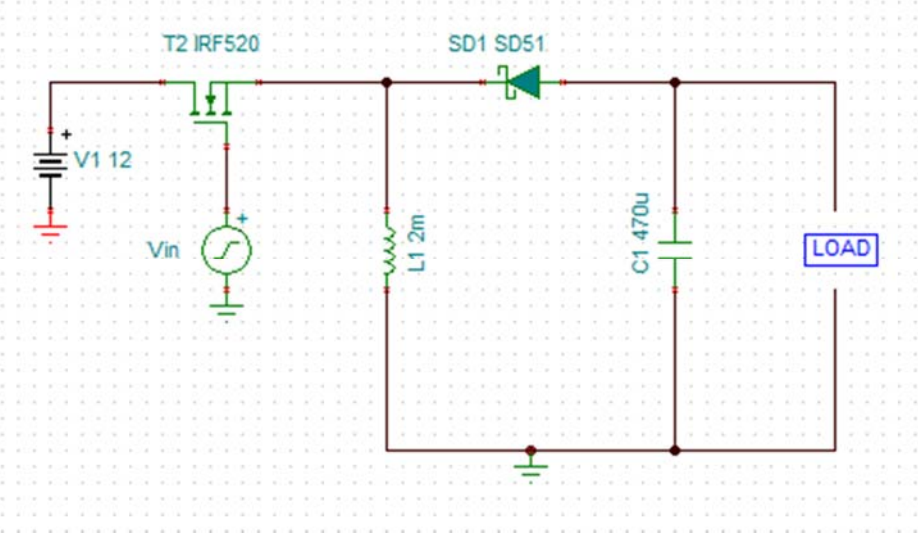

Figure 39: MPPT NMOS Gate Switching Buck Converter

5.4 PCB Design

The role of the microcontroller can be broken up into many different sections. At the top level of discussion, the microcontroller should get sensor readings from the device in order to determine the angle of rotation, calculate the maximum power point using the buck boost DC-DC converter, and manage communication between the device hardware peripherals and the mobile application.

In order to design a system as such, a custom PCB will be utilized for all of the maximum power point circuitry as well as the microprocessor traces. The PCB will be designed using a circuit board creation software, such as Eagle PCB Design by CadSoft. One major requirement specification we are attempting to achieve is to fit these elements onto one board for durability and sleek appearance. Too often is the solar market flooded with complicated hardware that needs interfacing. This may increase the cost factor as the PCB will be larger, so these constraints will be weighed as the factors are laid out more concretely throughout development. Due to the high number of traces off of the PCB for pulse width modulated signals and sensor readings, this one PCB design may prove to be even more challenging.

It is important to take note of the signals required when designing the PCB. Shown in Table 9 are the maximum possible analog signals required for the project thus far. These may be cut down due to limited ADC channels on the CC3220. Another solution may be to multiplex these signals, and reduce the sampling rate, as the sampling rate of the CC3220 is fixed, and indeed well above the minimum sampling rate we would require to account for weather changes. Note that the time to calculate the maximum power point should be kept under 5 seconds; therefore reducing the sampling rate by a factor of four, for example, would theoretically quadruple the time it would take to calculate the maximum power point.

Table 9: All Possible Analog Signals

Sensor	Function	Location	Frequency
Optical Sensor	Determine tilt	Top-face	3-4
Optical Sensor	Non-CPV Comparison	Top-face	2
Temperature Sensors	Monitor internal temperature	Inside each cell	2
Voltage Sensors	Monitor voltage	Solar cell, battery	2
Current Sensors	Monitor current	Solar cell, battery	2

5.5 Solar Tracking

The solar tracking system design is based around multiple control options that allow different forms of control for the solar concentrator device. These control options will be further known as modes. The solar tracking system we are implementing has three different modes that it could be in. These modes and their control signals are described in table 10.

Table 10: Device tracking methods

Mode	Name	Controlled
Mode 1	Sunlight Tracking	Sunlight sensors
Mode 2	Absolute Position	Latitude, Longitude
Mode 3	User Determined (Manual)	Mobile application

The default mode is dual-axis sunlight tracking. This is implemented using a pinhole and an quadrant photodiode (QPD) as shown in Figure 40. The light enters a pinhole and depending on the angle of incidence it hits a different quadrant of the photodiode. Using the output of the QPD, the microcontroller calculates the new adjusted angle that the concentrator should move to, and creates a PWM signal that is sent to the servos in order to maintain this angle. The new adjusted angle is calculated by the microcontroller by moving the concentrator towards the sensor with the highest intensity using a threshold of change to ensure that the solar concentrator system isn't wasting power or computing time on miniscule changes in the sunlight readings from the corner sensors.

The fallback mode is a tracking algorithm that calculates the position of the sun based on the latitude and longitude of the device. From these variables and the

time of day, we are able to estimate the position of the sun in the sky, bypassing the need for a sunlight sensor on the top face of the concentrator. This method is only to be used when the sunlight sensor readings do not fit the constraints of the first mode/algorithm. For example, if the top face sunlight sensor is producing readings that are outside of the normal boundaries of the signal, then we should revert to another method, since the current sensor mode isn't behaving appropriately. This may happen in the scenario that the sensors stop working or are disconnected. In this situation, we would like to notify the user of the reason of the algorithm switch, displayed in a readable format that is easy to understand.

The third mode is a dual-axis user controlled mode that allows the user to turn off the first two modes and take over in setting the specific angle at which the solar concentrator should be set. In this mode, the user will have a screen on the mobile application to set each axis at a particular angle and submit the request to the concentration. The information is then sent over WiFi to the microcontroller that checks for and accepts these requests in the main communication loop (namely in the checkForUpdatesFromMobile(); function in our pseudo code example above). These signals are then translated to a PWM signal that is connected and sent to the respective servos to rotate the solar concentrator along those axes.

5.5.1 Solar Position Sensor Systems

In this section, we will compare two different designs that will detect the position of the sun. These devices are necessary when the device is in sunlight tracking mode. The two designs considered are a quadrant photodiode (QPD) pin hole setup and a 2x2 light detecting resistor array. These designs are shown in Figures 40 and 41. Quadrant photodiodes are very accurate position sensors that are often used to measure the position of the spot of a laser. To use them to detect the position of the sun, we can put the QPD inside a cylinder with a pinhole in the top. The sunlight will pass through the pinhole and depending on the angle of incidence, it will be incident onto a different quadrant of the QPD. The problem with this setup is that the angle of acceptance is limited if the distance between the pinhole and QPD, L, is large. If L is reduced, the percision of the device is reduced as well.

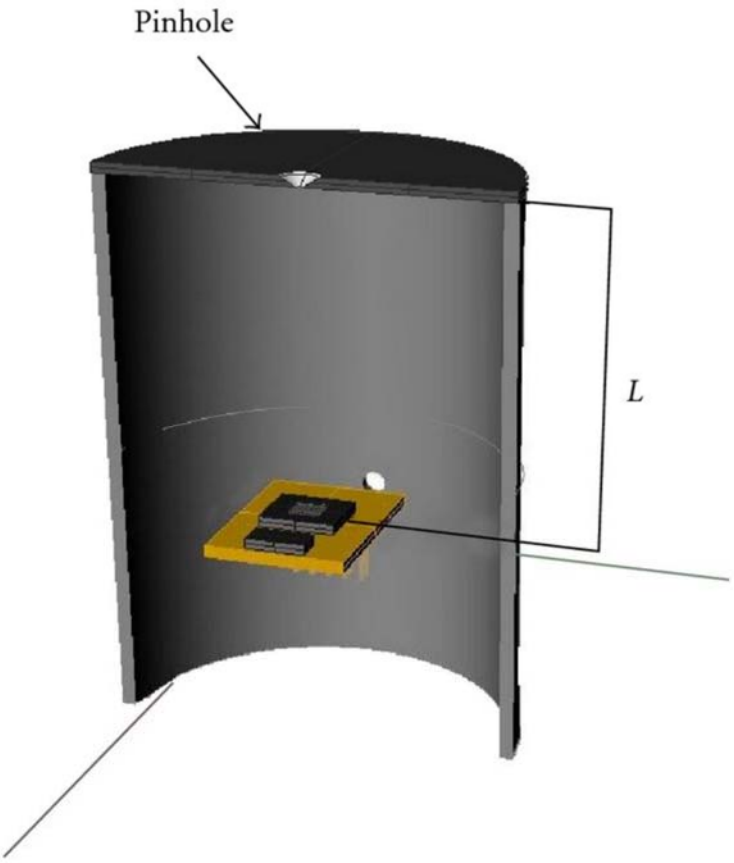

Figure 40: Pinhole and Quadrant Photodiode Position Sensor

In contrast, the array of LDRs functions by placing large walls between the LDRs in the array. If the device is not directly facing the sun, these walls will cast a shadow onto one or more of the LDRs. When that happens, the device can adjust the angle until it is facing the sun. The problem with this setup is that the accuracy is limited by angle that is formed by the base, the LDR, and the top of the wall. Compared to the QPD and pinhole setup, this one is much better at getting the device to point toward the sun in a general way, but it is unable to make fine adjustments to reach the precise 90 degree angle required.

After considering these two tracking systems, we have decided to use the pinhole and QPD system for precision adjustments in conjunction with a latitude and longitude based estimate to make the coarse adjustment. Further work needs to be done to find the optimal L for this application, because the trade off between precision and acceptance angle is important.

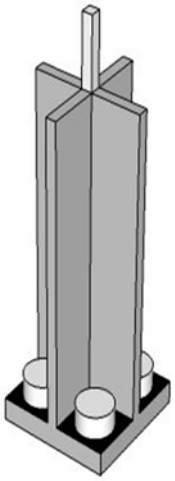

Figure 41: LDR Position Sensors

5.6 Base Design with Servos

The base servo design we wanted to create had to be able to have the solar panel mounted on top of it, be able to hold both servos, and rotate in the desired range that we had chosen. After thorough research, we found a pan and tilt bracket designed by Karlsson Robotics that we can mount the servos on. There is a place on the mounting bracket where the solar panel can be placed. A diagram of the mounting bracket is seen below.

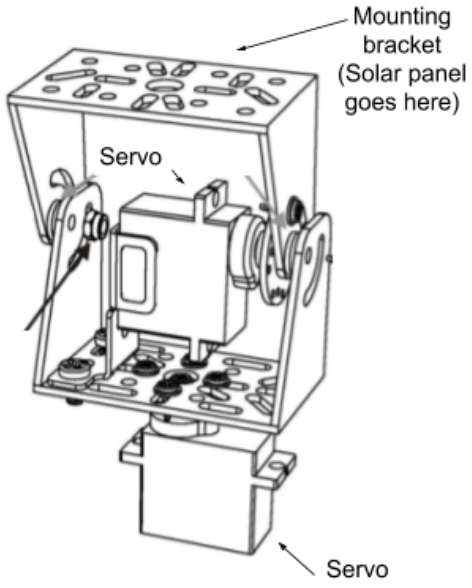

Figure 42: Solar Tracking Mechanism [32]
Permission Requested from: Karlsson Robotics

This design, in comparison to other multi-tiered axis designs, provides a smaller profile for the shape of the concentrator to mount on. Other designs we considered had two outer rings of axis control, which during our planning stages proved to be too bulky. This design allows for rotation around a point as well as tilt on that point, giving us the two axis feature that we desire

5.7 Summary of Hardware Design

As a whole, the hardware components are comprised of a few notable topic areas. The solar concentrator described above functions as the optical redirect for the solar energy and interfaces with the solar cells on the side of the device. The solar cells are then connected to the microcontroller, in which the signals are routed to the maximum power point tracking circuit to step down the voltage and step up the current to a manageable level. This resulting signal is placed over the battery load to charge the battery. In addition to this main energy flow, optical sensors described above placed on the top face of the solar concentrator dispel signals that are utilized by the microcontroller to rotate and tilt the device to face the sun at the optimal angle.

These electrical hardware components will all be housed within a weather-proof electronics box, and sensor cables will be routed in a safe and secure manner to the microcontroller.

Due to these additional electrical components such as the microcontroller, servos, etc. that require more power than the proof of concept level output from the solar concentrator, an additional battery bank will be included to run the hardware necessary. It is import to note that on a larger scale solar concentrator, these elements will not need to be increase while scale increases. Therefore they are a fixed cost, as opposed to the optical elements that will vary as scale increases. The battery bank will consist of a relatively large (2000mAh for testing purposes) battery to power the microcontroller at 3.6V, the servos at 5V and the sensors at their respective voltage described in Section 3. These additional elements will require a DC-DC converted similar to the buck-boost circuit described in Section 3, however in the low power case, the voltage will be bucked down (reduced) while the current remains the same. This design is known as a step down circuit or a transformer.

6 Project Software Design Details

The software side of the solar concentrator will be implemented on the breadboard, single axis tracker, and MPPT. A mobile android application will be created that will take readings from the sensors attached to the PCB board via a built-in wifi chip on the board and will output a variety of data information onto the android phone of the user. The main tasks of the mobile application are to provide the user access to output energy readings of the solar concentrator, display the status of the direction of the solar concentrator, and allow multiple tracking modes for the user to choose from.

6.1 Software Design Overview

This section pertains to the software side of the design project. The functions that will be created to operate the solar concentrator, retrieve information and display statistics to the user are mentioned here. The following topics will be discussed:

- Mobile application design and features
- Connecting between mobile application, server, and Microcontroller via Wi-Fi
- Programming microcontroller to read, store and send values to mobile application

As shown in Figure 43, the microcontroller will store data on the server and the android app will read data from the server. The data stored will be power generation readings at a given time, tilt status, and battery level.

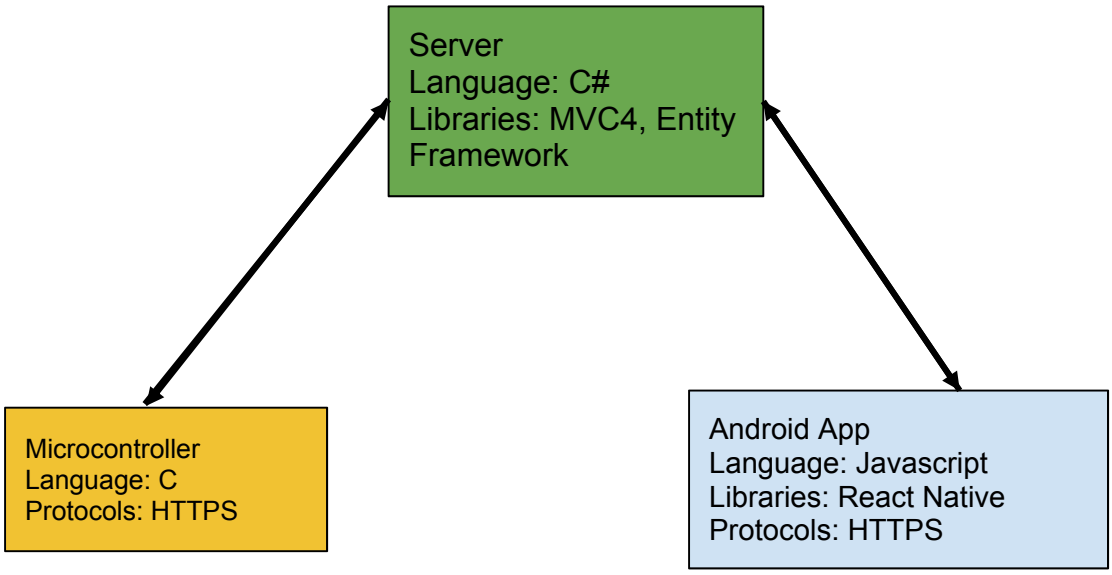

Figure 43: High Level Architecture

6.2 Mobile Application Design

The mobile application that we chose to go with is React Native. React Native is an application that allows the software engineers to build mobile apps using only JavaScript. It uses the same fundamental UI building blocks as regular Android applications. The mobile application is going to be the information hub for the user to understand how their solar device is operating, how it is saving them money on their electricity bill, and how they can make modifications to ensure that the solar device is performing to its best of its ability.

React Native uses the Fetch API for networking properties. It will request data and information over the network and retrieves a response to the request. The requests may come when the user selects one of the options, periodically throughout the day, or indefinitely.

6.2.1 Primary Features of Mobile Application

These are the features of the software that are going to be made available to the user so they can interact with their solar device.

6.2.1.1 Power Generation

Purpose: To monitor the photovoltaic energy generated from the solar concentrator. This part of the mobile application reads in the voltages from the board and outputs how much power has been generated. When the user selects the “show power readings” on the application, the application will output the current energy being generated by the solar tracking device. The power generated will be measured by day, month, year, and lifetime. The data will be displayed on a power vs time graph. The time the solar panels are running will be recorded and displayed on the x axis and the power that is generated from each the solar cells will be displayed on the y axis. There will be multiple tables that show the power generated over the course of the day, week, year and lifetime.

The mobile application will be saving the energy readings periodically throughout the day. Each hour the amount of energy generated (in kWh) will be saved in a variable. Since there are only a certain amount of hours that the sun is out throughout the day, there will be a certain amount of variables that will store the energy generated at that hour. The graph will show the amount of energy being generated between 7AM and 7PM, a 12-hour window. Each hour added through the day will add on to the graph. At the end of the day, the total amount of energy generated will be saved in another variable, called “dayX”, X being the day in the month (ex: day17 will be the 17th day in the month). At the end of the month, the

total amount of energy generated by the solar tracking device will be stored in a variable, called “monthX”, X being the month of that year. The monthly graph will show the amount of energy generated each day of month. The yearly graph will show the amount of energy generated each month. The overall amount of energy being generated will be stored in another variable that will be used to calculate the payback time that it will take for the user to start earning a profit from the systems. The graph below is the solar power generated vs time graph (time is in hours). A preliminary version of the power generation vs time user interface is shown in Figure 44.

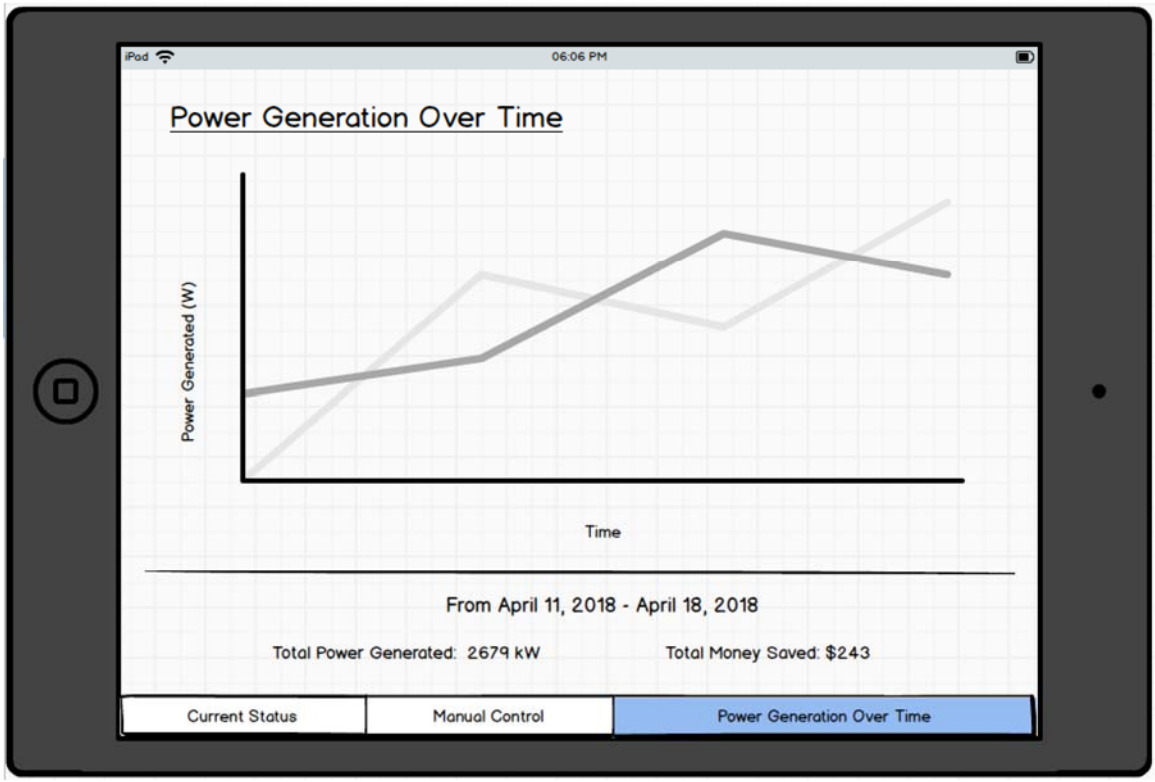

Figure 44: Power Generation Over Time User Interface

6.2.1.2 Battery Charge

The purpose of this feature is to display the current charge level of the battery. Using this indicator, the user can monitor how effective the system is at generating energy. The initial capacity of the battery will be stored stored as a constant in the application. By comparing the level of charge that the battery is at current, the battery charge level can be calculated.

$$battery\ charge\ = \frac{current\ charge\ level}{capacity\ of\ battery}$$

This battery charge level will be shown as a percentage when requested by the user. If the user wishes, a notification will be created when the battery is fully charged.

6.2.1.3 Current Tilt Status

The purpose of this feature is to inform the user about the direction the solar concentrator is facing. Since the solar tracker has the ability to track the movement of the sun, having this data available to user will allow them to know how the concentrator is facing the sun and if it is absorbing the maximum amount of energy. If it is not, then the user can take necessary actions to ensure that the tracker is working to its optimal level.

Ideally, the solar panels can absorb the maximum amount of energy from the sun when the sun rays are beaming on the panels at a perfect perpendicular angle. There are certain parameters that determine how that angle is determined. The orientation that the panels have from the surface of the sun and the angle of the panel from the surface of the sun are two primary factors that are used to establish the correct angle that the solar panels should be at when absorbing the sun's energy.

Software Pseudocode instructions

1. User selects the "tilt status" button.
2. Mobile application sends request to the microcontroller via wifi.
3. Microcontroller reads the angle that the servos are set at.
4. Microcontroller sends the data to the mobile application via wifi.
5. Mobile application converts data and outputs it on the user's phone.

The default view of the application will display the current status of the device as shown in Figure 45.

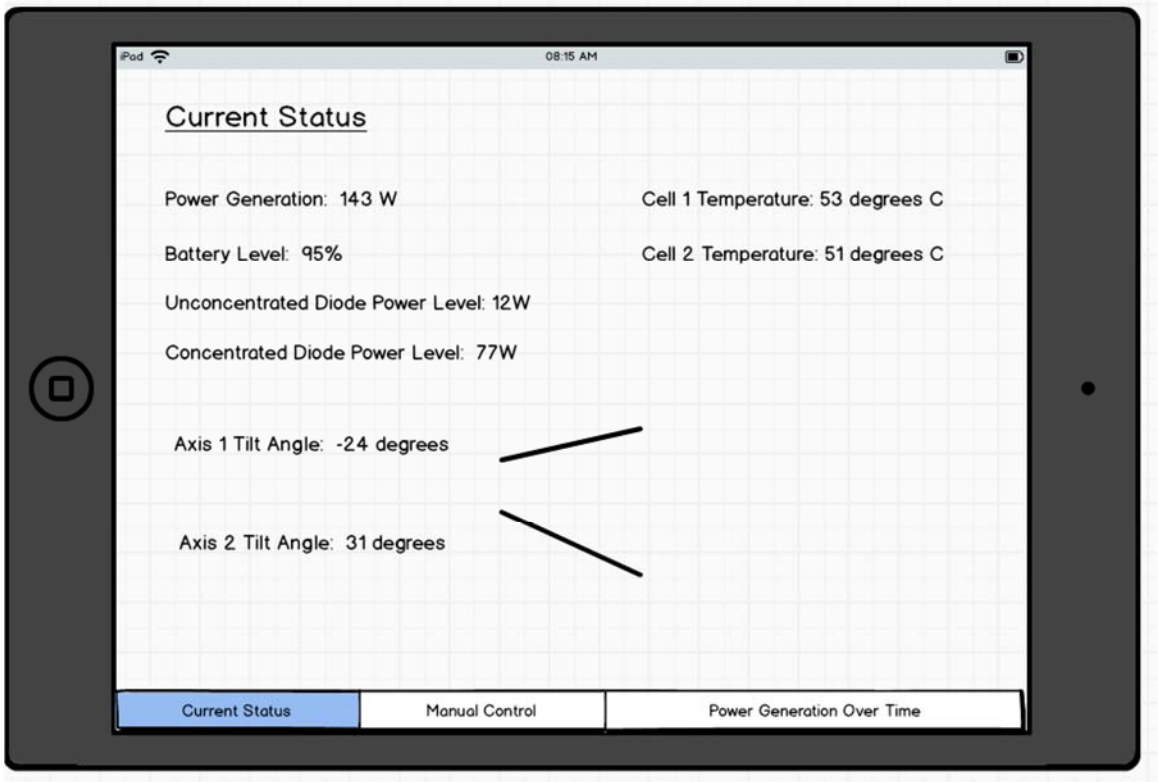

Figure 45: Current Status User Interface

6.2.1.4 Tracking Mode

The tracking mode feature is an attribute that not many current solar tracking applications are offering to their consumers. The feature that we are intending to offer to the user is the ability to select how they want their solar device to track the movement of the sun to obtain the maximum solar energy absorbed. This allows the user to directly interact with the solar device and make changes based on their own observations and calculations. There are three main tracking modes that we've decided on that the user can select.

1. Sensor readings - The sensors connected to the microcontroller track the movement from the sun. The microcontroller calculates if the sensors are in a position where the sun rays are directly aimed at the solar panel and alerts the servos to change the direction the solar panel is facing so that it is getting a direct 90 degree angle adjacent to the sun rays.

2. Predetermined path - Depending on the time of the day, year, or season, the mobile application will store the position that the servos should be set at so that it would ideally be receiving the maximum amount of solar energy. This option is used in the case that the sensors used to track the sun are malfunctioning, or the panels are not adjusting to optimal performance.

3. Manual (User-Controlled) - The user can manually control the movement of the solar device on the mobile application. There will be four buttons on the application that the user can press. This will send a pulse signal to the servos to rotate the solar panel between a certain range. Each button represents the four directions the panels can move at (north, south, east, west). The application will also be displaying the angle that the solar panels are at so that the user can make calculations and record data. The purpose of this option is in the case that the sensors that track the sun are inoperable. The user would be able to manually control the solar device. Another reason why this options is available is so that the user would not have to touch the solar device and risk possible injury. The solar device is meant to be able to operate without having anyone alter it physically. An image of what this feature should look like on the mobile application is seen below.

Software Pseudocode instructions

1. User selects “tracking mode” on mobile application.
2. User chooses one of the tracking options that are available (sensor readings, predetermined path, or manual).
3. If the user selects “sensor readings”, then the application will highlight “sensor readings” and the application will return the user to the selection screen.
4. If the user selects “predetermined path”, then the application will highlight “predetermined path” and the application will return the user to the selection screen.
5. If the user selects “manual” then the application will highlight “manual” and the application will go to another screen with four arrow buttons and the current tilt status.
    a. If the user selects the “up” arrow, then the solar panel will rotate up and update the current tilt status.
    b. If the user selects the “down” arrow, then the solar panel will rotate down and update the current tilt status.
    c. If the user selects the “left” arrow, then the solar panel will rotate to the left and update the current tilt status.
    d. If the user selects the “right” arrow, then the solar panel will rotate to the right and update the current tilt status.
6. Application returns to the selection screen.

The diagram below shows what the manual mode screen on the user’s phone should look like.

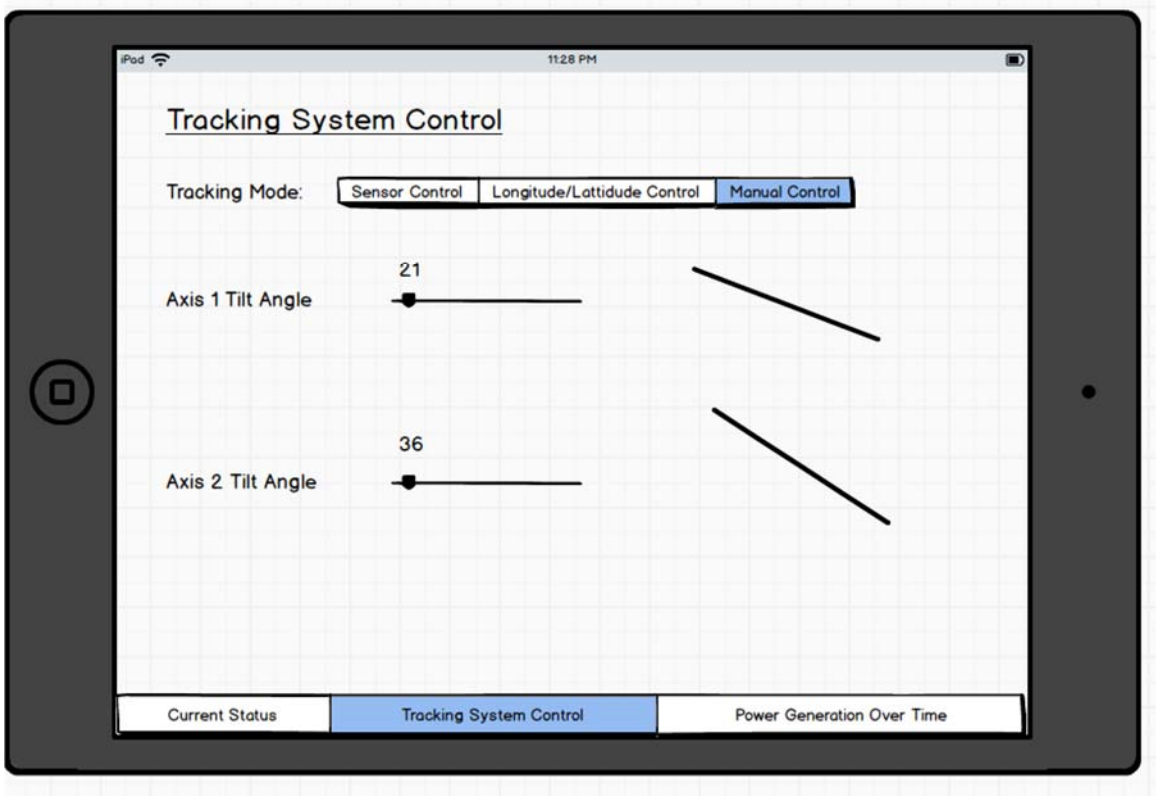

Figure 46: Tracking System Control User Interface

6.2.2 Additional Software Features

These additional features are secondary to the previous features listed above. Compared to the others, these features are truly secondary in nature and aren't hard objectives in our mobile software model. These simply assist the user in understanding what is going on behind the scenes within the device to bridge the technical gap.

6.2.2.1 Temperature Monitoring

The temperature monitoring feature checks the temperature of the solar panel throughout the day to check if there is any overheating occuring. The solar panels are designed to operate within a range of temperature values, so monitoring the temperature of the panel would be beneficial for the user to be able to take necessary steps to ensure that there won't be any heating issues or degradation of the panel. Any damage done to the panel would cause multiple cost issues such as costs for replacement and repair. The application will show the current temperature of the panel as well as offer the option to display a temperature vs. time line graph to show the user the times when the solar panel reaches its highest temperature in the day. The application will also send an alert to the user's phone when the solar panel's temperature is reaching a dangerous level that may cause any damage

6.2.2.2 Battery Health

The most common way to check the status of a battery is by measuring the voltage in order to determine the state of charge. [26] The “state of health” measurement is specifically related to the actual battery capacity in comparison to the design capacity of the battery. As time goes on, and the battery cycles multiple times, the battery’s state of health will degrade. This calculation can be determined in many different forms that can take into account certain variables including charge acceptance, voltage, and internal resistance.

Capacity is a common method to determine battery health, as batteries that degrade will slowly have less capacity within the battery to hold a charge. Since we are already determining the battery capacity through voltage sensors for the user front-facing mobile application, it makes sense to take advantage of these sensor readings to make an educated guess for the user as to the health and future ability of the current connected battery.

Therefore, within the microcontroller, the battery health will be determined by a capacity over time calculation. As the overall capacity of the battery decreases, the user will be notified that the battery health is degrading. The user will be notified that the battery health declining, and that the battery will need to be replaced soon. After a threshold of less than 60% design capacity, the user will be notified to replace the battery.

6.2.2.3 Long Term Value

An additional feature that the mobile application will be able to do is calculate when the user will be able to start earning a profit from using our solar tracking device. The average cost for solar panels as well as installation, maintenance, warranty and taxes ranges between about $11,000 and $15,000 (depending on the type of system [33]. The application would calculate the amount of money the user is saving from using our solar device. There are many factors that are involved in calculating how much time it would take the user to pay back the cost of the solar device. The factors are listed below:

- Overall cost of solar panel system (cost of device, cost of installation, cost of equipment)
- Financial incentives available in the user’s location
- Average monthly electricity usage cost
- Electricity generated from solar panel device
- Financial benefits from going solar (only available in some areas)

The program will then calculate the combined costs (financial incentives, overall cost of solar panel systems) and the annual benefits (financial benefits and

avoided electricity cost from using solar panel). Combined costs divided by annual benefits will give the user the amount of time it will take to pay back the cost of the solar device and begin earning a profit and saving more money.

6.2.3 User Interface

Figure 47 shows what the user is capable of doing in the mobile application. They have the option of selecting to view the power readings, which include how much energy has been produced by the solar cell. Inside of that option, the user can select to view the long term values, which show how much money the user is saving at that moment. The user can also select to view the current tracking mode, as well as choose the change the tracking mode if they want. They can also choose to view the charge level on the battery. This will output how much voltage is stored on the battery and the life status of the battery (if the capacity stored is good or not). The current tilt status will be displayed on the user interface as well as on the manual tracking mode option. The tilt status will update whenever the user controls the linear actuators. The user will also have the option of seeing the temperature readings of the solar cells at the current time. The PCB will be sending information via wifi.

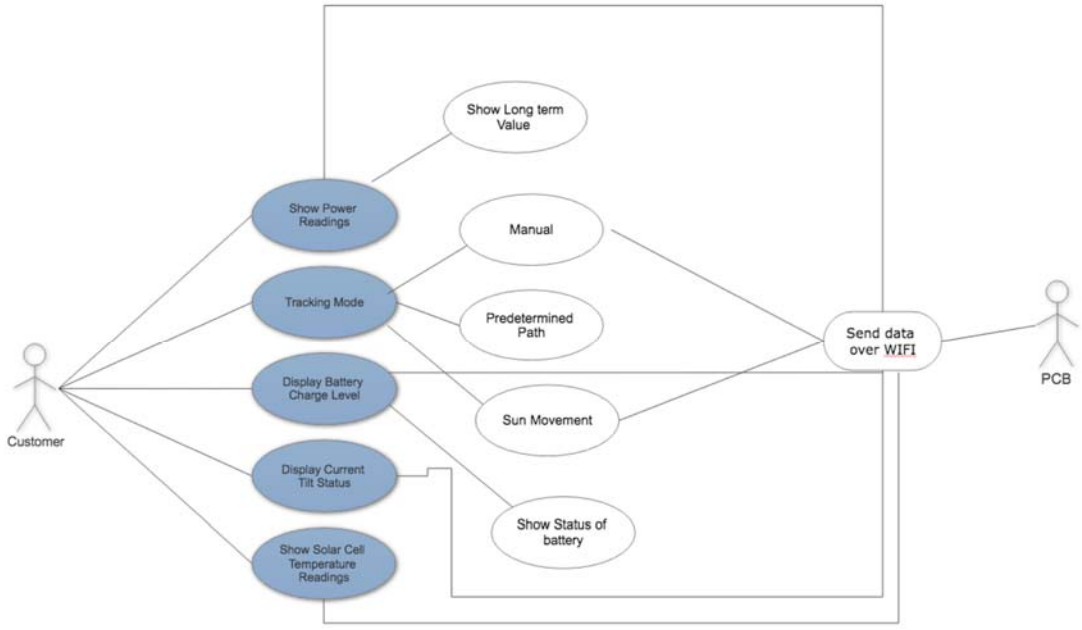

Figure 47: Use Case Diagram

6.2.4 React Native Details

React native works primarily through a main render function and event handlers. The render function returns some markup in a custom markup language called JSX. The styles are also applied with a markup tag. Event handlers can be added inline to interactable components such as buttons or textboxes. However, they also can be handled using two way bindings. Any JSX markup can contain a javascript statement. Markup containing theses expressions will automatically update whenever the underlying variable updates. This paradigm enables rapid development, because it eliminated the need to manually update the view when the model changes.

6.3 Microcontroller Software Design

The role of the microcontroller can be broken up into many different sections. At the top level of discussion, the microcontroller should get sensor readings from the device in order to determine the angle of rotation, calculate the maximum power point using the buck boost DC-DC converter, and manage communication between the device hardware peripherals and the mobile application. Below is a rough break down using pseudocode of the important functions that the microcontroller software must call.

Microcontroller pseudocode main loop:

```
getSensorStatuses();
computeTrackingPWMSignal(); // depending on tracking mode
computeMPPT();
sendUpdatesToMobile();
checkForUpdatesFromMobile();
```

6.3.1 Connecting over Wi-Fi

To program the microcontroller, the programmer must have the CC3220S-LAUNCHXL board connected to a computer running Windows 7 or above and must have an 802.11b/g/n (2.4GHz) Wireless Access Point (AP). The windows computer must also have the latest version of the CC3220 Software Development Kit (SDK) installed as well as Code Composer Studio

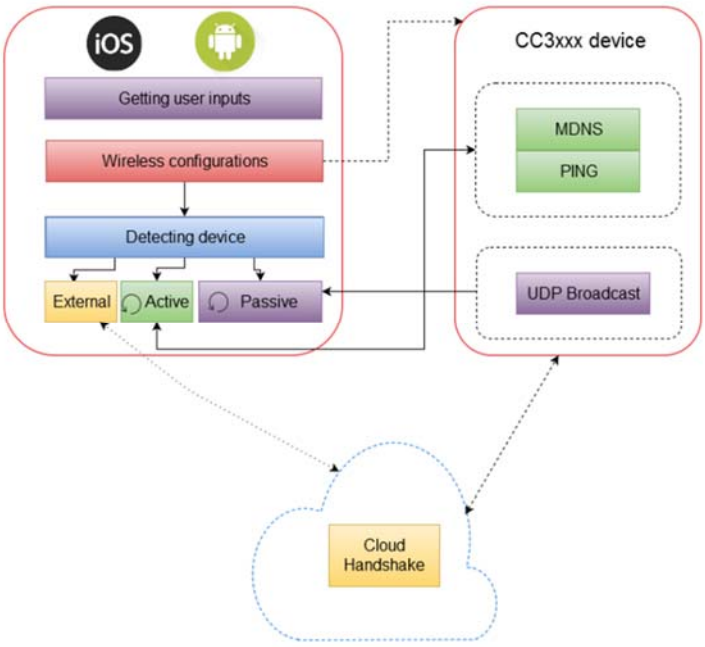

Figure 48: CC3220 Top Level Architecture [49]
Permission Requested from: Texas Instruments

Using SmartConfig, the mobile application can connect to the microcontroller by provisioning. There are four steps for provisioning:

1. User Inputs - The user gives the information on the network. Necessary information that the user has to provide are the network SSID and network password (if a secured network is being used).

2. Sending configurations - The mobile application sends configuration information to the non-configured device. While the device is listening for any information that is being transferred over the network, the mobile application should be sending the information. The device intercepts the information and stores it in a profile that now allows the device to be connected to the same network as the mobile device.

3. Finding the device on the network - The IP address of the device after it is connected to the Wi-Fi network needs to be found, and the IP address from the DHCP server needs to be found as well. If the network is not isolated, the mobile application will detect the device on the network by:
    a. Listening to UDP broadcast packets from the device specifying the name and IP address
    b. Listening to UDP multicast packets from mDNA on the network, and filtering by services supported by the device
    c. Sending broadcast ping packets and catching ping response packets from the devices on the network.

6.3.2 Tracking the sun

The device will track the sun by monitoring the readings from the 4 quadrants of the photodiode. As shown in the hardware section in Figure 40, the sunlight will pass through a pinhole first, then it will be incident on a quadrant photodiode that as shown in Figure 49. Each quadrant in Figure 49 indicates an independent diode. The angle that the device is creating with the incident sunlight can be calculated based on the differences between the photocurrents of the diodes.

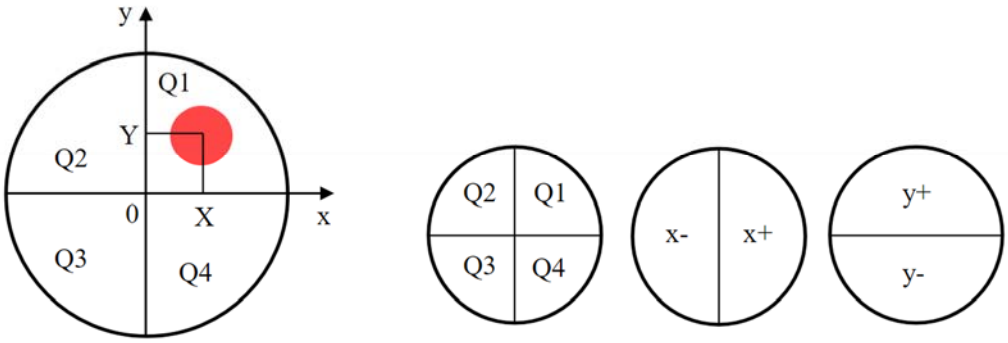

Figure 49: Quadrant Photodiode
Permission Requested from: UCF CREOL

Using the image in Figure 49 as an example, we can calculate the X and Y coordinates of the center of the spot. The equations used to calculate the coordinates are shown in Figure 50.

$$X = \frac{(x+)-(x-)}{Q1+Q2+Q3+Q4} = \frac{(Q1+Q4)-(Q2+Q3)}{Q1+Q2+Q3+Q4} = \frac{X_{Diff}}{SUM}$$

$$Y = \frac{(y+)-(y-)}{Q1+Q2+Q3+Q4} = \frac{(Q1+Q2)-(Q3+Q4)}{Q1+Q2+Q3+Q4} = \frac{Y_{Diff}}{SUM}$$

Figure 50: Quadrant Photodiode Equations

6.3.3 Hill Climbing Algorithm

As described throughout the maximum power point research section, the hill climbing algorithm is simple to implement, effective in practice, and intuitive in design. The hill climbing algorithm, also known as a perturb and observe algorithm, in its basic form increases the acceptance voltage of the solar cells to the battery

through the use of a impedance matching circuit so long as the power is increasing. Once the steps of increasing voltage results in a loss of power, we know that the maximum power point has been passed, and we should step the voltage down until we notice another loss in power.

Within the microcontroller, this is implemented by sampling the voltage at the solar cell (V2), the current at the solar cell (I2), the voltage at the battery (V1), and the current at the battery (I1) shown in Figure 50. By sampling the voltage and current at the battery, we can determine the power output value of the circuit and subsequently the pulse-width modulated signal.

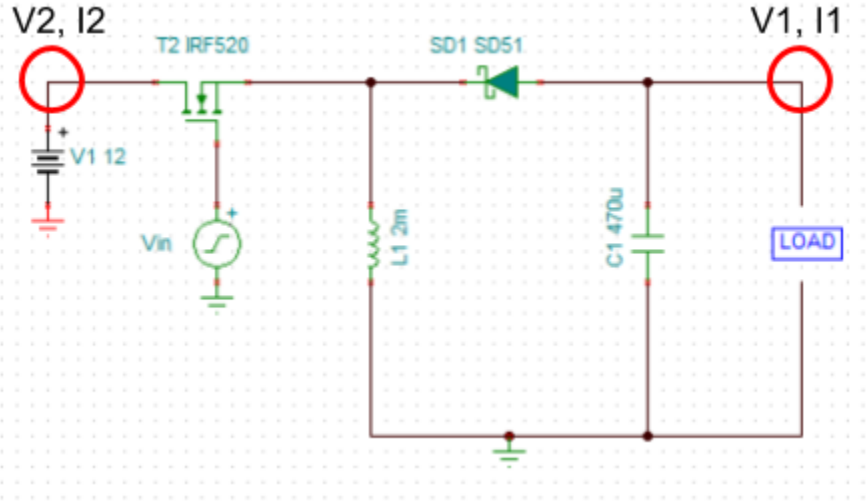

Figure 50: Circuit Sampling Points

6.4 Code Flow Chart

The diagram below shows the flow of code in our design. Information will be continuously flowing between the mobile application and the microcontroller. When the user requests information to be shown, a request package will be sent to the microcontroller via Wi-Fi asking to send certain values. The microcontroller will read the request and send back the requested information, which will then be displayed to the user through the mobile application.

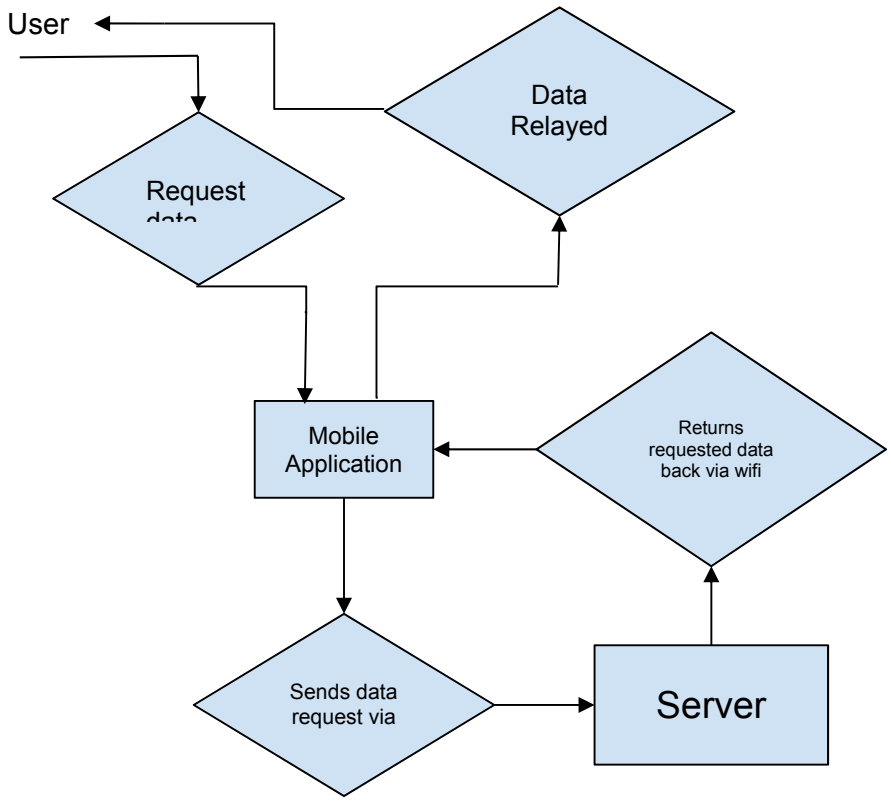

Figure 51: Code Flow Chart

In order to save on resources for the microcontroller, the external server can be utilized and the microcontroller is then referenced for sensor polling. This also allows for the phones internal storage to be disconnected, while the information regarding the performance of the system is stored on a webserver in the cloud. The user then pulls this information down as requested depicted in the above figure.

7 Prototype Construction and Testing

Our project contains a number of unknown factors that will affect future performance and design of the system as a whole. The following section describes in detail, how we will approach different testing methods and resolve issues that may arise throughout production.

7.1 Solar Concentrator Testing

The refractive indexes of each piece of the concentrator will be tested prior to assembly. Each refractive index will be measured with a refractometer. As the concentrator is assembled, it will be tested after each piece is added. Losses will be measured by passing a laser through the device. The power of the laser will be measured before it passes through the device and the aftwards. These two powers will be compared to calculate a percentage loss. Testing the losses after adding each component will allow us to record the source of the largest losses. Knowing the source of the losses will help us know which component needs the most improvement. A coupling prism may be required to couple the laser beam out of the device in order to measure the losses.

First, the losses due to reflection at the air - polycarbonate interface. Then, the mirrors will be deposited onto the prisms and the losses due to absorption will be measured. Then, the prisms will be glued together using an index matched resins and the losses due to mismatched resins will be measured. The prism assembly will then be glued to the high index gradient index later (n = 1.65 - 1.80.) The losses due to Fresnel reflection will then be measured. The process of gluing on a component and then measuring losses will continue until all pieces are assembled and the final optical losses can be measured.

The intensity profile will be tested next. The assembled concentrator will be placed in the sun and positioned such that the angle of incidence is approximately 0 degrees. A optical sensor will then be moved to different positions on the output area. The intensity will be measured at each point on each side. These intensities will be visualized via a heat map style diagram so that the intensity profile may be studied.

After the intensity profile is measured, two optical sensors will be mounted onto the concentrator. One will be mounted parallel to the surface of the plexiglass. The other sensor will be mounted on the side of the concentrator to measure the concentrated light. The ratio of the the powers that these two sensors measure, along with the losses that were measured in previous steps, can be used to estimate the actual concentration level. During operation, these two sensors can be compared to confirm that the concentrator is still working and to detect if the concentrator is degrading in some way. One potential problem is that the indexes

of the resins may change with temperature. The constant testing provided by these sensors will detect this kind of problem.

7.2 Solar Cell Testing

When the solar cells arrive, they need to be tested and characterized. The open circuit voltage, short circuit current, fill factor and efficiency must be measured. To find these parameters, a source, optical setup, circuit and multimeter are required.

Ideally, a solar simulator would be used as a source. However, to reduce expenses, a white LED array that is collimated and focused onto the solar cell will be used. The power of the light will be measured with an optical power meter. Then, the solar cell will be placed at a distance away from the focusing lens that allows the light to cover the solar cell. This way, we will know the optical power that is incident on the solar cell. This setup is shown in Figure X.

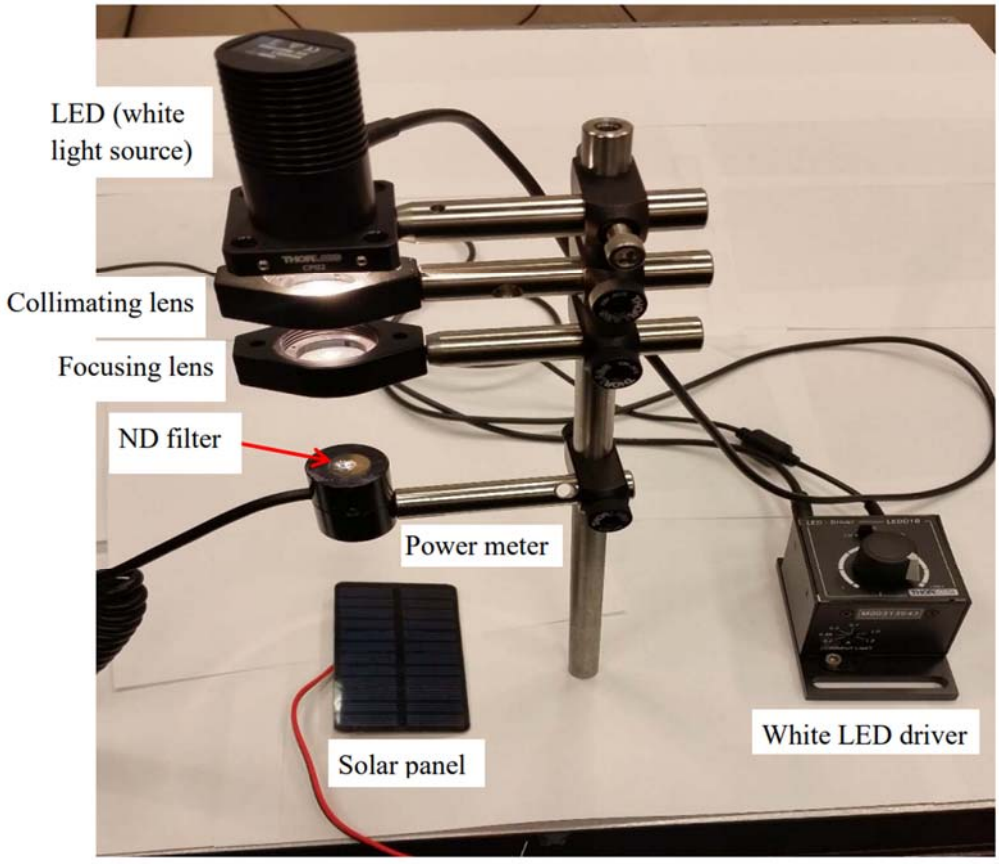

Figure 52: Solar Cell Characterization Setup.

Once the optical power incident on the solar cell is known, the open circuit voltage and short circuit current will be measured. To do this, the solar cell will be placed in the circuit pictured in Figure 53.

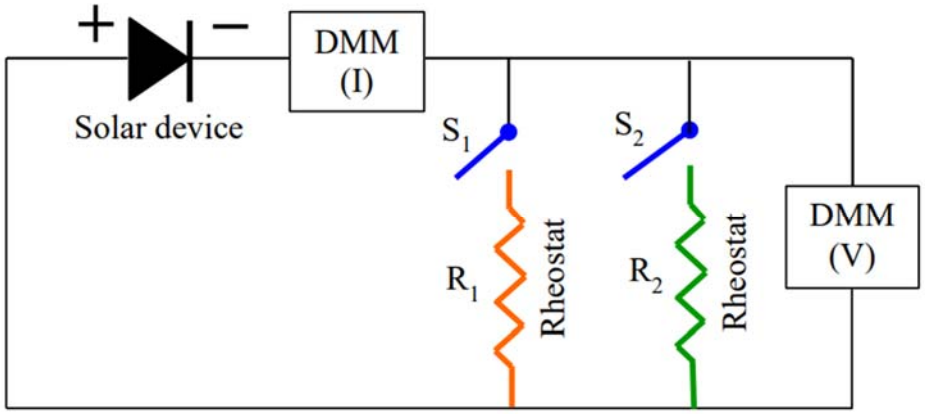

Figure 53: Solar Cell Test Circuit
Permission Requested from: UCF CREOL

The resistance in the circuit will be varied and the current and voltage will be measured as the resistance changes. Then, the intensity of the light on the solar cell will be increased and the process will be repeated. In this way, the open circuit voltage, short circuit current, fill factor and efficiency will be measured under different light intensity conditions. To find the efficiency, the following equation will be used:

$$Efficiency = V_m I_m / P_i$$

Vm and Im are the voltage and current at which the cell operates at maximum power. Vm and Im can be found when the area of the rectangle in Figure 54 is maximized. Since we have already measured Pi, we can calculate the efficiency at a certain light intensity. By comparing efficiencies at different intensities, we can discover the relationship between intensity and efficiency.

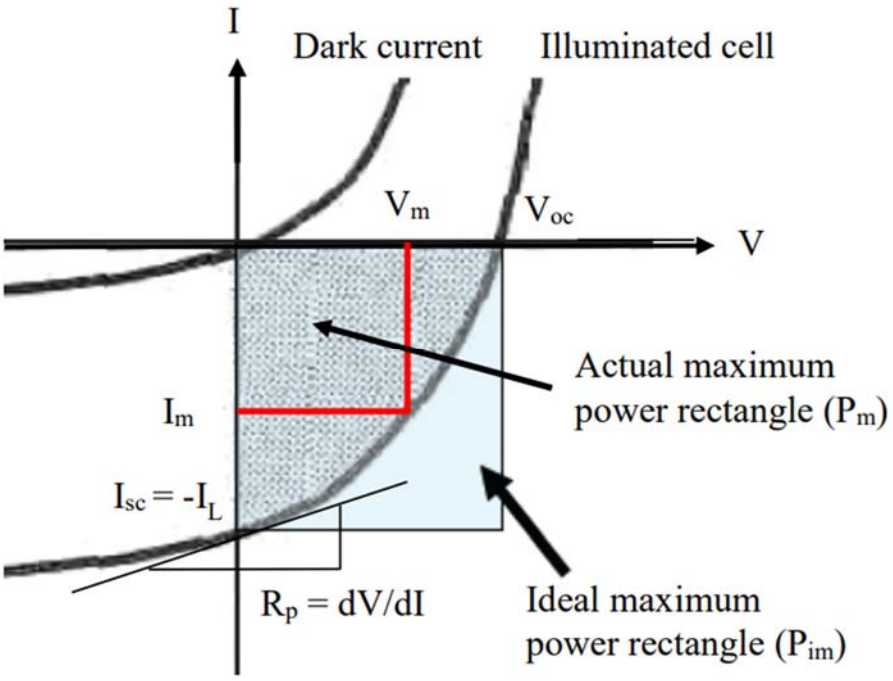

Figure 54: Fill Factor Rectangle
Permission Requested from: UCF CREOL

7.3 Hardware Testing

Testing all of the hardware components to ensure they are in proper working order as they are assembled is imperative early on in order to not disturb the flow of the milestone goals set in section 8. All hardware including the microcontroller development board, custom PCB with their associated parts, servos, and battery will be tested on arrival, and continually tested during assembly as needed.

The battery (as described in 7.6.2) will be tested for discharge rate and capacity, as well as behavior during slight voltage and current overload. It is important to know how the battery will react during undefined behavior, in order to prevent dangerous situations if any of the DC-DC converters aren't working properly. The microcontroller development board will receive the most testing, as we will be using it to develop and test our code base before programming the CC3220. Through this development board, we can send specific low voltage signals to other parts such as the servos to test the connection, response time, and behavior as if they were achieving a signal response from the optical sensors. In addition to the servos, the optical, voltage, and current sensors will all be tested for accuracy as the data sheets state from the manufacturer.

After preliminary tests have been completed, combinations of these components will be put together to form a dummy version of the solar concentrator. The optical components to the solar concentrator will take some time to achieve. Therefore, it

is imperative to design a development version of the solar device to see if the optical sensors, microcontroller, and servos will behave in an appropriate manner. This entails getting a piece of wood or plastic material approximately the same size as the final concentrator and loosely mounting the hardware to test if these components will work together seamlessly in the final product. Tweaks will be made as necessary.

7.4 Simulation

As design iterations improve, testing the hardware circuitry with programs such as Multisim, LTSpice, or TINA will allow us more insight as to the function and behavior behind the circuit an allow us to better analyze each individual step of the process as the signal passes through. Currently, the circuit from Figure 39 has been simulated and tweaked to achieve the appropriate values shown. Moving forward, we plan to replace passive element values as we see fit through simulation, as well as the diode element. Multiple passive component value have been simulated to achieve the current maximization so imperative to charging our battery in a fast manner.

Adding onto this circuit will be current caps/limits to stop the battery from charging at a rate faster than is recommended by the manufacturer, as well as a voltage regulator to ensure the signal entering the battery is at a strong and steady value, rather than fluctuating wildly. These new additions will be simulated for appropriate component values and added as the design matures and progresses in its later stages of development.

7.5 Software Testing

Testing the software is one of the most important components to ensuring that the solar tracking system is performing up to its standards. Before software testing can begin, there needs to be and initial setup of the software:

- The system will need to be able to power up correctly.
- Sensors need to be calibrated.
- Microcontroller needs to be connected to a Wi-Fi access point.
- User’s phone must be connected over same Wi-Fi access point.
- The mobile application needs to be running on the user’s Android phone as well.

Once all of these conditions have been satisfied, testing of the Native React application may begin. Below shows the steps for testing the application.

1. User selects “show power readings”
    a. User selects “day”
    b. User selects “month”

    c. User selects “year”
2. User selects “tracking mode”
    a. User selects “sensor readings”
    b. User selects “predetermined path”
    c. User selects “manual”
        i. User presses up arrow
        ii. User presses down arrow
        iii. User presses left arrow
        iv. User presses right arrow
3. User selects “select battery charge level”
4. User selects “display current tilt status”
5. User selects “show solar cell temperature readings”
6. User selects “battery health”
7. User selects “Payback time”
    a. User inserts overall cost of solar panel system
    b. User inserts financial incentives
    c. User inserts average monthly electricity bill from past 6 months
    d. User inserts financial benefits from using solar system

7.6 Longevity Predictions

Longevity problems are issues that could possibly come up after using the solar system for a certain period of time.
Heat over time? Components that need to be replaced? Solar cells not working/damage?

7.6.1 Solar Cell Lifetime

The lifetime of a solar cell is considered to be the amount of time it can operate until it is operating at 80% of the original efficiency. According to the National Renewable Energy Lab, the efficiency of silicon solar cells decreases an average of 0.8 percent per year. [35] However, the SunPower solar cells that we have chosen have a degradation rate of 0.3 percent per year. However, both of these values were measuring the cells under 1 sun conditions. Silicon solar cell degradation under concentrated settings is rare, but the data we have indicates that the lifetime of a solar cell under concentrated conditions will be reduced. The data given in [36] for 2.5 times concentration indicates that those cells degraded at a rate of 1.2 percent per year. Extrapolating this linearly, we can infer the lifetime of our solar cells under concentration as shown in Figure X. We calculate the lifetime of our solar cells and compare it to the average solar cell lifetime in Figure 55.

$$t = Efficiency\ reduction\ \%/(degradation\ rate\ per\ year + (C - 1) * concentrator\ degradation)$$

Typical Solar Cell Under 1 Sun: t = 20/.8 = 25 years
Sunpower Solar Cell Under 6 Suns: t = 20/(.3 + (6-1)*.3) = 11.1 years

Figure 55: Solar Cell Lifetime Calculations

7.6.2 Battery Life Degradation

The battery life degradation tests will consist of constantly power cycling a test battery to see how the model of battery chosen will continue to work under suitable conditions. Noted in Mutagekar's paper [39], cycling batteries to their degradation point is a long and arduous process. In order to sell a new battery model, battery manufacturers must test a battery model rigorously to ensure the expected cycle count of the battery is accurate. These numbers are difficult to test on the consumer side though, as it takes significant time and effort to constantly charge and discharge a battery.

Without the use of an autonomous battery cycler such as the one Mutagekar describes, the two main options are to trust the battery manufacturer or to manually test to degradation. To avoid wasting time manually testing the battery to the death of 500+ cycles, we will instead run the battery through numerous cycles and at each cycle plot the voltage, current, and power results over time through discharge. This may look like something similar to Figure 56, in which the overall battery capacity is measured throughout multiple cycles of the battery and compared to the design specifications presented by the manufacturer.

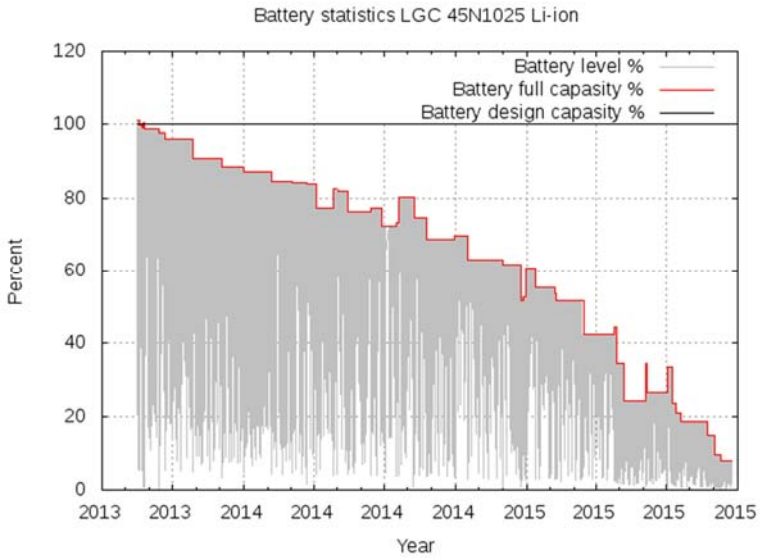

Figure 56: Li-ion Battery Capacity Over Time [40]
Permission Requested from: Reinholdtsen

As time elapses the battery degradation increases, and eventually the battery will cross a threshold point in which the user will be notified of these issues. Below 80% the user will be notified to replace the battery soon. Below 60% the user will be notified to replace the battery as soon as possible.

8 Administrative Content

This section reviews administrative break downs including distribution of work, and budget determinations after researching and strategically picking our hardware and software components.

8.1 Project Roles

During research and planning, a natural divide has segmented our focus between the group. Kyle Merritt, Matthew Armogan, and Justin Kolnick will be referenced by their first names throughout this subsection. Kyle, as the optics and photonics student, focused on the optical design of the solar concentrator including but not limited to the gradient index layered concentrator design, solar cell composition, and sensor mechanisms in order to monitor the entire device. Justin focused mainly on hardware design and low level embedded software including how it interfaces with the mobile application software. Matthew focused on the higher level software design and implementation including React Native development for mobile applications and general interfacing between the microcontroller and the user controlled device using WiFi communication.

All of these project role breakdowns and not rigid, and include heavy overlap to ensure that our entire team is aware of how the system is functioning. This is imperative in a group project, notably due to the tunnel vision effect that can occur when designing each system section.

8.2 Budget

The following section goes over the entire budget for the product broken down into quantity and price shown in Table 11. Due to the high cost of optical components, we have decided to size down the project, but depending on budgetary sponsors, the scale could increase.

Table 11: Budget

Item	Quantity	Price Estimate
Metal Framing Material	1	$20
Metal Support Material	1	$10
Resistance Temperature Detectors	2	$40
Quadrant Photodiode	1	$90

Tube with Pinhole for Quadrant Photodiode	1	$10
Servos	2	$30
Batteries	1	$100
Custom PCB	1	$30-$100
CC3220 LaunchPad	1	$45
Circuitry components	1	$25-$65
Buck Converter Components	1	$20
Microcontroller	1	$20
Microcontroller wifi chip	1	$15
Voltage regulators	2	$20
Gem Refractometer	1	$98
Gem Refractometer Liquid	2	$122
Various Tools for Glass Component Assembly	1	$60
Laser Diode for Testing Concentrator	1	$40
Optical Bench Setup for Testing Concentrator	1	$120
High index glass samples (~3cm^2)	5	$50
Large high index glass sheet	2	$200
Plexiglass sheet	2	50
Anamorphic Prism Pairs	20	$1100
Silver nitrate salt	100g	$60
TOTAL		~2,055

8.3 Project Milestones

This section details a timeline of milestones for each topic area including concentrator (Table 12), tracking (Table 13), and software (Table 14) in order to simplify and organize the tasks required to realize the device design.

Table 12: Concentrator Milestones

#	Milestone	Week of Completion
1	Design and build apparatus for testing planar gradient index material	2/18
2	Begin testing ion exchange process on 5 - 10 small samples of glass	2/25
3	Finalize choice of gradient index glass materials	3/11
4	Bond 2 samples with resin and test optical properties under varying temperatures	3/25
5	Fabricate a molded glass slump of zig-zag pattern	4/1
6	Deposit mirror onto zig-zag size of glass	4/8
7	Bond polycarbonate directly to glass	4/15
8	Assemble a working mini prototype	4/29
9	Order materials for full scale prototype	8/19
10	Fabricate a full size gradient index sheet and fuse polycarbonate layer to it	8/26
11	Fabricate a full size zig-zag glass piece	9/16
12	Deposit Mirror onto full size zig-zag piece	9/23
13	Attach mirrored zig-zag piece to assembly	9/30
14	Attach solar cells to concentrator	10/14
15	Integrate concentrator assembly with tracking system	10/31

Table 13: Tracker Milestones

#	Milestone	Week of Completion
1	Complete and finalize tracker design	2/11
2	Complete design of MPPT circuit	3/11
3	Place order for parts that will interface with microcontroller (for testing)	3/11
4	Complete design of battery bank and converter circuits	3/18
5	Test moving parts by connecting them to microcontroller and purchase remaining parts including sample solar cells	3/25
6	Test solar cell efficiency	4/4
7	Review parts received and confirm that they wlll work as expected	4/11
8	Assemble MPPT circuit and test with a solar cell	8/23
9	Assemble frame for concentrator	9/9
10	Test a solar cell, MPPT circuit and battery bank system	9/16
11	Assemble support frame and linear actuators	9/30
12	Integrate electronics with microcontroller	10/7
13	Test movement of entire tracking system with microcontroller	10/14
14	Integrate with concentrator	10/31
15	Test manually with concentrator attached	11/7
16	Test fully integrated system	11/14

Table 14: Software Milestones

#	Milestone	Week of Completion
1	Define the problem the mobile application is trying to solve	2/4
2	Define the feature set of the application	2/11
3	Choose mobile platform, framework, and libraries, choose ~~and order microcontroller~~ (how to get info via wifi, start dummy app), charting, wifi, github sharing	2/25
4	Design mobile application user experience	3/4
5	Stub out mobile application	3/11
6	Implement connection between microcontroller and mobile application	3/25
7	Test interface with moving parts by controlling them with microcontroller	3/25
8	Design microcontroller application	4/8
9	Finalize design & test with mock data	4/22
10	Implement microcontroller control of tracking system	8/23
11	Implement microcontroller wifi endpoints	9/9
12	Implement mobile app part 1 and integrate implementation with microcontroller app	9/16
13	Implement mobile app part 2 and	9/23
14	Implement mobile app part 3 (scope depends on user experience design)	9/30
15	Complete mobile app implementation	10/14
16	Test fully integrated system	11/14

9 Conclusion

This project is comprehensive in solar energy efficient technologies to provide the user with the best experience possible in their hand and on their wallet. From energy capture to energy storage, this project encompasses a number of techniques to ensure that the maximum amount of power is transferred from point a to point b. By reducing the size and quantity of necessary solar cells, funds could be focused on fewer, more expensive, more efficient cells in order to maximize the solar energy captured within the CPV optics. This solar energy, once trapped within the final gradient index layer closest to the top, is concentrated to C=6, motivating the need for a higher end cell. A maximum power point tracking switching circuit and algorithm are implemented to ensure that sufficient voltage is maintained when energy moves throughout the system from the cell to the battery, all the while maximizing the current (within a particular threshold limit) to speed up the charging process.

In addition to broad and comprehensive solar energy technology, the software side of the project introduces new and interesting problems. As we move into the embedded system design, the scope of the project broadens to that of computer engineering problem solving through the use of the new CC3220 microprocessor. This microprocessor is powerful and new on the market; writing software for the ARM Cortex M4 will prove to be challenging yet informative moving forward. All the way to the top of the software design, we are shaping the user experience through the use of graphical user interface elements on a mobile application. This is our best attempt to bridge the gap of today's consumer, which is so undoubtedly linked to smart devices all the time and solar technology which may come off as something completely foreign to the layman.

Through this planning phase, we have completed sufficient research in each topic area to ensure that proper precautions and previous experience of other projects is heeded. As we move forward with the testing phase, and eventually the final construction phase, we are all excited to see our vision come to fruition and develop a concentrated photovoltaic system that has the user in mind.

9.1 Future Improvements

Moving forward, one of our biggest constraints is budgetary, due to the high cost of optical elements related to the concentrator. At the moment, our current design is a proof of concept and includes a small surface area where the sunlight can be captured, mainly due to the high cost of the anamorphic prisms beneath the flat gradient index layers. As we determine the source of funding, one area we would like to see improve is the optical cost decrease. Access to a professional kiln and a platinum crucible in order to melt high indexed glass frit would be ideal, but unfortunately not readily available. Moving forward, we would also like to see improvements in the maximum power point tracking circuit as well as the PCB

design as a whole. However, these elements will mainly be improved with iteration, simulation, and testing.

Throughout software development we will continue to tweak the MPPT algorithm duty cycle to ensure that an appropriate maximum power point is being achieved in a timely and effective manner without constant oscillations. Other MPPT algorithms that we researched in Section 3 are still under consideration. In regards to the higher level software, testing the user interface with peers and colleagues will be our main testament to the quality and intuitiveness of our design. Through these findings we will continue to improve the UI design, as this is one of our main objectives.

10 References

[1] IEA, Key Energy World Statistics 2017, International Energy Agency, http://www.iea.org/publications/freepublications/publication/KeyWorld2017.pdf

[2] Höök, M. and X. Tang (2013). "Depletion of fossil fuels and anthropogenic climate change—A review." Energy Policy 52: 797-809.

[3] Sustainable Development Goals Report 2017, United Nations, https://unstats.un.org/sdgs/files/report/2017/TheSustainableDevelopmentGoalsReport2017.pdf

[4] “Solar Industry Research Data.” SEIA, www.seia.org/solar-industry-research-data.

[5] J.J. Droher, S.E. Squier, Performance of the Vanguard Solar Dish-Stirling Engine Module, EPRI AP-4608, Electrical Power Research Institute, Palo Alto, CA, 1986.

[6] “Dish/Engine System Concentrating Solar Power Basics.” Energy.gov, www.energy.gov/eere/solar/articles/dishengine-system-concentrating-solar-power-basics.

[7] “Power System.” How Efficient Are Solar Panels?, www.qrg.northwestern.edu/projects/vss/docs/power/2-how-efficient-are-solar-panels.html.

[8] “US6029475A - Batching of Molten Glass in the Production of Graded Index of Refraction Glass Bodies.” Google Patents, Google, patents.google.com/patent/US6029475.

[9] Roman Rogoziński , “Ion Exchange in Glass –The Changes of Glass Refraction“ http://cdn.intechopen.com/pdfs/40698/InTech-Ion_exchange_in_glass_the_changes_of_glass_refraction.pdf

[10] Klaus Jäger, Olindo Isabella, Arno H.M. Smets, René A.C.M.M. van Swaaij, Miro Zeman “Solar Energy Fundamentals, Technology, and Systems“ https://courses.edx.org/c4x/DelftX/ET.3034TU/asset/solar_energy_v1.1.pdf

[11] “Fixed Tilt vs axis tracker solar panels.” Kiewit, www.kiewit.com/plant-insider/current-issue/fixed-tilt-vs-axis-tracker-solar-panels/.

[12] Sharp, Photodiode/Phototransistor Application Circuit, http://physlab.org/wp-content/uploads/2016/03/Photodiode_circuit.pdf

[13] P., Garg H., and Prakash J. Solar Energy Fundamentals and Applications. Tata McGraw-Hill Pub. Co., 2007.

[14] “CONTROLLING THE REFRACTIVE INDEX OF EPOXY ADHESIVES.” Conservation OnLine - CoOL, cool.conservation-us.org/jaic/articles/jaic28-02-006.html.

[15] Sun, Jian, “Pulse-Width Modulation” https://pdfs.semanticscholar.org/7e5b/9378d9100f66cebf496aa4e9b6514f88da77.pdf

[16] “SOLAR ENERGY STANDARDS ACT -.” Florida Solar Energy Industries Association, www.flaseia.org/education/solar-laws/solar-energy-standards-act/.

[17] Meng, W., et al. (2016). "The Recycling of Leaded Glass in Cathode Ray Tube (CRT)." Procedia Environmental Sciences 31: 954-960.

[18] “Pulse Width Modulation Used for Motor Control.” Basic Electronics Tutorials, 16 Feb. 2018, www.electronics-tutorials.ws/blog/pulse-width-modulation.html.

[19] Silicon Labs, “Which ARM Cortex Core Is Right for Your Application: A, R or M?“ https://www.silabs.com/documents/public/white-papers/Which-ARM-Cortex-Core-Is-Right-for-Your-Application.pdf

[20] ARM, DSP Capabilities of Cortex M4 and Cortex M7, https://community.arm.com/cfs-file/__key/telligent-evolution-components-attachments/01-2142-00-00-00-00-73-48/ARM-white-paper-_2D00_-DSP-capabilities-of-Cortex_2D00_M4-and-Cortex_2D00_M7.pdf

[21] “Silicon Concentrator Solar Cells.” SpringerLink, Springer, Berlin, Heidelberg, 1 Jan. 1970, link.springer.com/chapter/10.1007%2F978-3-540-68798-6_3.

[22] “BU-205: Types of Lithium-Ion.” Types of Lithium-Ion Batteries – Battery University, batteryuniversity.com/learn/article/types_of_lithium_ion.

[23] Choosing the Detector for Your Uniquie Light Sensing Application, www.johnloomis.org/ece445/topics/egginc/tp4.html.

[24] “How To Select And Use The Right Temperature Sensor.” How to Select and Use the Right Temperature Sensor, www.pyromation.com/TechInfo/WhitePapers/How_to_Select_and_Use_the_Right_Temperature_Sensor.aspx.

[25] “Concentrator Photovoltaic Market.” Concentrator Photovoltaic CPV Market - Industry Analysis, Forecast 2024, www.transparencymarketresearch.com/concentrator-photovoltaic-market.html.

[26] “BU-903: How to Measure State-of-Charge.” Measuring State-of-Charge - Battery University, batteryuniversity.com/learn/article/how_to_measure_state_of_charge.

[27] “State of Health (SOH) Determination.” Battery State of Health Determination, www.mpoweruk.com/soh.htm.

[28] Robinson, John W, and Brian W Raichle. “PERFORMANCE COMPARISON OF FIXED, 1-, AND 2-AXIS TRACKING SYSTEMS FOR SMALL PHOTOVOLTAIC SYSTEMS WITH MEASURED DIRECT BEAM FRACTION.”*Https://Pdfs.semanticscholar.org/bb19/41451e027f73d814d07332a9deebec0cadeb.Pdf*, Semantic Scholar, pdfs.semanticscholar.org/bb19/41451e027f73d814d07332a9deebec0cadeb.pdf.

[29] Hamza Hijazi, Ossama Mokhiamar, Osama Elsamni, Mechanical design of a low cost parabolic solar dish concentrator, Alexandria Engineering Journal, Volume 55, Issue 1,2016, Pages 1-11, ISSN 1110-0168, https://doi.org/10.1016/j.aej.2016.01.028. (http://www.sciencedirect.com/science/article/pii/S111001681600034X)

[30] Collins, Danielle. “Servo Motor Basics.” *Linear Motion Tips*, Linear Motion Tips, 19 Jan. 2017, www.linearmotiontips.com/servo-motor-basic/.

[31] Drury E., Lopez A., Denholm P., and Margolis R. (2014), Relative performance of tracking versus fixed tilt photovoltaic systems in the USA, *Prog. Photovolt: Res. Appl.*, 22, pages 1302–1315, doi: 10.1002/pip.2373

[32] “Pan/Tilt Bracket.” Karlsson Robotics, www.kr4.us/pantilt-bracket.html?gclid=CjwKCAjwq_vWBRACEiwAEReprGy1y6S0p6G48CobzVUxJ44RKUKb7TY2Eg7BjJeAAU9BdEewbNgU-BoC7z8QAvD_BwE.

[33] Figure 6. Distribution of Hourly Photovoltaic Energy Generation [12] : Simulation of a ZEB Electrical Balance with AHybrid Small Wind/PV : Science and Education Publishing, pubs.sciepub.com/rse/2/1/2/figure/6.

[34] Fontani, et al. “Pointing Sensors and Sun Tracking Techniques.” International Journal of Photoenergy, Hindawi, 5 May 2011, www.hindawi.com/journals/ijp/2011/806518/.

[35] Jordan, Dirk C, Kurtz ,Sarah R., Photovoltaic Degradation Rates — An Analytical Review, NREL, June 2012

[36] Jordan, Dirk C., et al. “Compendium of Photovoltaic Degradation Rates.” Progress in Photovoltaics: Research and Applications, Wiley-Blackwell, 7 Feb. 2016, onlinelibrary.wiley.com/doi/full/10.1002/pip.2744.

[37] Adafruit Industries. “Standard Size - High Torque - Metal Gear Servo.” Adafruit Industries Blog RSS, www.adafruit.com/product/1142.

[38] “501833 280mAh 3.7v Lithium Li Ion Polymer Rechargeable Battery For Bluetooth Headset Smart Watch Sports Bracelet Mouse-in Rechargeable Batteries from Consumer Electronics on Aliexpress.com | Alibaba Group.” Aliexpress.com, www.aliexpress.com/item/501833-280mAh-3-7v-lithium-Li-ion-polymer-rechargeable-battery-For-Bluetooth-Headset-Smart-watch-Sports/32825692554.html.

[39] Sushant Mutagekar, John P Kurian, Ashok Jhunjhunwala, Prabhjot Kaur, Shivashankar Gunaki, "Designing a high performance battery life cycle tester", *Sustainable Green Buildings and Communities (SGBC) International Conference on*, pp. 1-4, 2016.

[40] “Petter Reinholdtsen.” Petter Reinholdtsen: The Life and Death of a Laptop Battery, people.skolelinux.org/pere/blog/The_life_and_death_of_a_laptop_battery.html.

[41] “IEEE Std 937-2007 (Revision of IEEE Std 937-2000) - IEEE Recommended Practice for Installation and Maintenance of Lead-Acid Batteries for Photovoltaic (PV) Systems.” IEEE 937-2007 - IEEE Recommended Practice for Installation and Maintenance of Lead-Acid Batteries for Photovoltaic (PV) Systems, 22 Mar. 2007, standards.ieee.org/findstds/standard/937-2007.html.

[42] “IEEE Std 1013-2007 (Revision of IEEE Std 1013-2000) - IEEE Recommended Practice for Sizing Lead-Acid Batteries for Stand-Alone Photovoltaic (PV) Systems.” IEEE 1013-2007 - IEEE Recommended Practice for Sizing Lead-Acid Batteries for Stand-Alone Photovoltaic (PV) Systems, 22 Mar. 2007, standards.ieee.org/findstds/standard/1013-2007.html.

[43] “IEEE Std 1526-2003 - IEEE Recommended Practice for Testing the Performance of Stand-Alone Photovoltaic Systems.” IEEE 1526-2003 - IEEE Recommended Practice for Testing the Performance of Stand-Alone Photovoltaic Systems, 11 Sept. 2003, standards.ieee.org/findstds/standard/1526-2003.html.

[44] 1561-2007 - IEEE Guide for Optimizing the Performance and Life of Lead-Acid Batteries in Remote Hybrid Power Systems - IEEE Standard, ieeexplore.ieee.org/document/4522641/.

[45] “ANSI/IEEE 1562-2007 - IEEE Guide for Array and Battery Sizing in Stand-Alone Photovoltaic (PV) Systems.” IEEE 1562-2007 - IEEE Guide for Array and

Battery Sizing in Stand-Alone Photovoltaic (PV) Systems, 5 Dec. 2007, standards.ieee.org/findstds/standard/1562-2007.html.

[46] IEEE Std 1661 - IEEE Guide for Test and Evaluation of Lead-Acid Batteries Used in Photovoltaic (PV) Hybrid Power Systems - IEEE Standard, ieeexplore.ieee.org/document/4449092/.

[47] P2030.3/D4, Dec. 2015 - IEEE Approved Draft Standard for Test Procedures for Electric Energy Storage Equipment and Systems for Electric Power Systems Applications - IEEE Standard, ieeexplore.ieee.org/document/7419221/.

[48] 29119-4-2015 - ISO/IEC/IEEE International Standard - Software and Systems Engineering--Software Testing--Part 4: Test Techniques - IEEE Standard, ieeexplore.ieee.org/abstract/document/7346375/.

[49] Instruments, Incorporated Texas. “SimpleLink™ Wi-Fi® CC3120 and CC3220 Provisioning for Mobile Applications.” SimpleLink™ Wi-Fi® CC3120 and CC3220 Provisioning for Mobile Applications.

[50] A. Gutierrez, H. R. Chamorro, J. F. Jimenez, L. F. L. Villa, C. Alonso, "Hardware-in-the-loop simulation of PV systems in micro-grids using SysML models", Control and Modeling for Power Electronics (COMPEL) 2015 IEEE 16th Workshop on, pp. 1-5, 2015.